UNIVERSITY
OF TRENTO

DIPARTIMENTO DI INGEGNERIA E SCIENZA DELL'INFORMAZIONE

38123 Povo – Trento (Italy), Via Sommarive 14
http://www.disi.unitn.it

FAILURE DETECTION IN LINEAR ARRAYS THROUGH COMPRESSIVE SENSING

G. Oliveri, P. Rocca, and A. Massa

June 2013

Technical Report # DISI-13-012

TEST CASE DESCRIPTION

Goal: THE TARGET I HAVE TO FOCUS ON IN THIS PROJECT IS THE CREATION OF A NEW SOFTWARE TOOL FOR FAILURE DETECTION. I HAVE TO MERGE TOGETHER DIFFERENT CODES TO REACH MY AIM. FROM THE LINEAR ARRAY EXPECTED FIELD RADIATION AND THE LINEAR ARRAY MEASURED FIELD RADIATION (BOTH COMPUTED BY MEANS OF THE ALREADY EXISTING CODE "GENERATION.BEAM.PATTERN") I SHOULD BE ABLE, THANKS TO MY TOOL, TO ELABORATE THE SPARSE VECTOR AS THE ALREADY EXISTING CODE BAYESIAN COMPRESSIVE SAMPLING OUTPUT.

1 Test Case Description

- Linear Array of point sources
- Number of elements: N
- Observation angle number: U
- Observation angle: u
- Reference pattern: Dolph or Taylor
- Element Spacing: z
- Percentage of failures: F
- Actual error (complex):e_n, it is the actual complex sparse error vector
- Detected error (complex): $\hat{e_n}$, it is the complex sparse error vector detected by the BCS algortihm
- Actual error magnitude and phase:$\mid e_n \mid$, $arg(e_n)$
- Detected error magnitude and phase:$\mid \hat{e}_n \mid$, $arg(\hat{e}_n)$
- Expected Pattern (complex): $F_{\{exp\}}(u)$
- Measured Pattern (complex): $F_{\{mea\}}(u)$
- The reliability is computed thanks to the following formula: $\eta = \frac{\sum_{n=1}^{N} |e_n^{mea} - e_n^{exp}|^2}{\sum_{n=1}^{N} |w_n|^2} < 10^{-4}$,

where $w_n$is the expected pattern weight.

1.1 FIRST SIMULATION RESULTS

1.1.1 First Case

Test Case:

- Linear Array of point sources
- Reference pattern: Dolph
- Number of elements: 40
- Observation angle number: from 1 to $2 * N + 1$
- Element Spacing: $\lambda/2$
- $dB = -20$
- Percentage of failures: 5%

Reliability about all simulations:

U	η
36	$1.60 * 10^{-9}$
37	$3.88 * 10^{-10}$
38	17.78
39	21.40
40	0
41	0
42	0
43	0
44	0

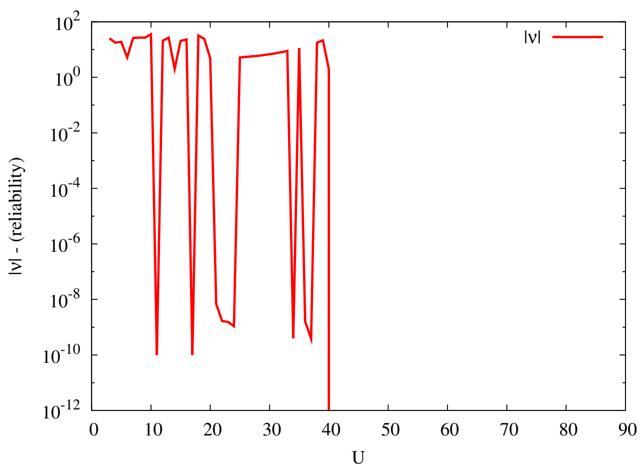

Fig.1 - Reliability

Results with $U = 41$:

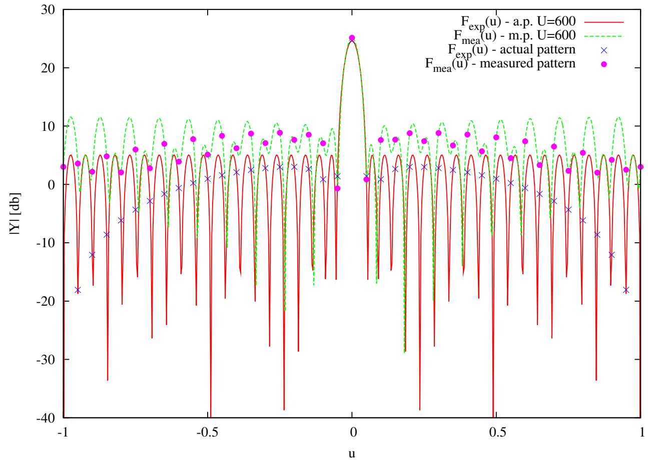

Fig.2 - Actual and measured patterns

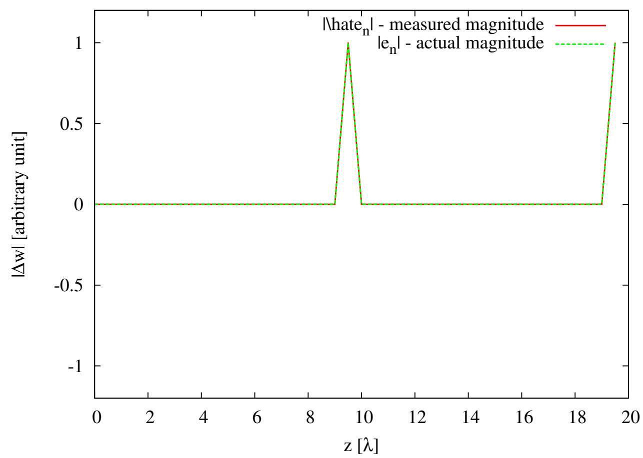

Fig.3 - Actual and measured magnitude

1.1.2 Second Case

Test Case:

- Linear Array of point sources
- Reference pattern: Dolph
- Number of elements: 40
- Observation angle number: from 1 to $2 * N + 1$
- Element Spacing: $\lambda/2$
- $dB = -30$
- Number of failures: 5%

Reliability about all simulations:

U	η
36	10.36
37	$9.79 * 10^{-9}$
38	$6.75 * 10^{-9}$
39	$9.97 * 10^{-9}$
40	6.97
41	$8.92 * 10^{-10}$
42	$8.92 * 10^{-10}$
43	$8.92 * 10^{-10}$
44	$8.92 * 10^{-10}$

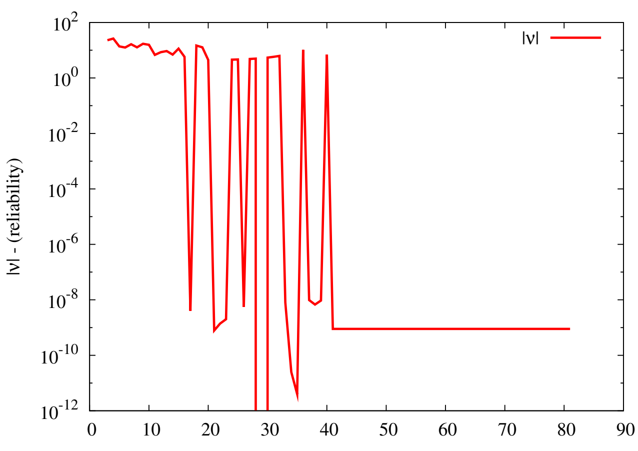

Fig.1 - Reliability

Results with $U = 41$:

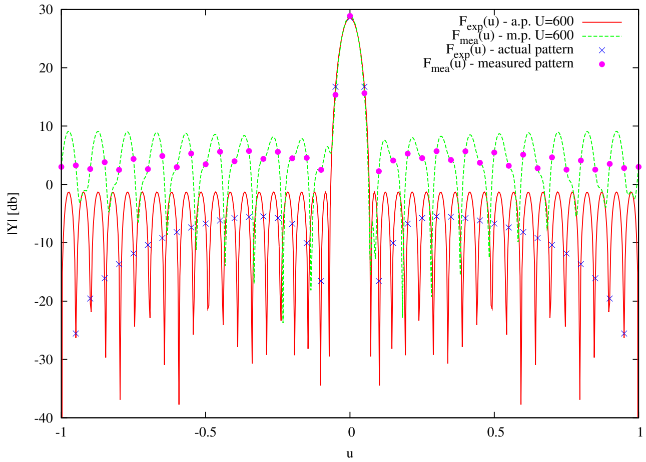

Fig.2 - Actual and measured patterns

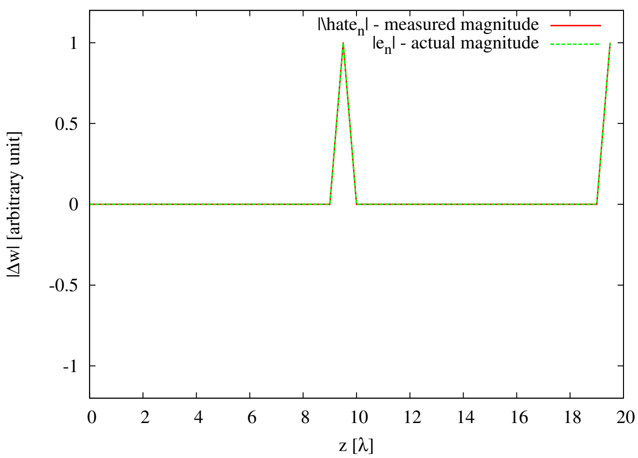

Fig.3 - Actual and measured magnitude

1.1.3 Third Case

Test Case:

- Linear Array of point sources
- Reference pattern: Dolph
- Number of elements: 40
- Observation angle number: from 1 to $2 * N + 1$
- Element Spacing: $\lambda/2$
- $dB = -40$
- Number of failures: 5%

Reliability about all simulations:

U	η
36	$8.10 * 10^{-11}$
37	$3.95 * 10^{-8}$
38	0
39	108.30
40	72.56
41	$1.60 * 10^{-8}$
42	$1.60 * 10^{-8}$
43	$1.60 * 10^{-8}$
44	$1.60 * 10^{-8}$
45	$1.76 * 10^{-8}$

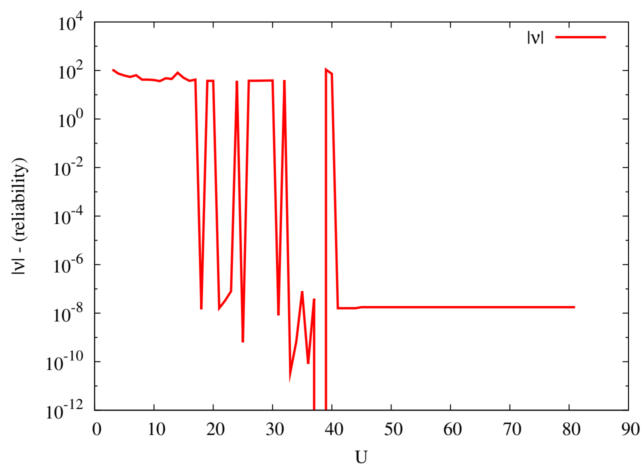

Fig.1 - Reliability

Results with $U = 41$:

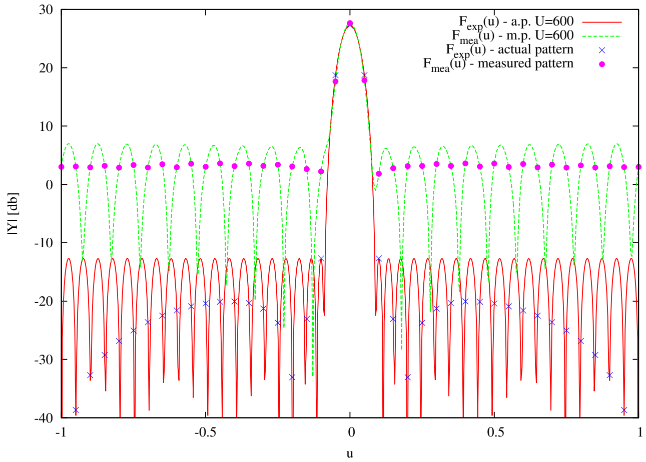

Fig.2 - Actual and measured patterns

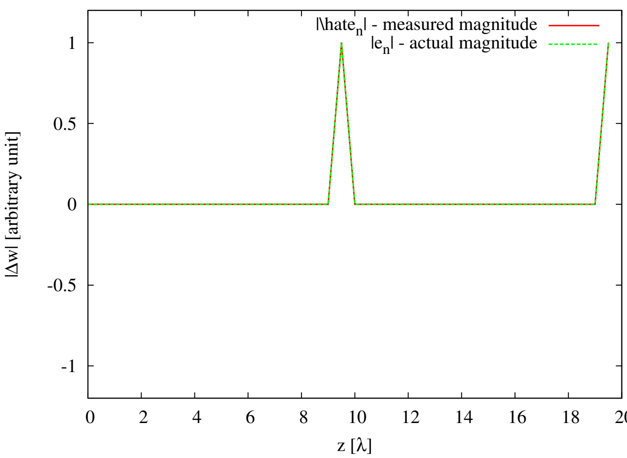

Fig.3 - Actual and measured magnitude

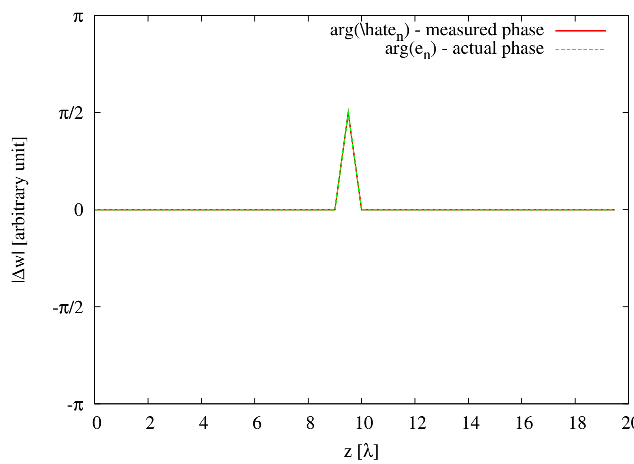

Fig.4 - Actual and measured phase

1.1.4 Fourth Case

Test Case:

- Linear Array of point sources
- Reference pattern: Taylor
- Number of elements: 40
- Observation angle number: from 1 to $2 * N + 1$
- Element Spacing: $\lambda/2$
- $dB = -20$
- Number of failures: 5%

Reliability about all simulations:

U	η
36	$7.84 * 10^{-10}$
37	$4.56 * 10^{-9}$
38	3.65
39	$1.16 * 10^{-9}$
40	3.13
41	$1.56 * 10^{-10}$
42	$1.56 * 10^{-10}$
43	$1.56 * 10^{-10}$
44	$1.56 * 10^{-10}$

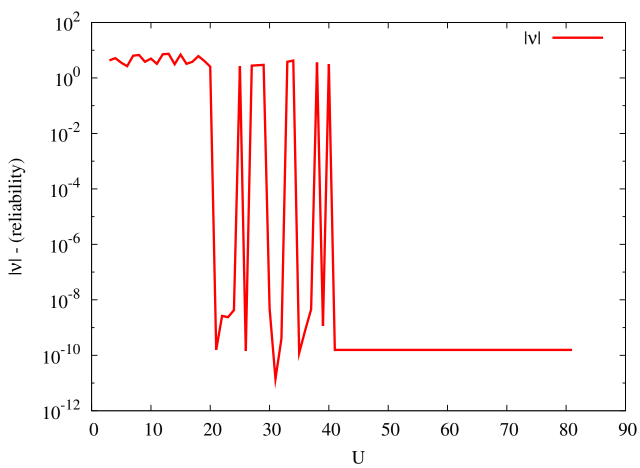

Fig.1 - Reliability

Results with $U = 41$:

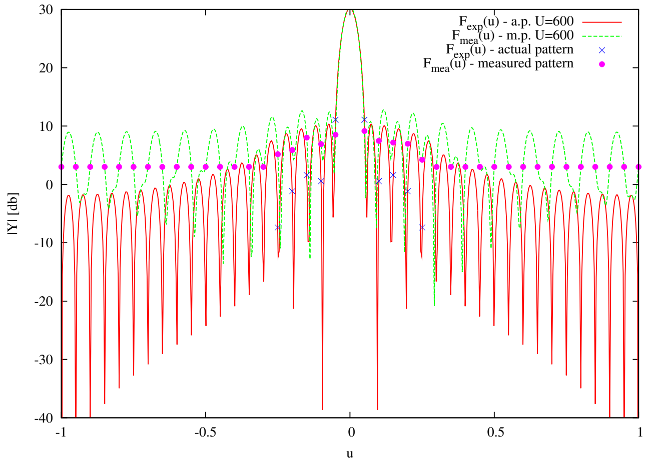

Fig.2 - Actual and measured patterns

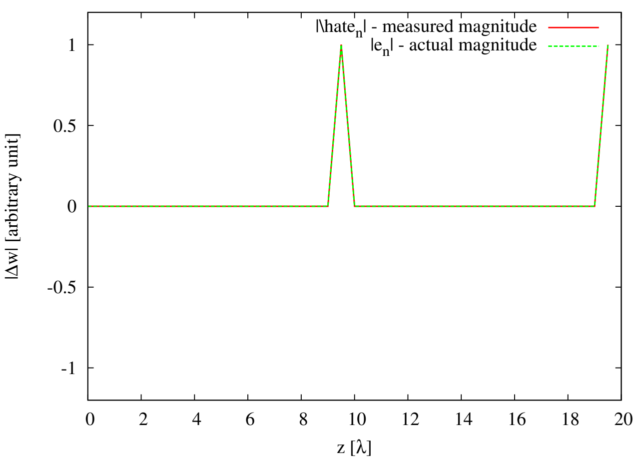

Fig.3 - Actual and measured magnitude

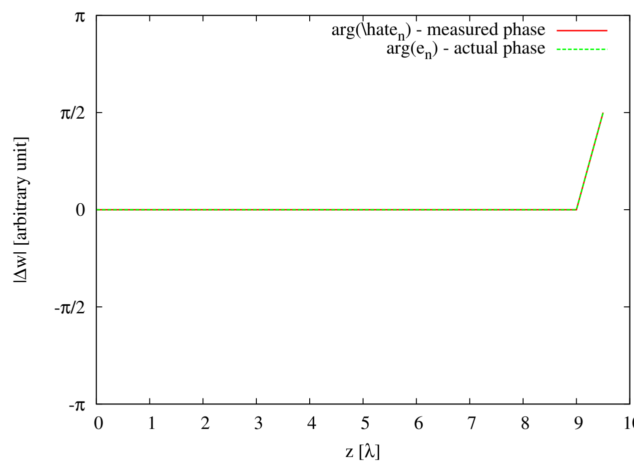

Fig.4 - Actual and measured phase

1.1.5 Fifth Case

Test Case:

- Linear Array of point sources
- Reference pattern: Taylor
- Number of elements: 40
- Observation angle number: from 1 to $2 * N + 1$
- Element Spacing: $\lambda/2$
- $dB = -30$
- Number of failures: 5%

Reliability about all simulations:

U	η
36	$2.72 * 10^{-9}$
37	$2.94 * 10^{-8}$
38	25.56
39	27.03
40	27.81
41	$1.70 * 10^{-8}$
42	$1.70 * 10^{-8}$
43	$1.70 * 10^{-8}$
44	$1.70 * 10^{-8}$

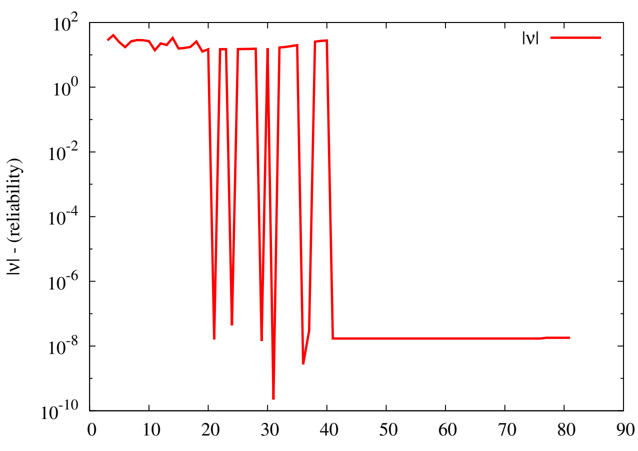

Fig.1 - Reliability

Results with $U = 41$:

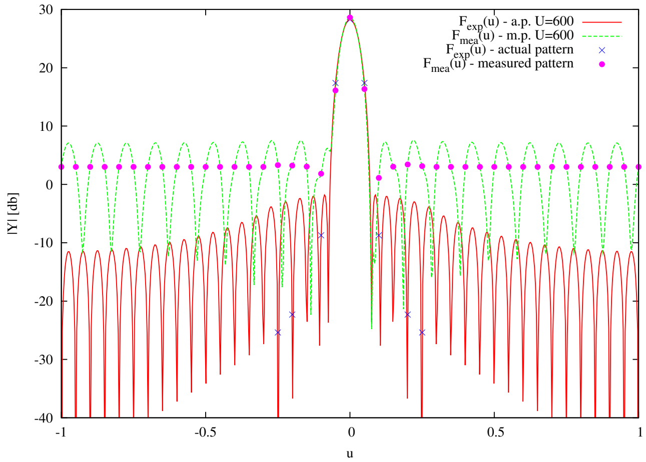

Fig.2 - Actual and measured patterns

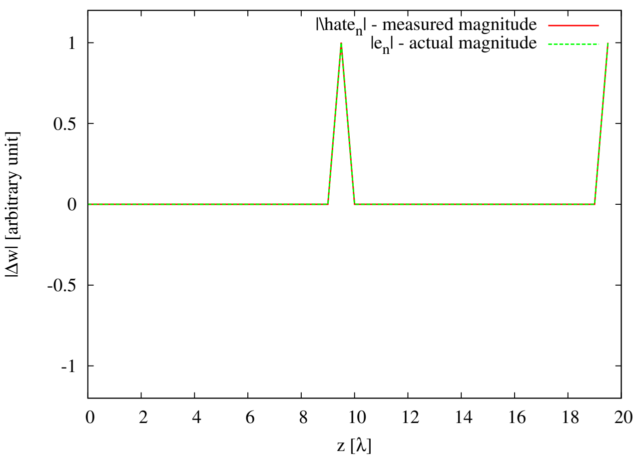

Fig.3 - Actual and measured magnitude

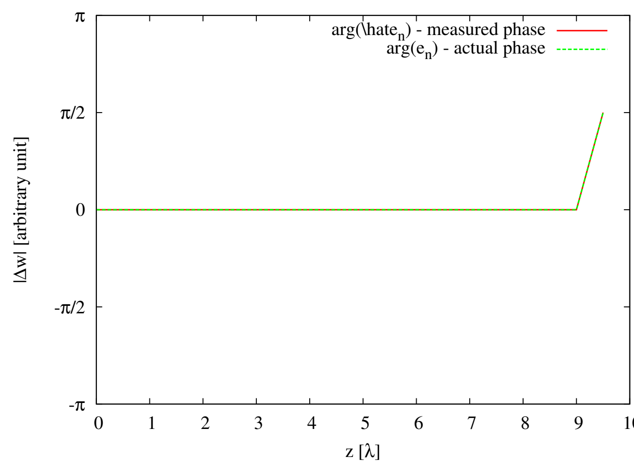

Fig.4 - Actual and measured phase

1.1.6 Sixth Case

Test Case:

- Linear Array of point sources
- Reference pattern: Taylor
- Number of elements: 40
- Observation angle number: from 1 to $2 * N + 1$
- Element Spacing: $\lambda/2$
- $dB = -40$
- Number of failures: 5%

Reliability about all simulations:

U	η
36	$5.72 * 10^{-8}$
37	$2.65 * 10^{-7}$
38	$2.38 * 10^{-7}$
39	$6.85 * 10^{-9}$
40	169.18
41	$6.17 * 10^{-8}$
42	$6.17 * 10^{-8}$
43	$6.17 * 10^{-8}$
44	$6.17 * 10^{-8}$

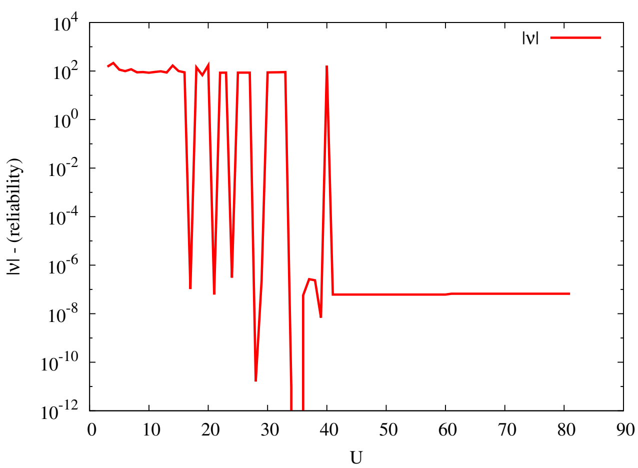

Fig.1 - Reliability

Results with $U = 41$:

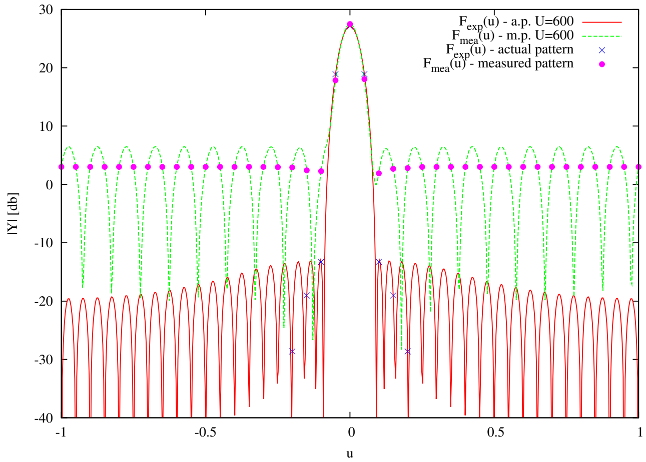

Fig.2 - Actual and measured patterns

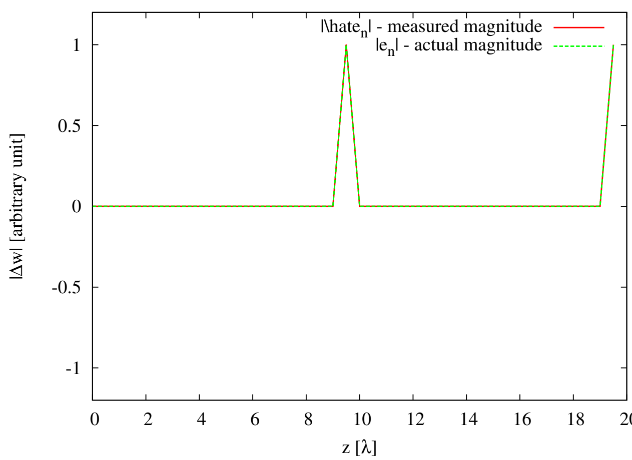

Fig.3 - Actual and measured magnitude

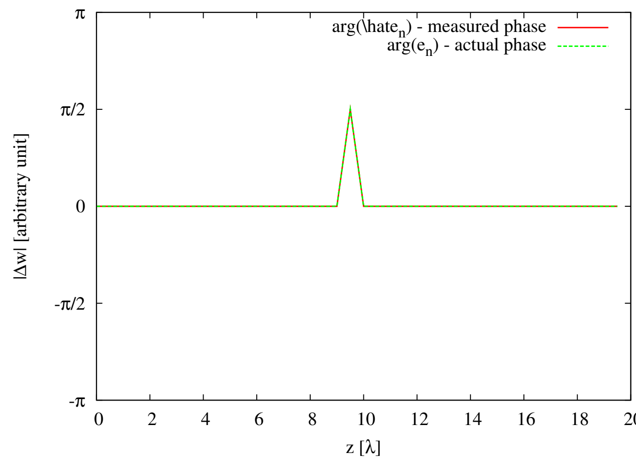

Fig.4 - Actual and measured phase

Observations

As we expected the failure detection works perfectly from a threshold up to infinite. In the case I have studied the threshold is always equal to $N+1$, where N is the number of array element. These results are valid for both Dolph and Taylor reference pattern. This threshold, if we think that the formula to it should be: $U_{opt} = 2 * K + 1$, is not satisfying in our test case.

1.2 SECOND SIMULATION RESULTS

1.2.1 First Case

Test Case:

- Linear Array of point sources
- Reference pattern: Dolph
- Number of elements: 20
- Observation angle number: 21
- Element Spacing: $\lambda/2$
- $dB = -30$
- Percentage of failures: $F \in [5, 10, 15, 20][\%]$

Reliability about all simulations:

$F[\%]$	η
5	0
10	$8.24 * 10^{-11}$
15	0
20	$1.12 * 10^{-10}$

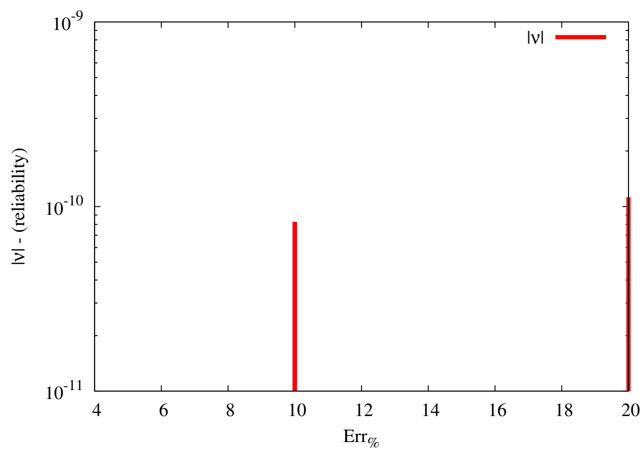

Fig.1 - Reliability

Results with $F = 5$:

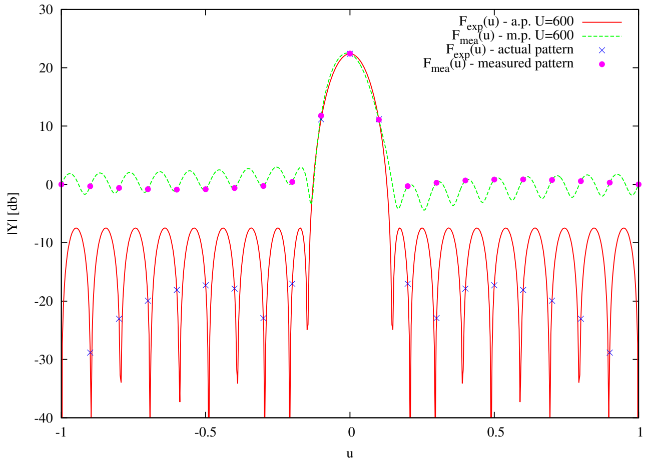

Fig.2 - Actual and measured patterns

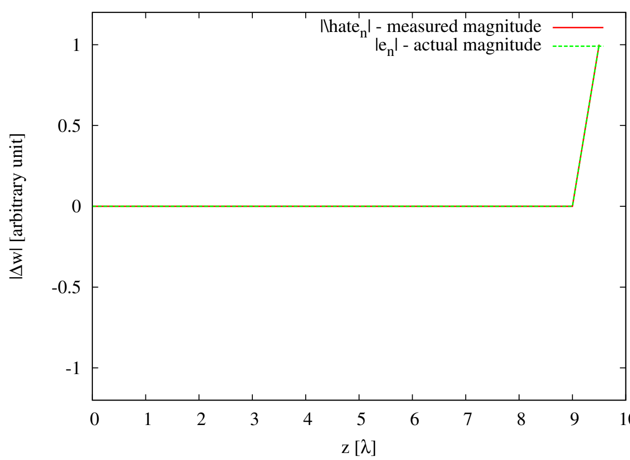

Fig.3 - Actual and measured magnitude

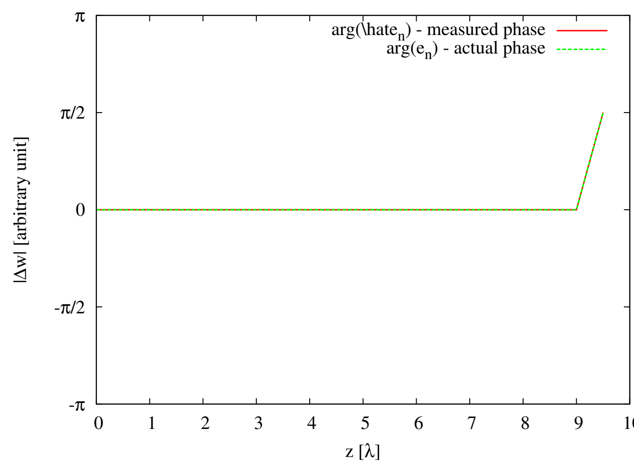

Fig.4 - Actual and measured phase

Results with $F = 10$**:**

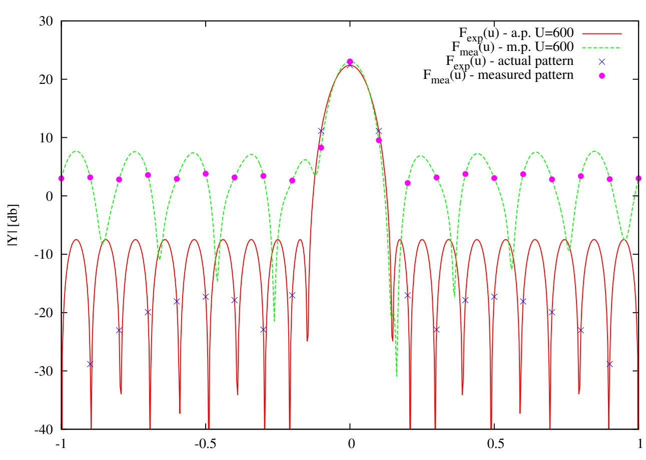

Fig.2 - Actual and measured patterns

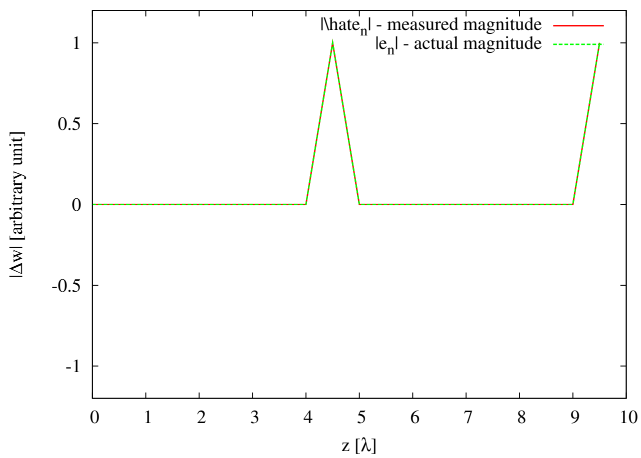

Fig.3 - Actual and measured magnitude

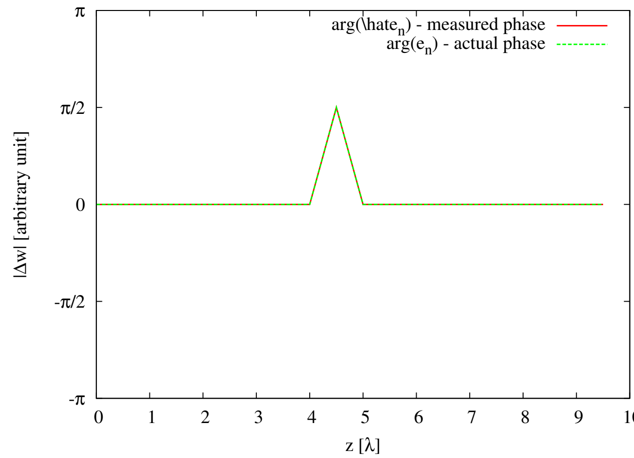

Fig.4 - Actual and measured phase

Results with $F = 15$:

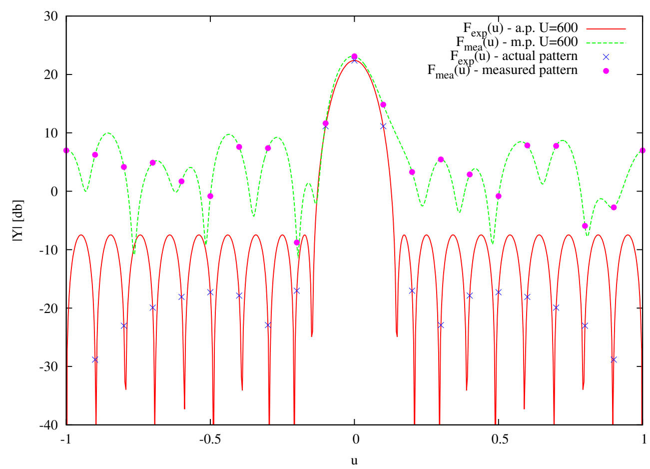

Fig.2 - Actual and measured patterns

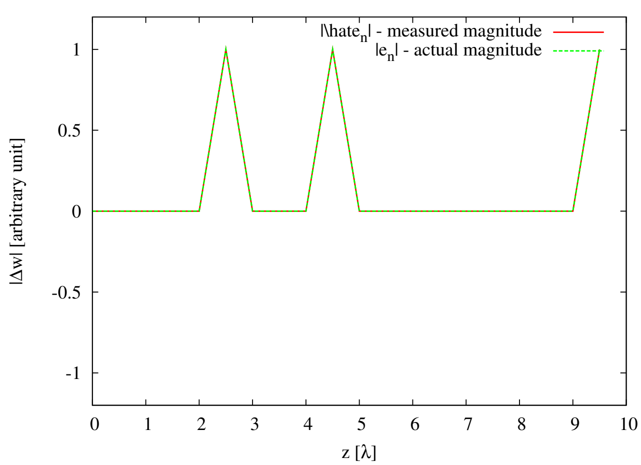

Fig.3 - Actual and measured magnitude

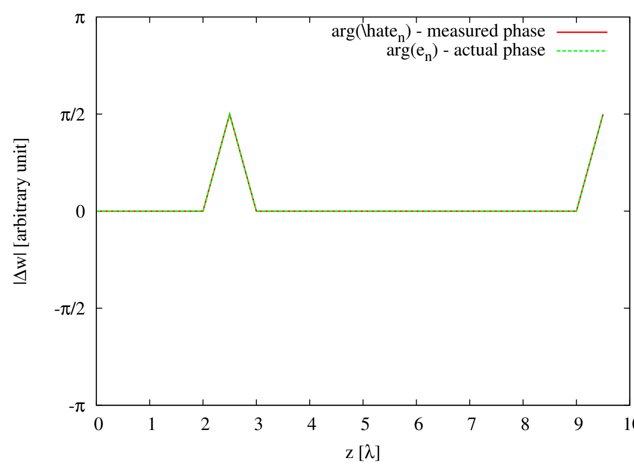

Fig.4 - Actual and measured phase

Results with $F = 20$:

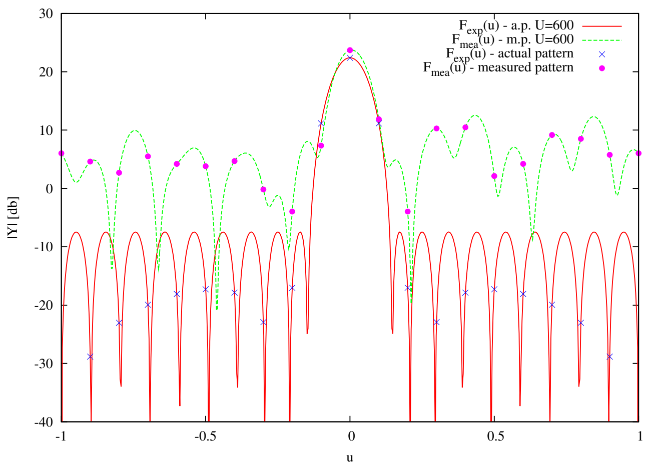

Fig.2 - Actual and measured patterns

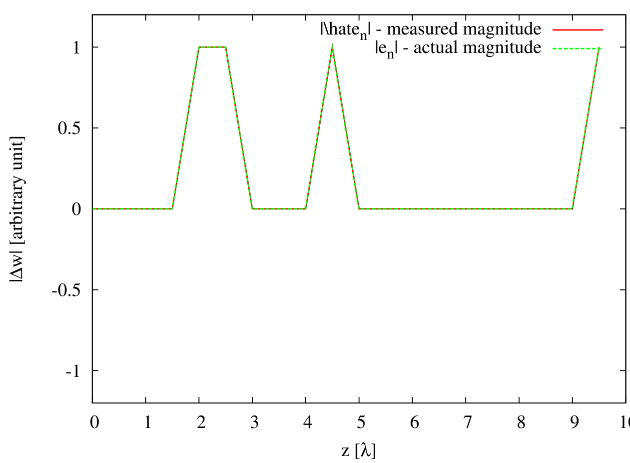

Fig.3 - Actual and measured magnitude

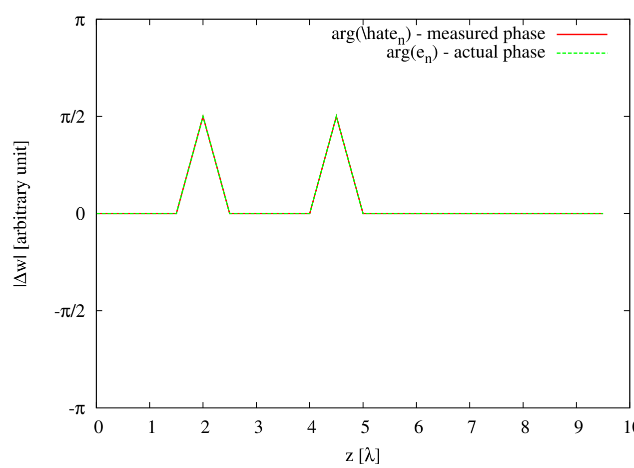

Fig.4 - Actual and measured phase

1.2.2 Second Case

Test Case:

- Linear Array of point sources
- Reference pattern: Dolph
- Number of elements: 30
- Observation angle number: 31
- Element Spacing: $\lambda/2$
- $dB = -30$
- Percentage of failures: $F \in [4, 7, 10, 14, 17, 20][\%]$

Reliability about all simulations:

$F[\%]$	η
4	0
7	$9.00 * 10^{-12}$
10	0
14	$1.50 * 10^{-9}$
17	$1.69 * 10^{-9}$
20	$2.66 * 10^{-9}$

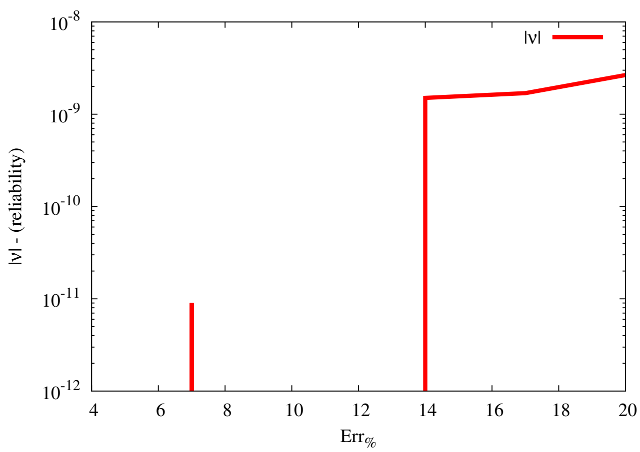

Fig.1 - Reliability

Results with $F = 4$:

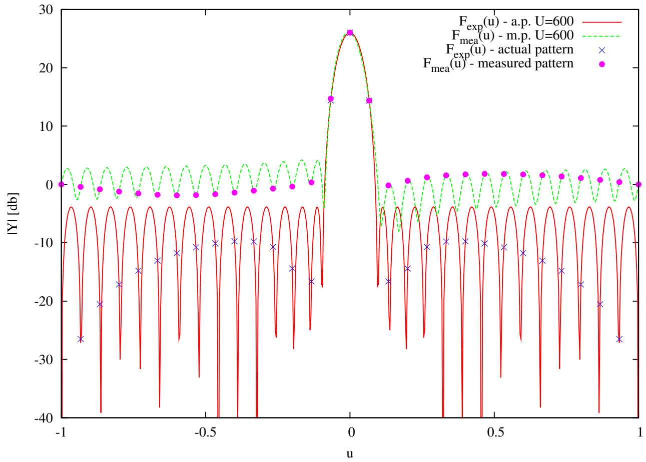

Fig.2 - Actual and measured patterns

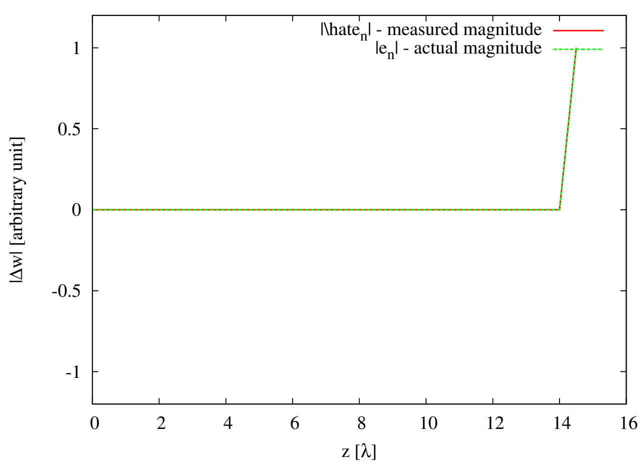

Fig.3 - Actual and measured magnitude

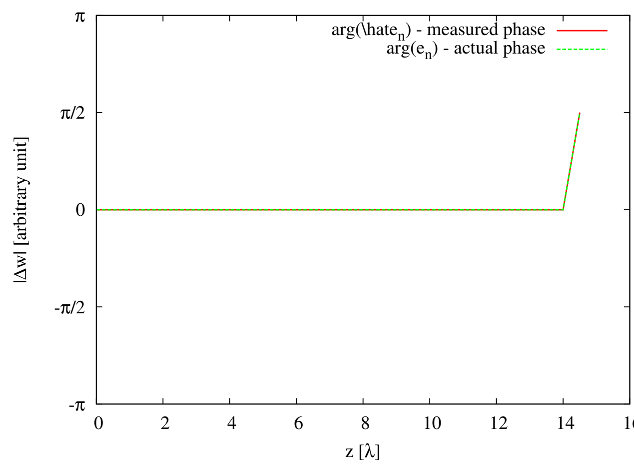

Fig.4 - Actual and measured phase

Results with $F = 7$:

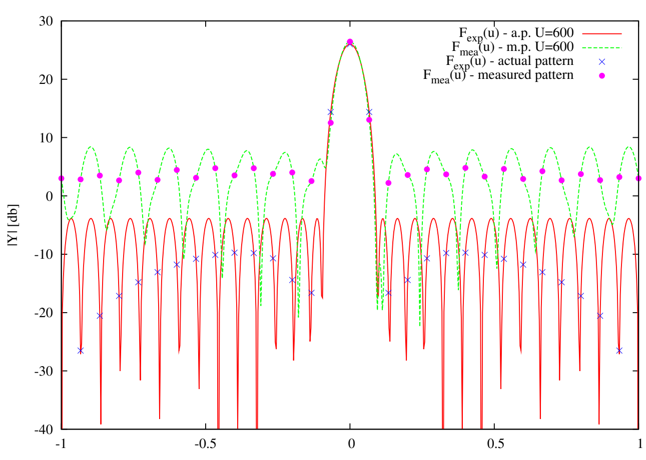

Fig.2 - Actual and measured patterns

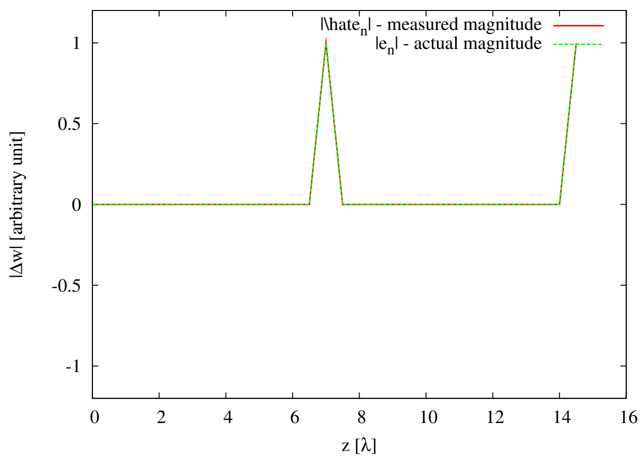

Fig.3 - Actual and measured magnitude

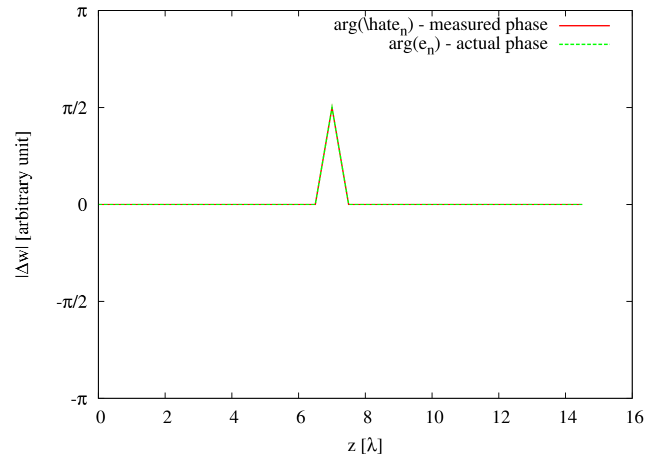

Fig.4 - Actual and measured phase

Results with $F = 10$:

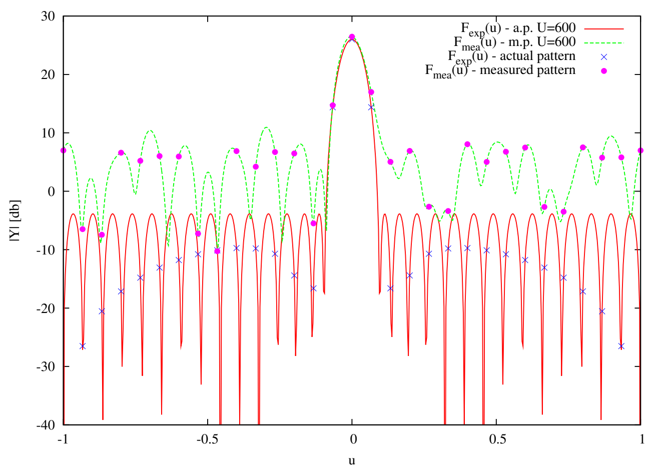

Fig.2 - Actual and measured patterns

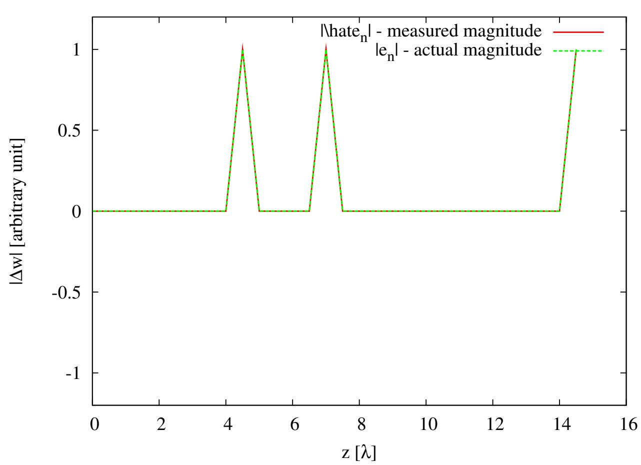

Fig.3 - Actual and measured magnitude

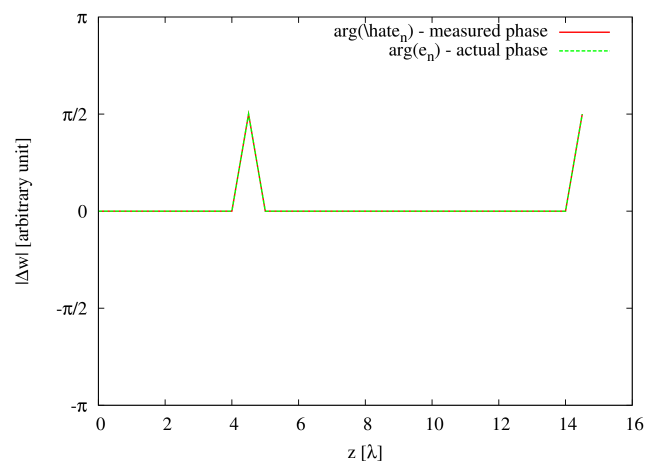

Fig.4 - Actual and measured phase

Results with $F = 14$:

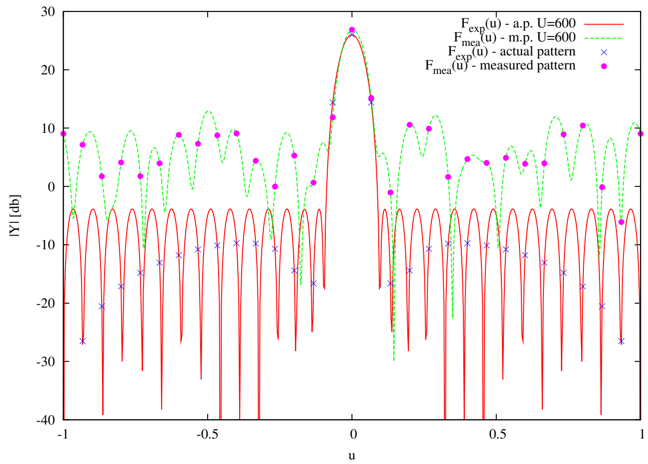

Fig.2 - Actual and measured patterns

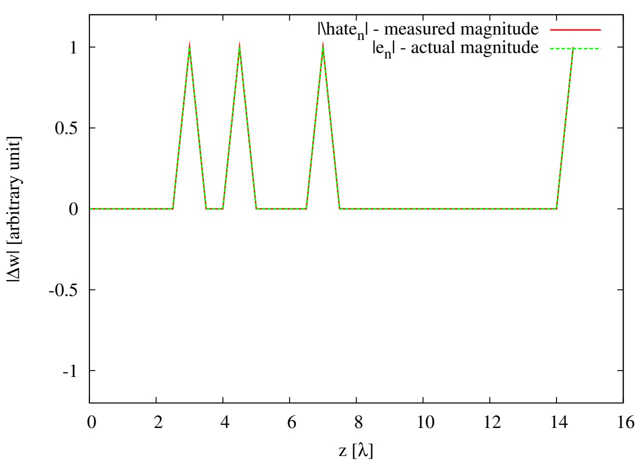

Fig.3 - Actual and measured magnitude

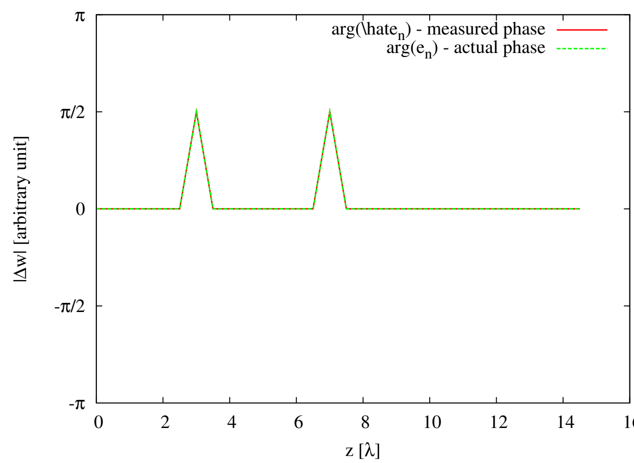

Fig.4 - Actual and measured phase

Results with $F = 17$:

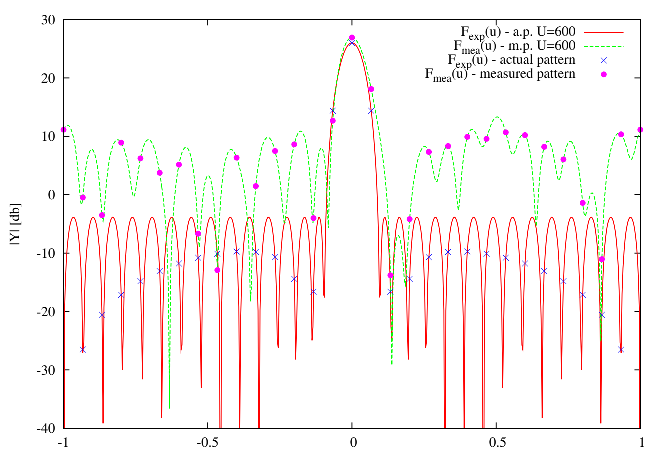

Fig.2 - Actual and measured patterns

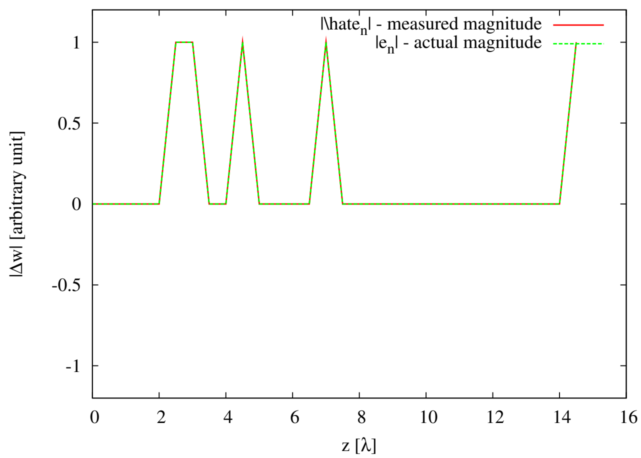

Fig.3 - Actual and measured magnitude

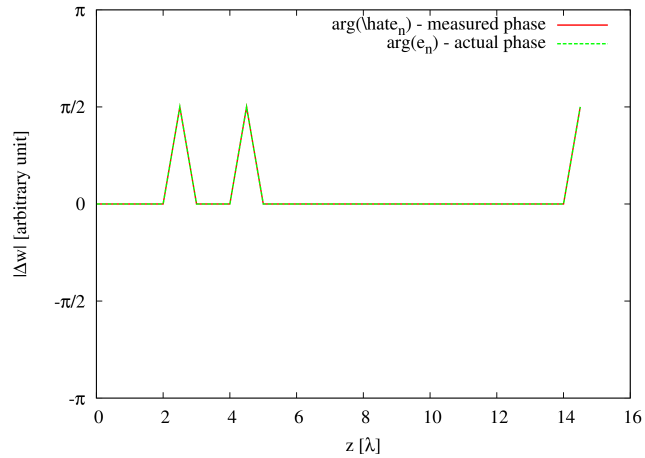

Fig.4 - Actual and measured phase

Results with $F = 20$:

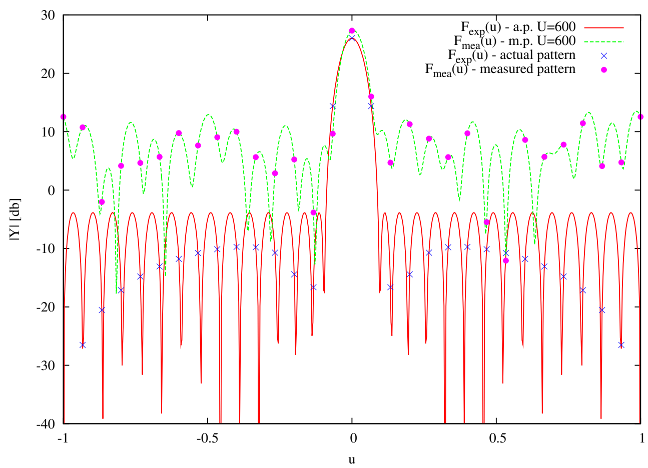

Fig.2 - Actual and measured patterns

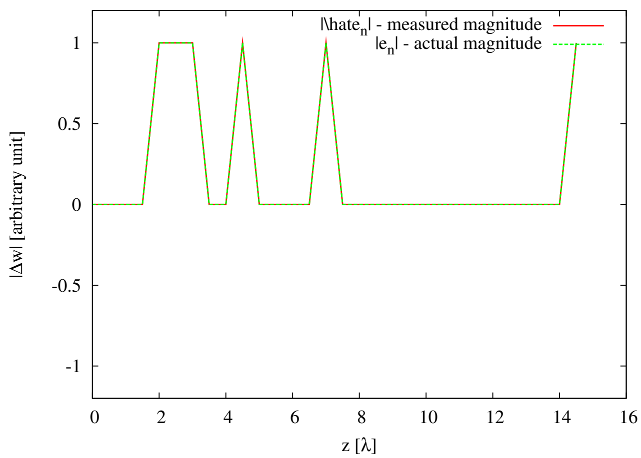

Fig.3 - Actual and measured magnitude

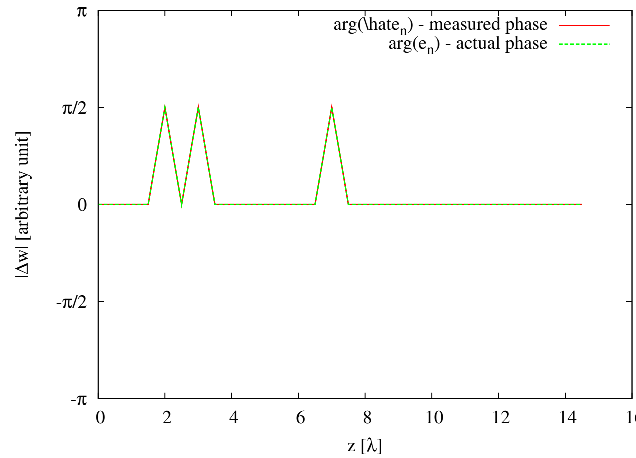

Fig.4 - Actual and measured phase

1.2.3 Third Case

Test Case:

- Linear Array of point sources
- Reference pattern: Dolph
- Number of elements: 40
- Observation angle number: 41
- Element Spacing: $\lambda/2$
- $dB = -30$
- Percentage of failures: $F \in [3, 5, 8, 10, 13, 15, 18, 20][\%]$

Reliability about all simulations:

$F[\%]$	η
3	0
5	$8.92 * 10^{-10}$
8	0
10	$3.93 * 10^{-9}$
13	$3.72 * 10^{-9}$
15	$7.58 * 10^{-9}$
18	$5.91 * 10^{-9}$
20	$1.57 * 10^{-8}$

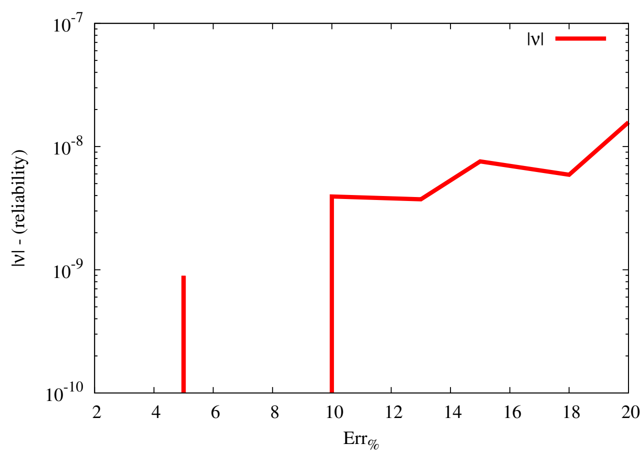

Fig.1 - Reliability

Results with $F = 3$:

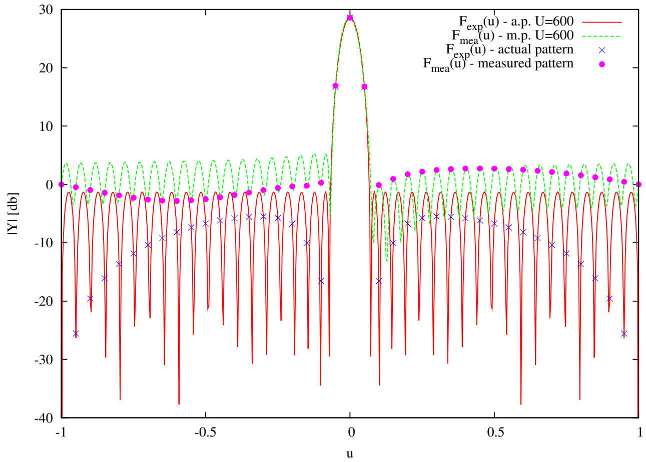

Fig.2 - Actual and measured patterns

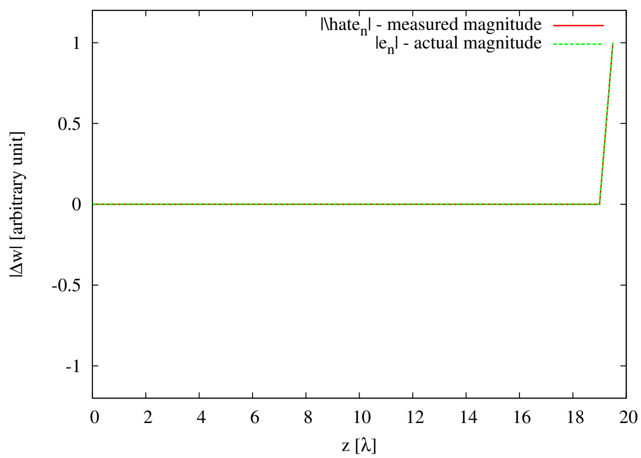

Fig.3 - Actual and measured magnitude

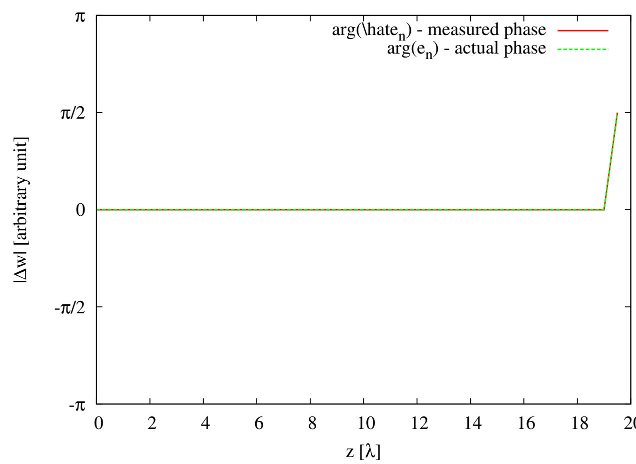

Fig.4 - Actual and measured phase

Results with $F = 5$:

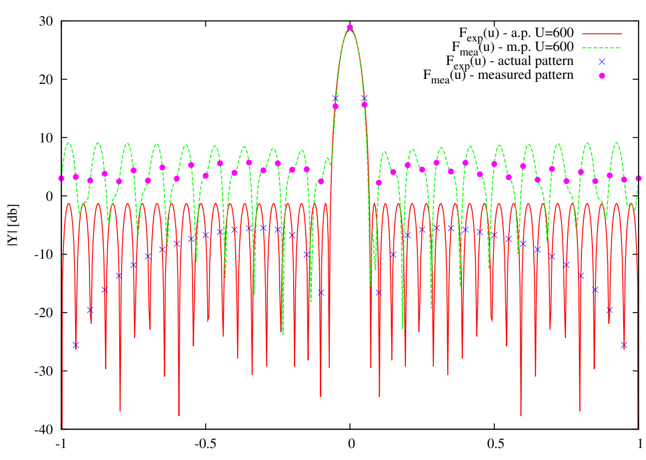

Fig.2 - Actual and measured patterns

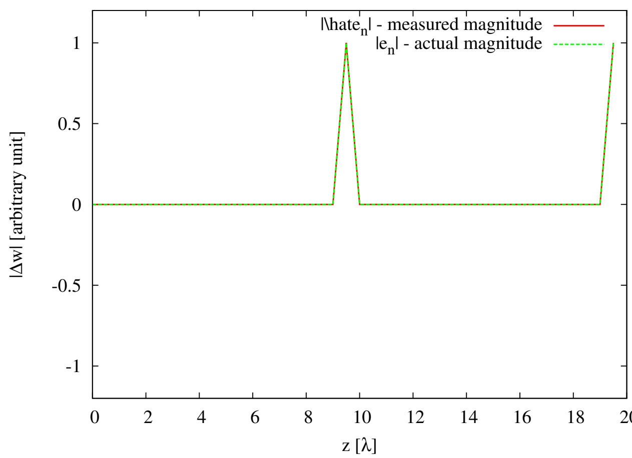

Fig.3 - Actual and measured magnitude

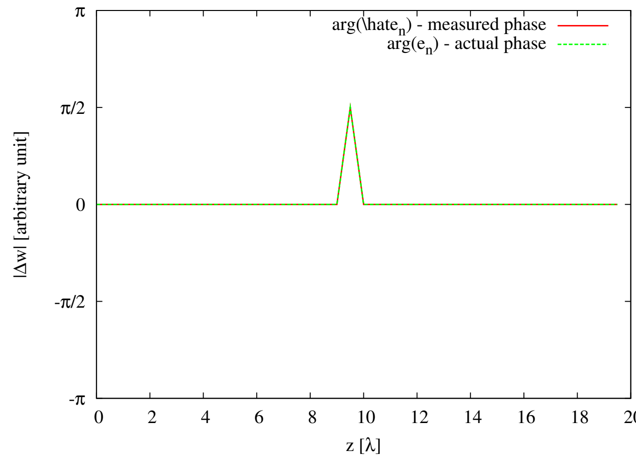

Fig.4 - Actual and measured phase

Results with $F = 8$:

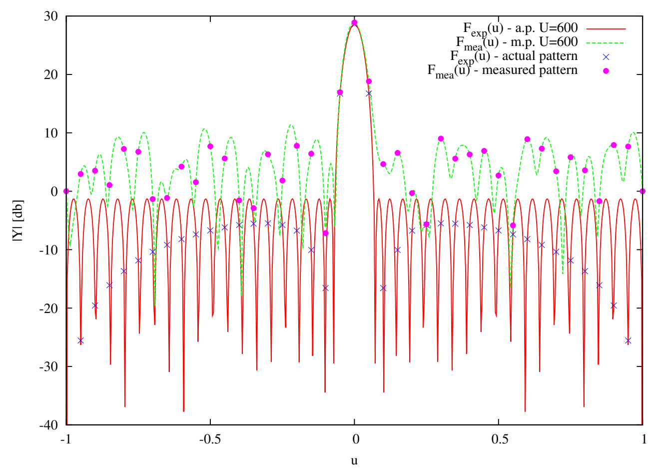

Fig.2 - Actual and measured patterns

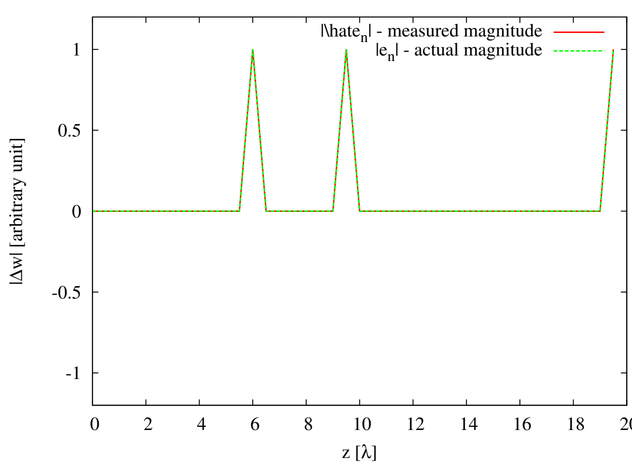

Fig.3 - Actual and measured magnitude

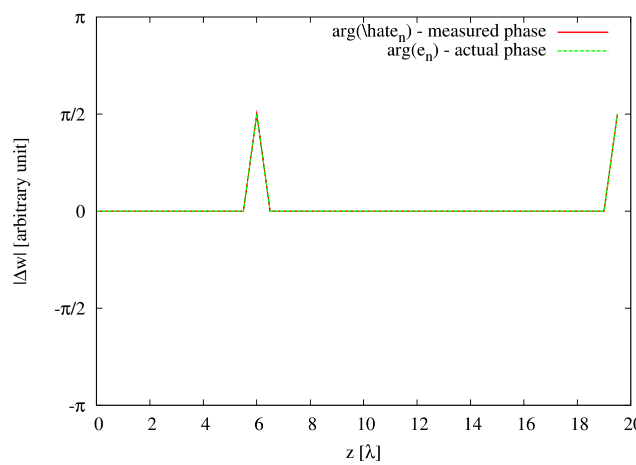

Fig.4 - Actual and measured phase

Results with $F = 10$:

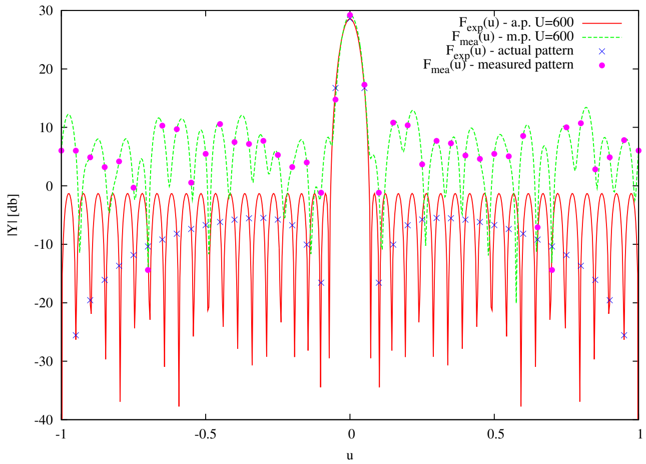

Fig.2 - Actual and measured patterns

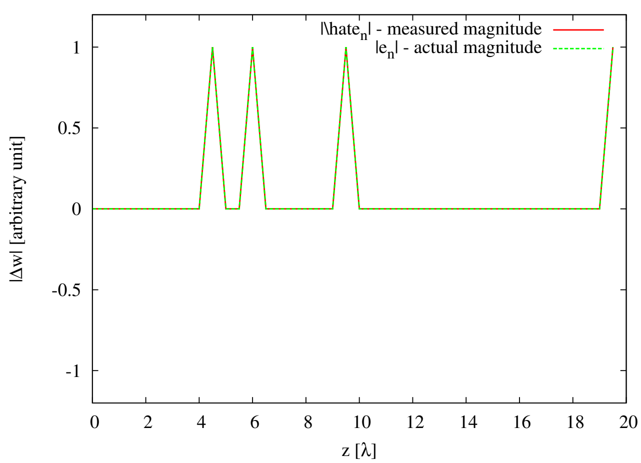

Fig.3 - Actual and measured magnitude

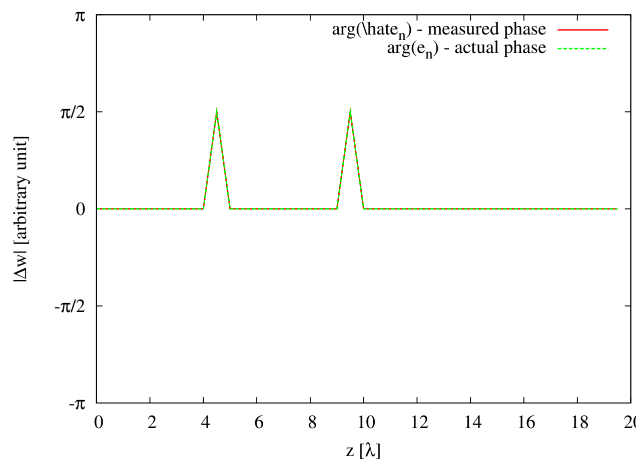

Fig.4 - Actual and measured phase

Results with $F = 13$:

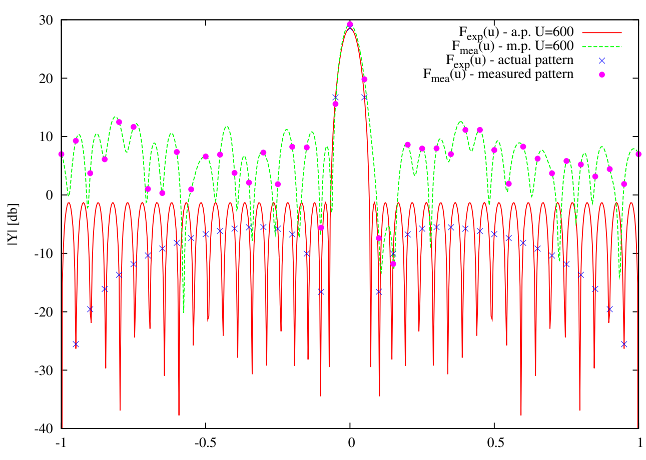

Fig.2 - Actual and measured patterns

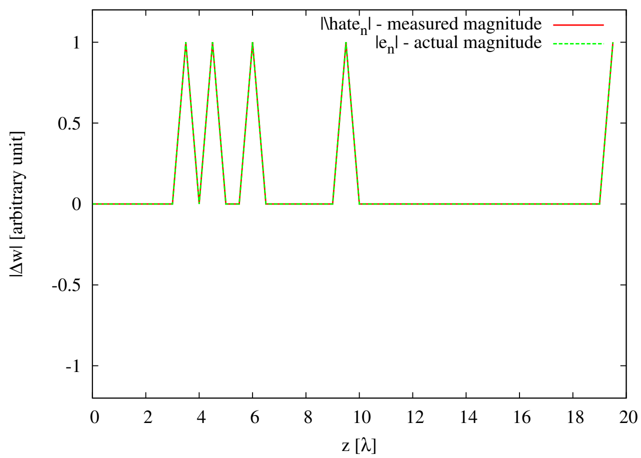

Fig.3 - Actual and measured magnitude

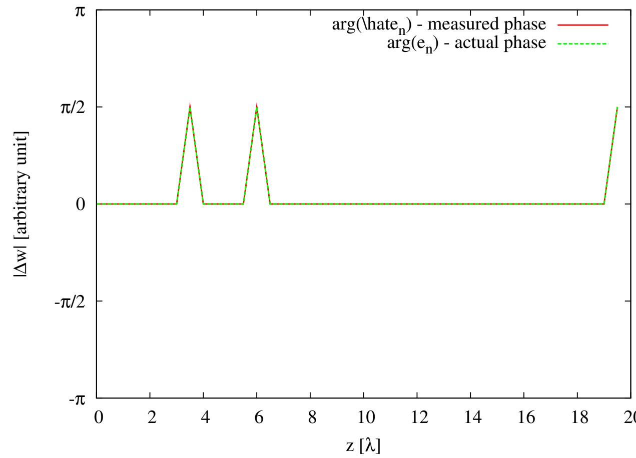

Fig.4 - Actual and measured phase

Results with $F = 15$:

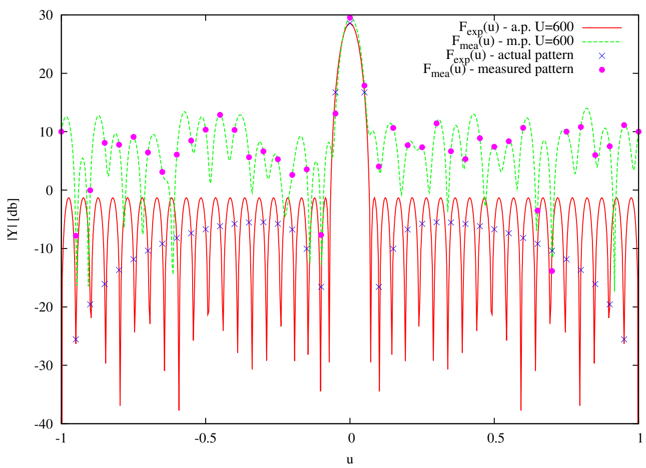

Fig.2 - Actual and measured patterns

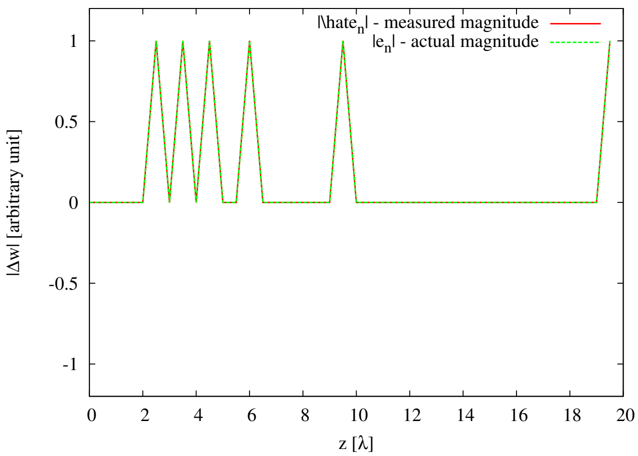

Fig.3 - Actual and measured magnitude

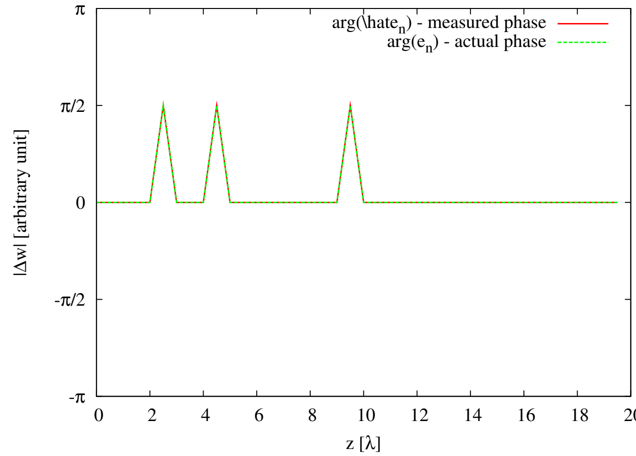

Fig.4 - Actual and measured phase

Results with $F = 18$:

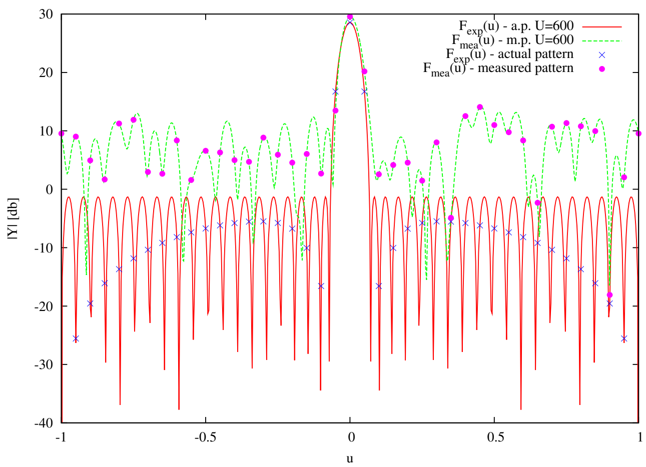

Fig.2 - Actual and measured patterns

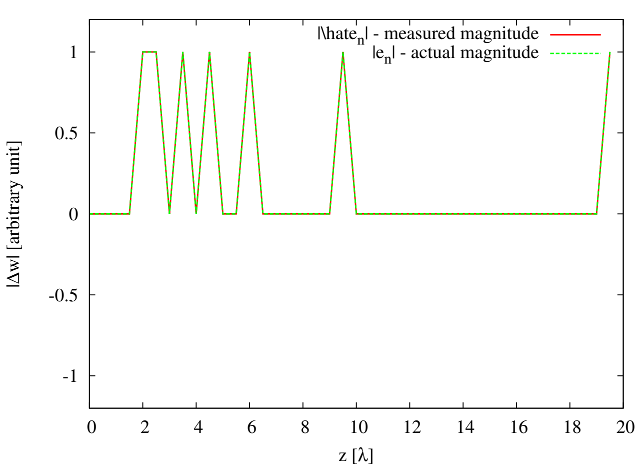

Fig.3 - Actual and measured magnitude

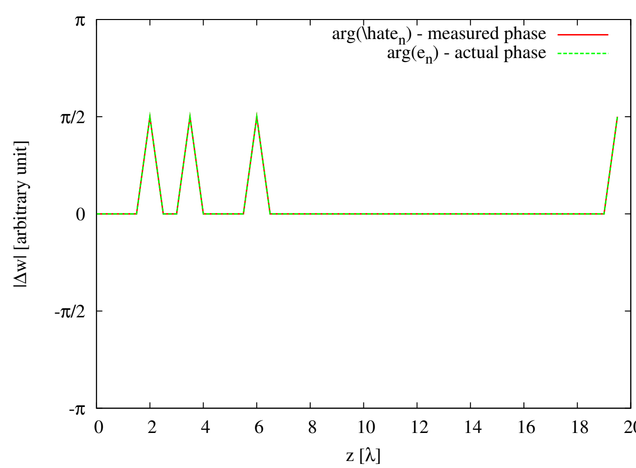

Fig.4 - Actual and measured phase

Results with $F = 20$:

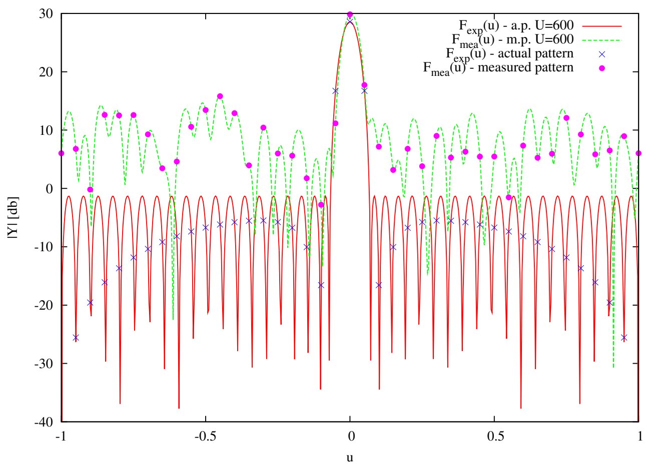

Fig.2 - Actual and measured patterns

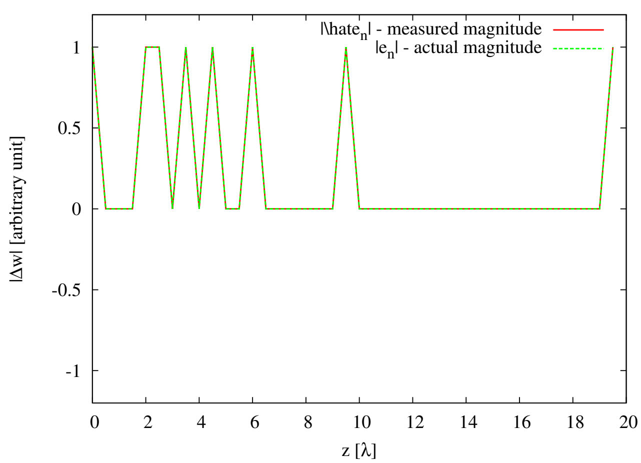

Fig.3 - Actual and measured magnitude

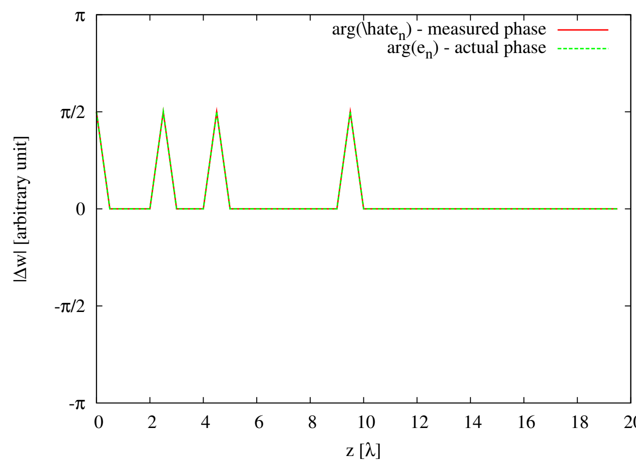

Fig.4 - Actual and measured phase

1.2.4 Fourth Case

Test Case:

- Linear Array of point sources
- Reference pattern: Taylor
- Number of elements: 20
- Observation angle number: 21
- Element Spacing: $\lambda/2$
- $dB = -30$
- Percentage of failures: $F \in [5, 10, 15, 20][\%]$

Reliability about all simulations:

$F[\%]$	η
5	0
10	$4.45 * 10^{-9}$
15	0
20	$5.91 * 10^{-9}$

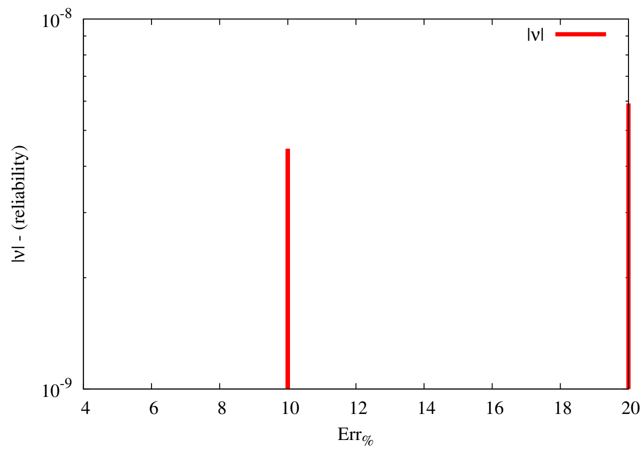

Fig.1 - Reliability

Results with $F = 5$:

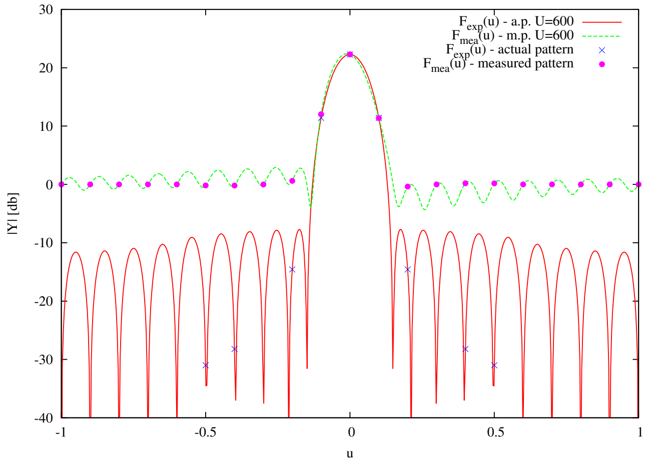

Fig.2 - Actual and measured patterns

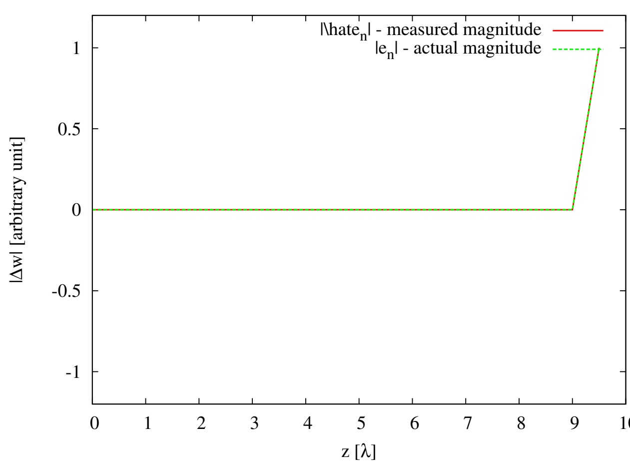

Fig.3 - Actual and measured magnitude

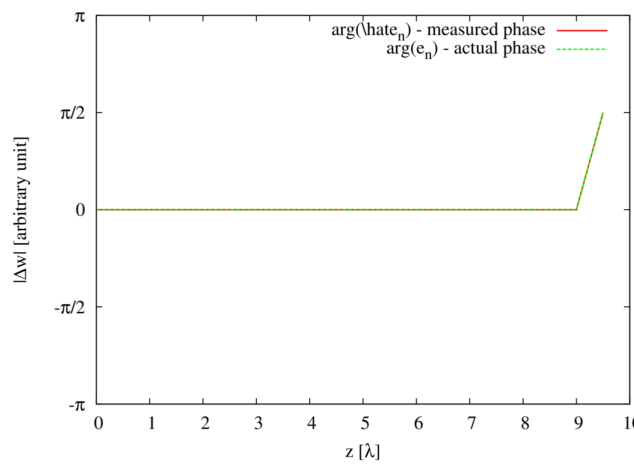

Fig.4 - Actual and measured phase

Results with $F = 10$:

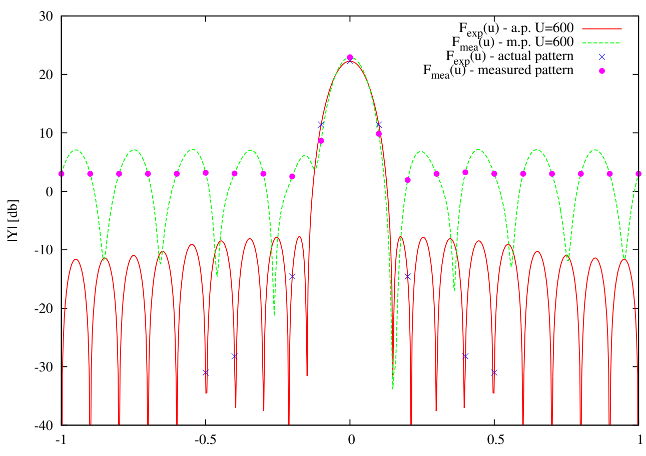

Fig.2 - Actual and measured patterns

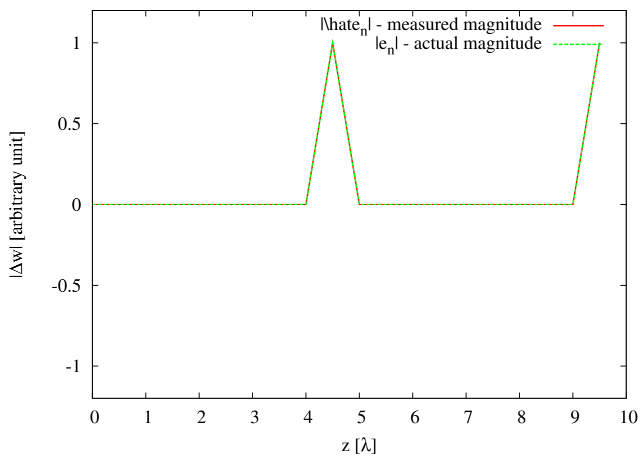

Fig.3 - Actual and measured magnitude

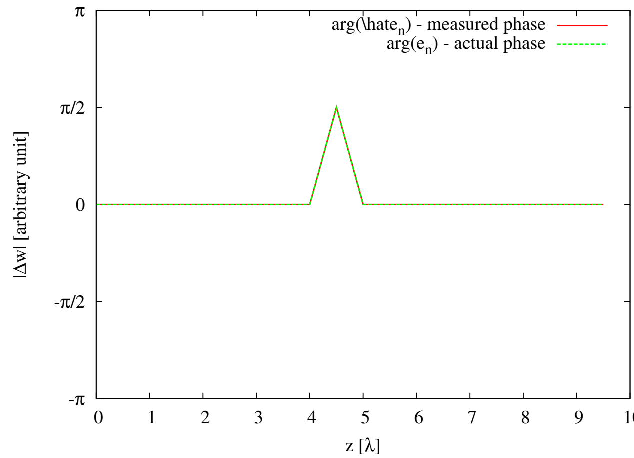

Fig.4 - Actual and measured phase

Results with $F = 15$:

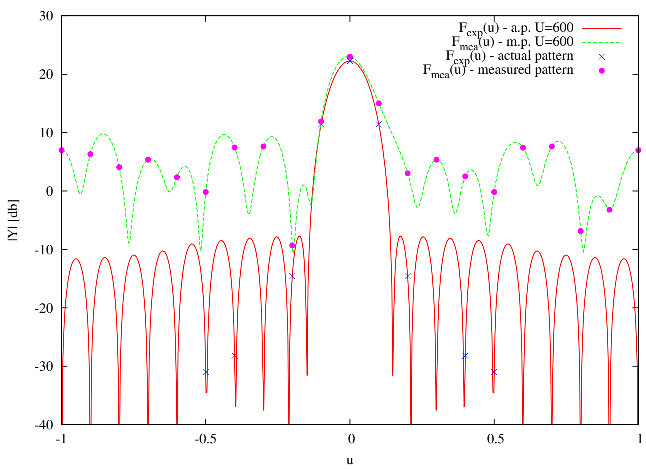

Fig.2 - Actual and measured patterns

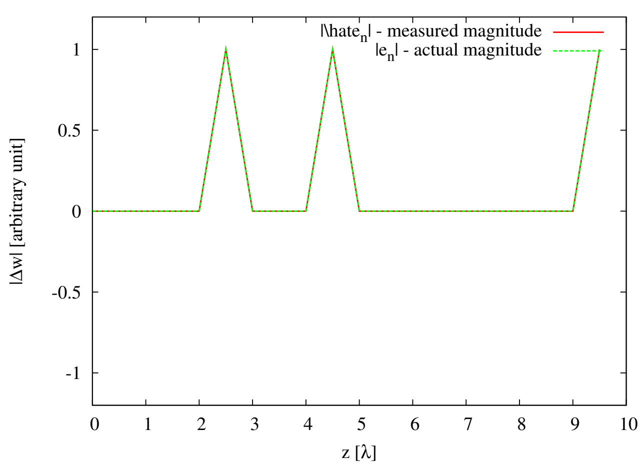

Fig.3 - Actual and measured magnitude

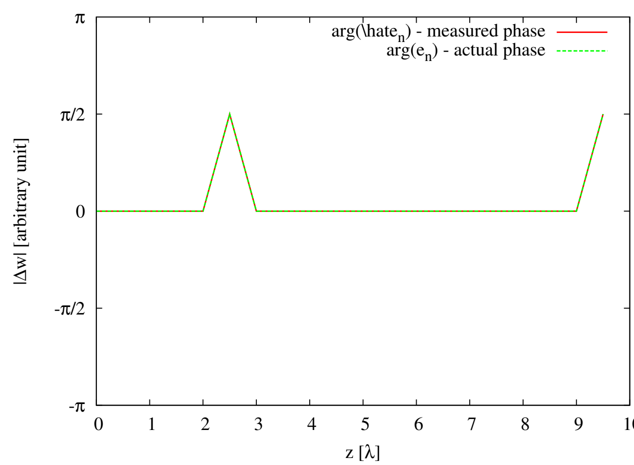

Fig.4 - Actual and measured phase

Results with $F = 20$:

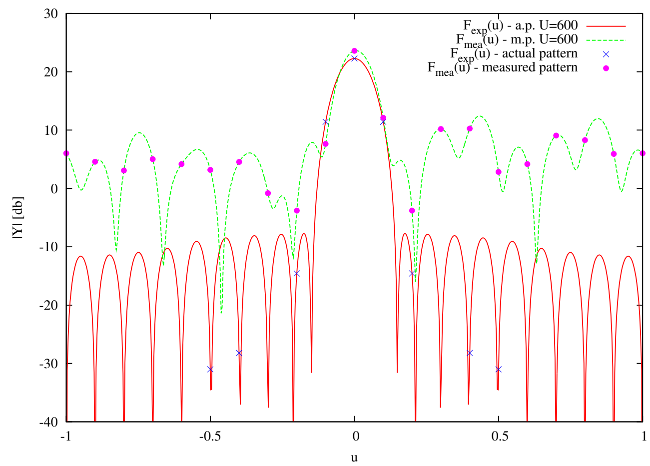

Fig.2 - Actual and measured patterns

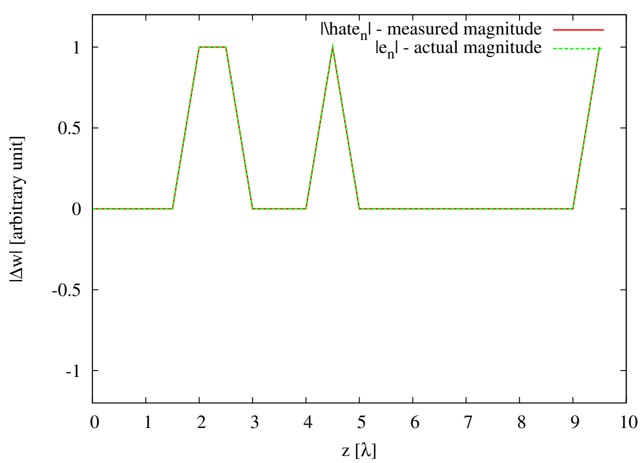

Fig.3 - Actual and measured magnitude

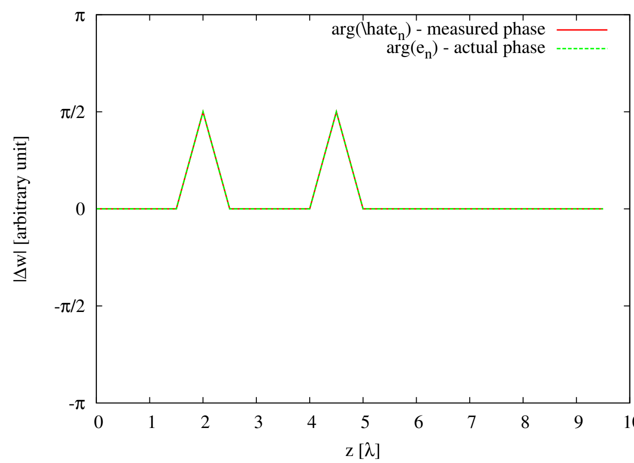

Fig.4 - Actual and measured phase

1.2.5 Fifth Case

Test Case:

- Linear Array of point sources
- Reference pattern: Taylor
- Number of elements: 30
- Observation angle number: 31
- Element Spacing: $\lambda/2$
- $dB = -30$
- Percentage of failures: $F \in [4, 7, 10, 14, 17, 20][\%]$

Reliability about all simulations:

$F[\%]$	η
4	0
7	$1.69 * 10^{-8}$
10	0
14	$1.66 * 10^{-8}$
17	$6.44 * 10^{-10}$
20	$2.32 * 10^{-8}$

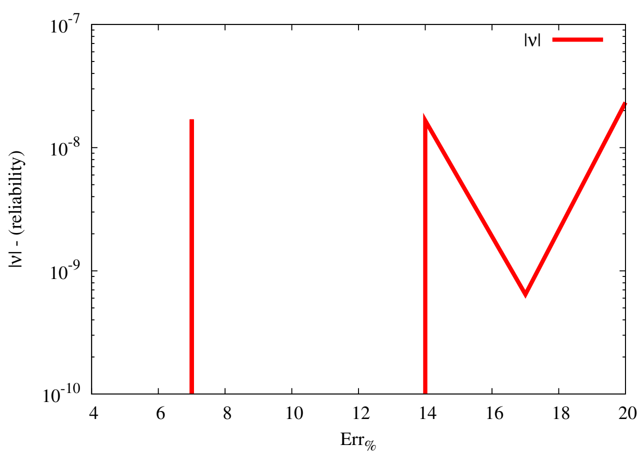

Fig.1 - Reliability

Results with $F = 4$:

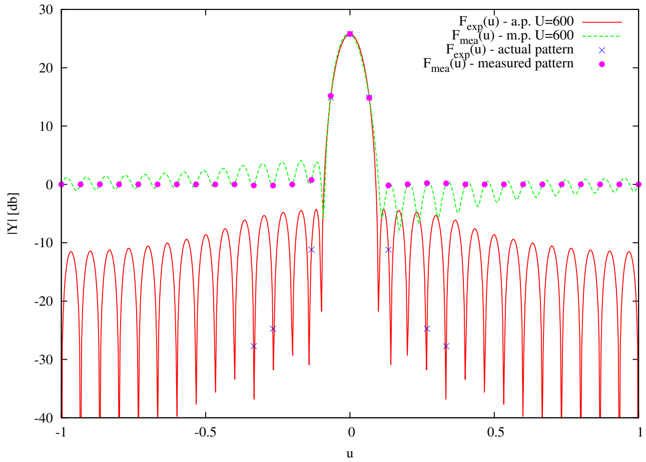

Fig.2 - Actual and measured patterns

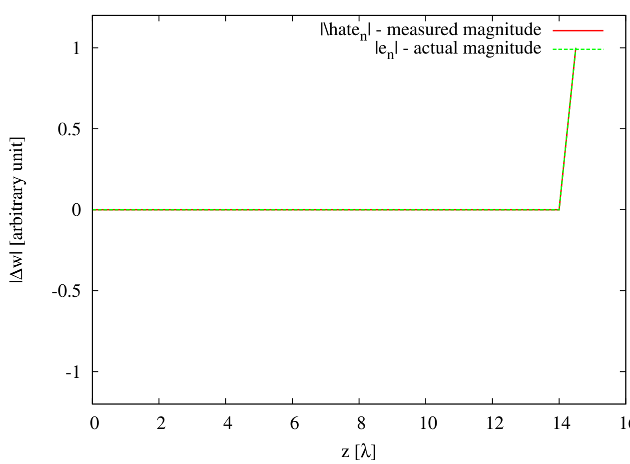

Fig.3 - Actual and measured magnitude

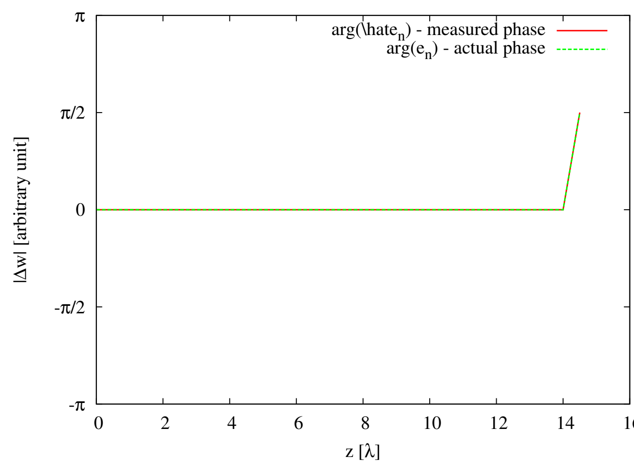

Fig.4 - Actual and measured phase

Results with $F = 7$:

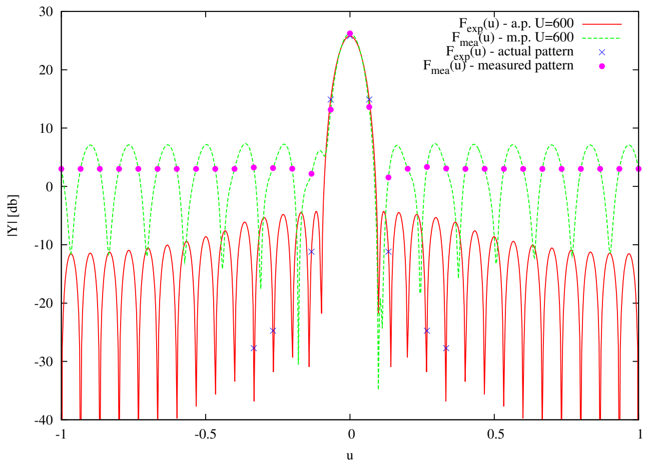

Fig.2 - Actual and measured patterns

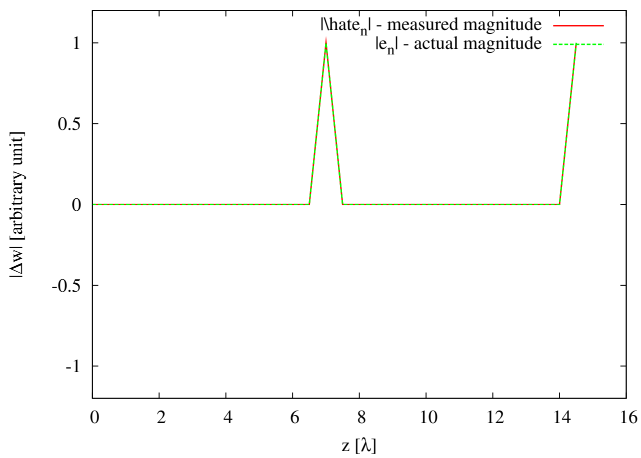

Fig.3 - Actual and measured magnitude

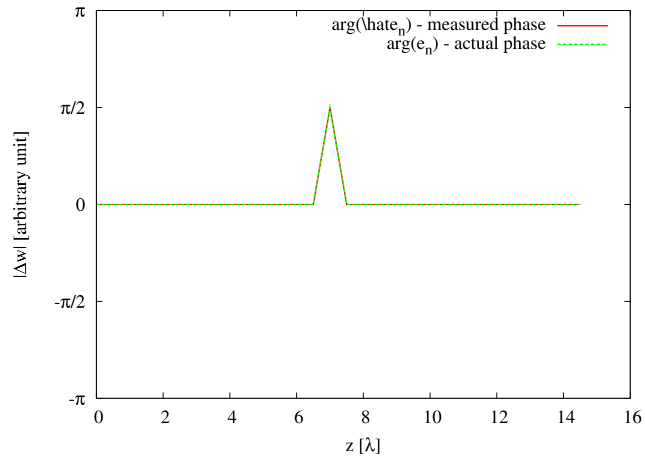

Fig.4 - Actual and measured phase

Results with $F = 10$:

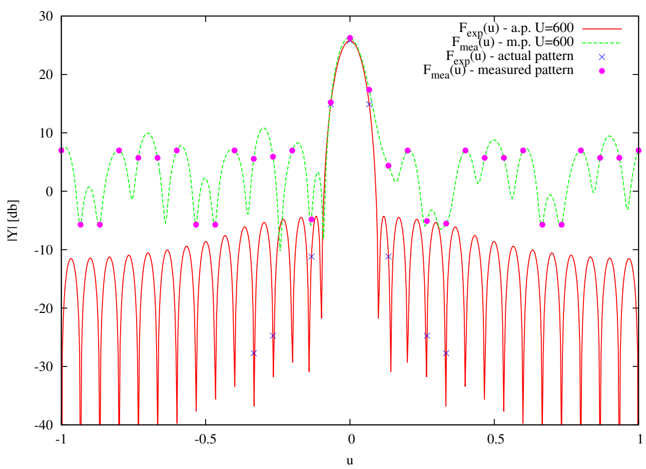

Fig.2 - Actual and measured patterns

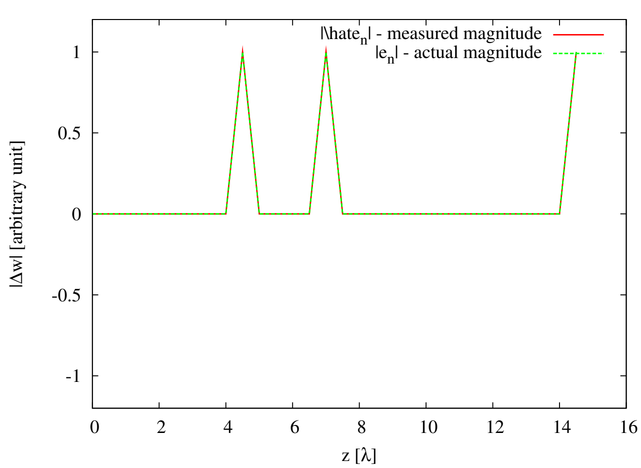

Fig.3 - Actual and measured magnitude

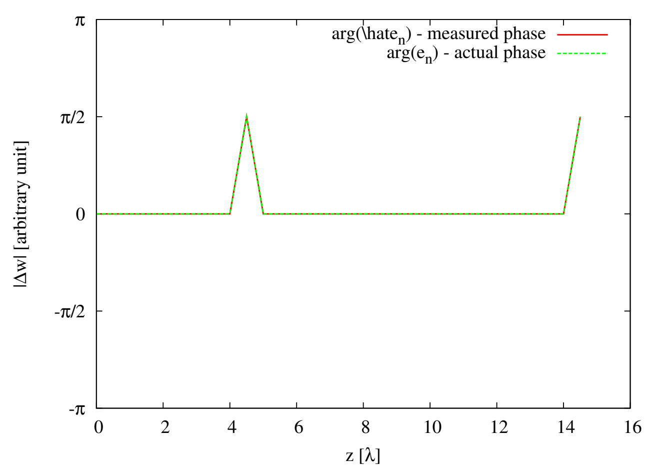

Fig.4 - Actual and measured phase

Results with $F = 14$:

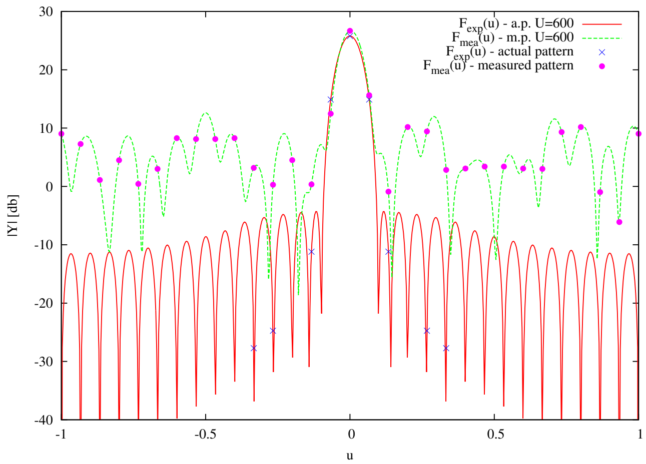

Fig.2 - Actual and measured patterns

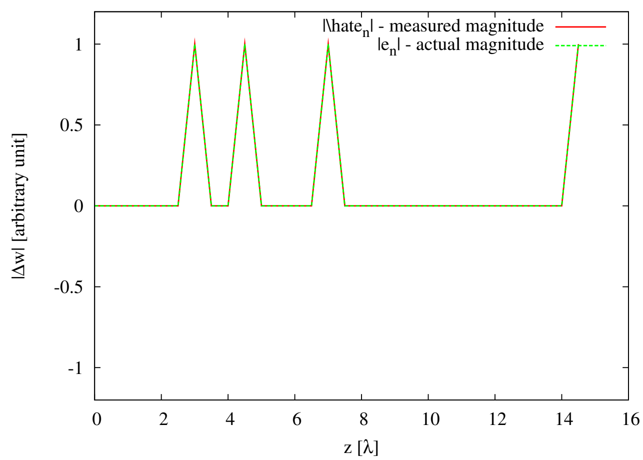

Fig.3 - Actual and measured magnitude

Results with $F = 17$:

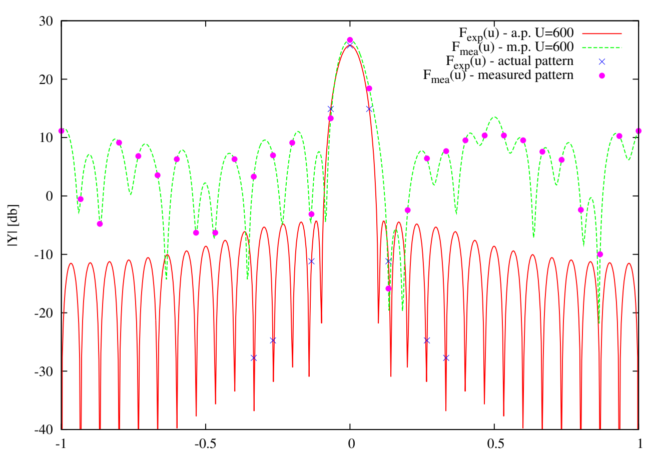

Fig.2 - Actual and measured patterns

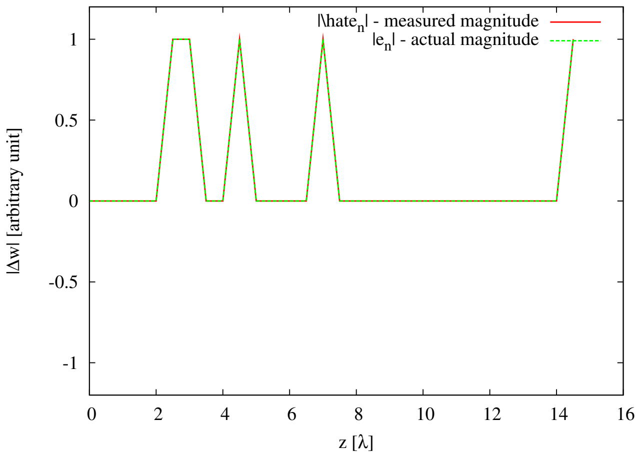

Fig.3 - Actual and measured magnitude

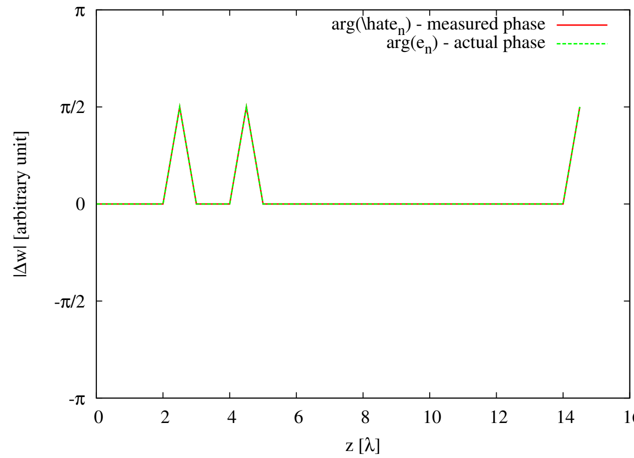

Fig.4 - Actual and measured phase

Results with $F = 20$:

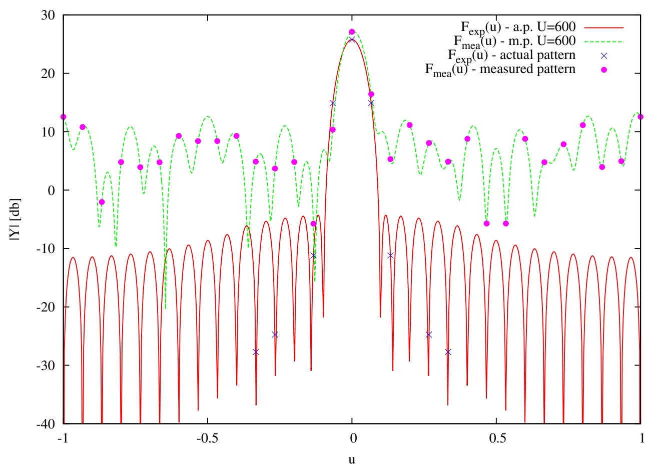

Fig.2 - Actual and measured patterns

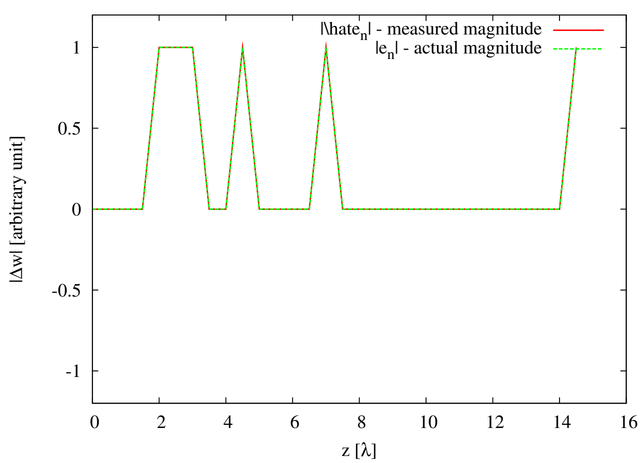

Fig.3 - Actual and measured magnitude

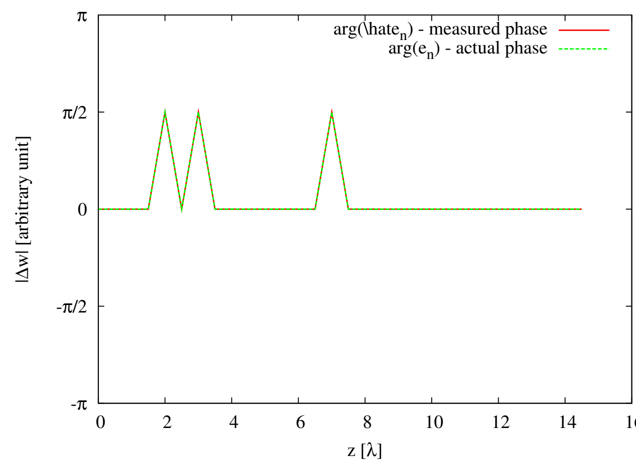

Fig.4 - Actual and measured phase

1.2.6 Sixth Case

Test Case:

- Linear Array of point sources
- Reference pattern: Taylor
- Number of elements: 40
- Observation angle number: 41
- Element Spacing: $\lambda/2$
- $dB = -30$
- Percentage of failures: $F \in [3, 5, 8, 10, 13, 15, 18, 20][\%]$

Reliability about all simulations:

$F[\%]$	η
3	0
5	$1.70 * 10^{-8}$
8	0
10	$3.26 * 10^{-8}$
13	$1.94 * 10^{-8}$
15	$4.07 * 10^{-8}$
18	$5.42 * 10^{-8}$
20	$5.49 * 10^{-8}$

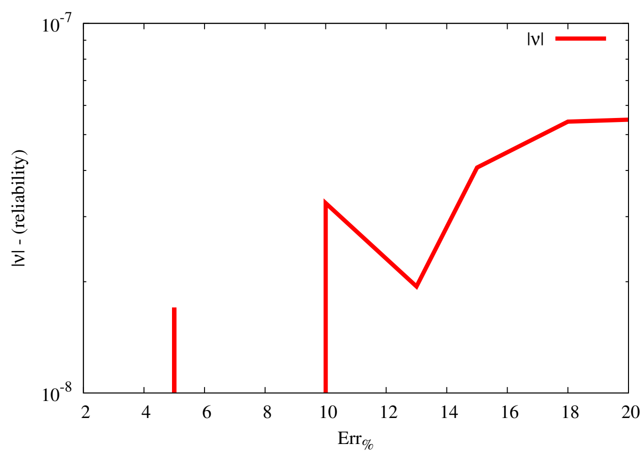

Fig.1 - Reliability

Results with $F = 3$:

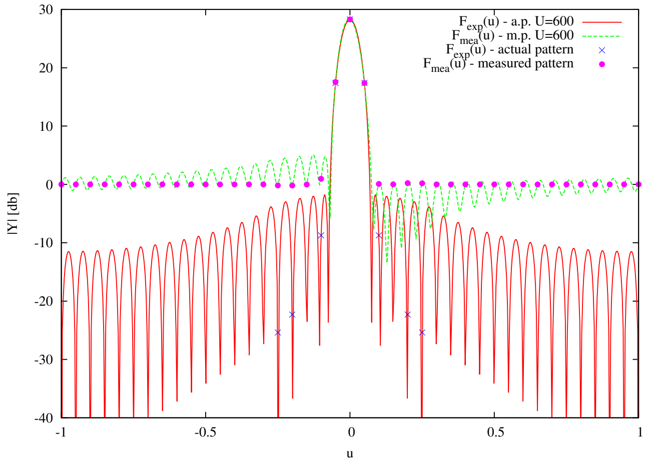

Fig.2 - Actual and measured patterns

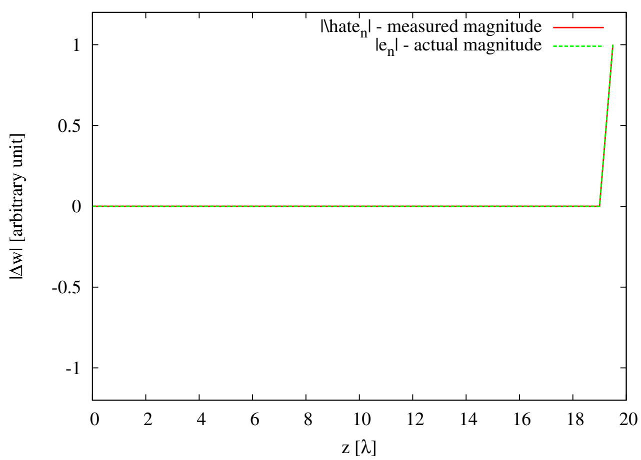

Fig.3 - Actual and measured magnitude

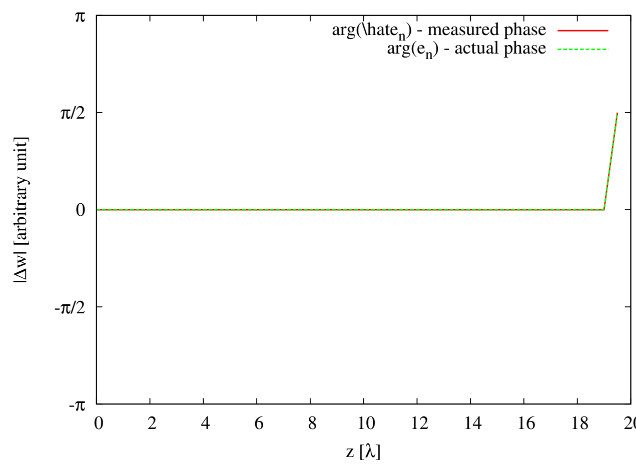

Fig.4 - Actual and measured phase

Results with $F = 5$:

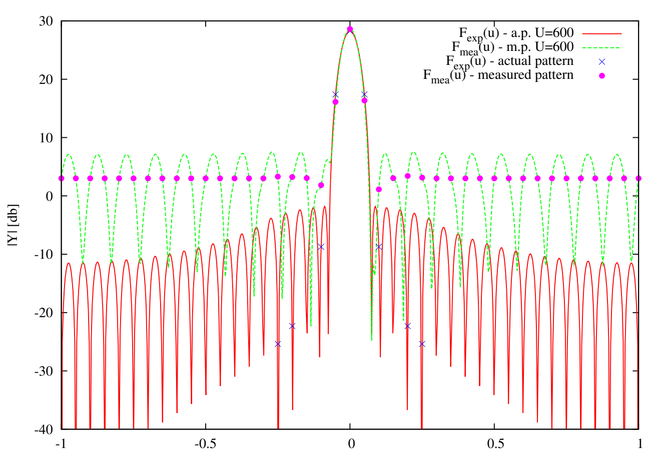

Fig.2 - Actual and measured patterns

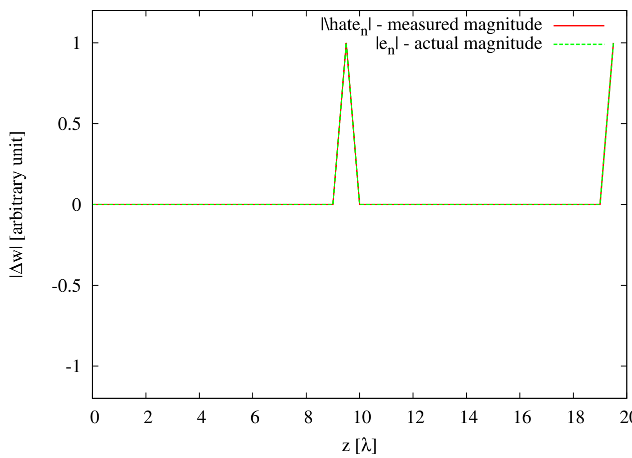

Fig.3 - Actual and measured magnitude

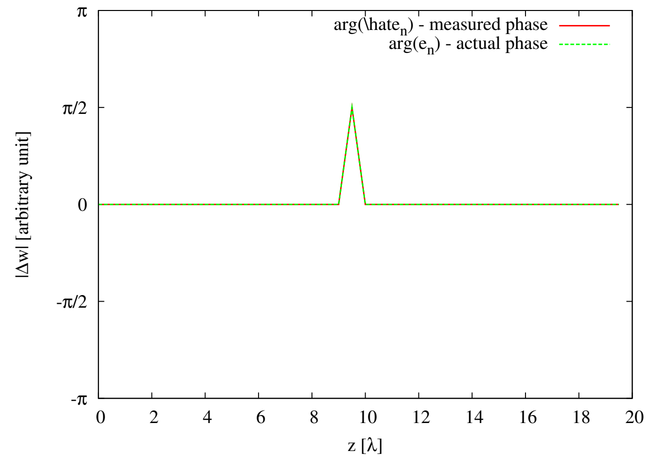

Fig.4 - Actual and measured phase

Results with $F = 8$:

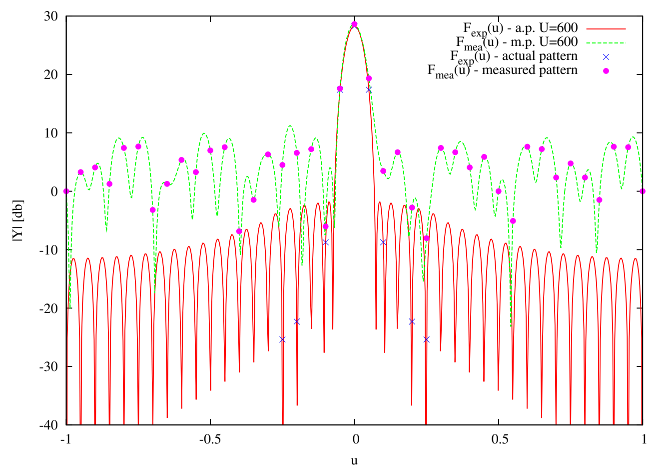

Fig.2 - Actual and measured patterns

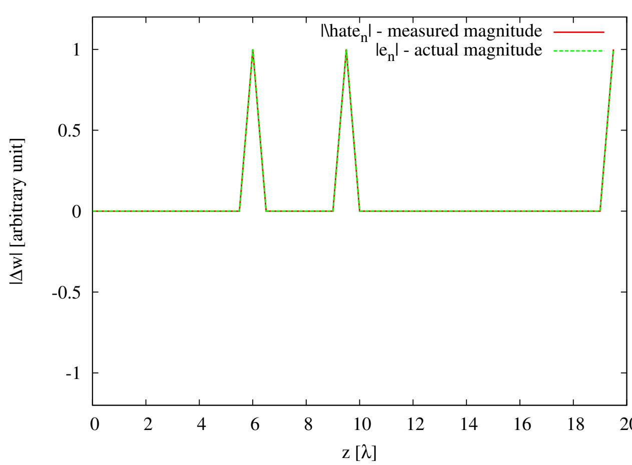

Fig.3 - Actual and measured magnitude

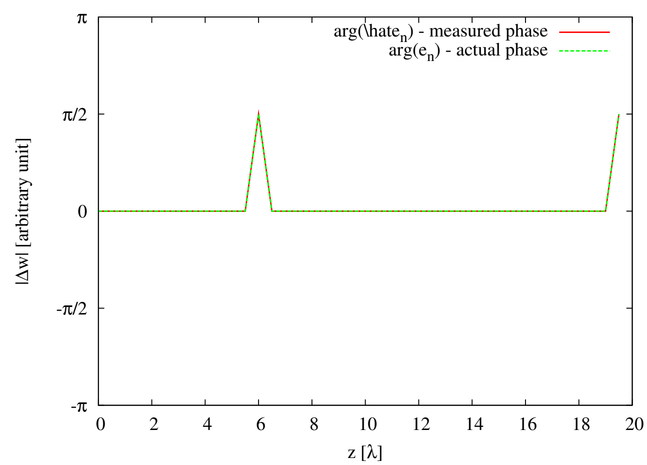

Fig.4 - Actual and measured phase

Results with $F = 10$:

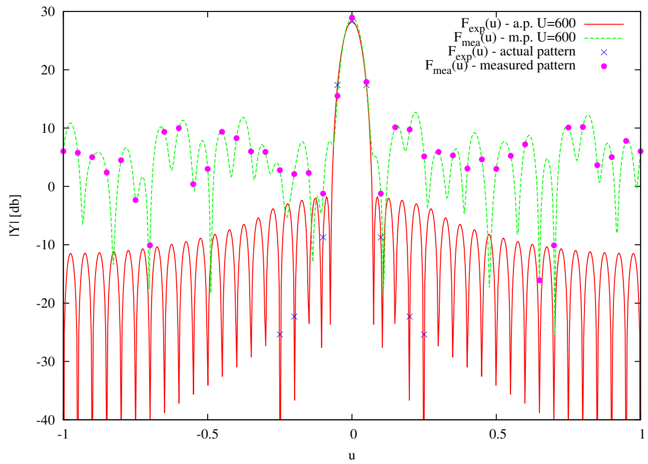

Fig.2 - Actual and measured patterns

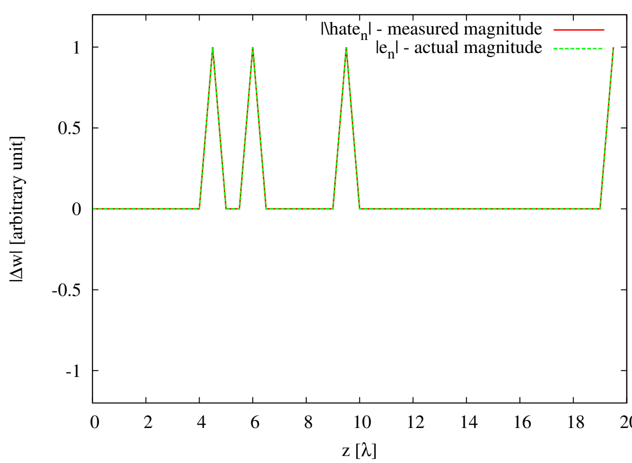

Fig.3 - Actual and measured magnitude

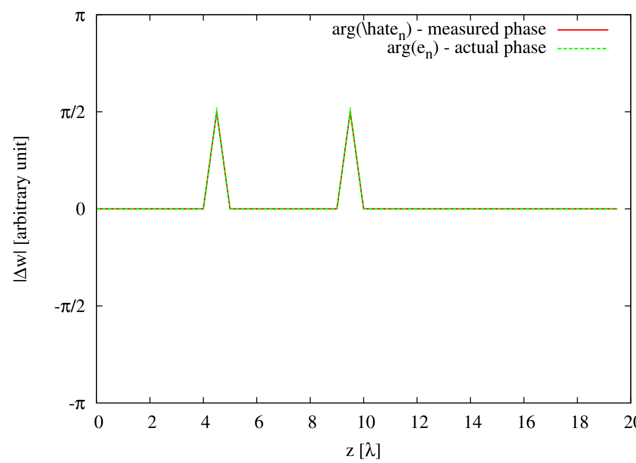

Fig.4 - Actual and measured phase

Results with $F = 13$:

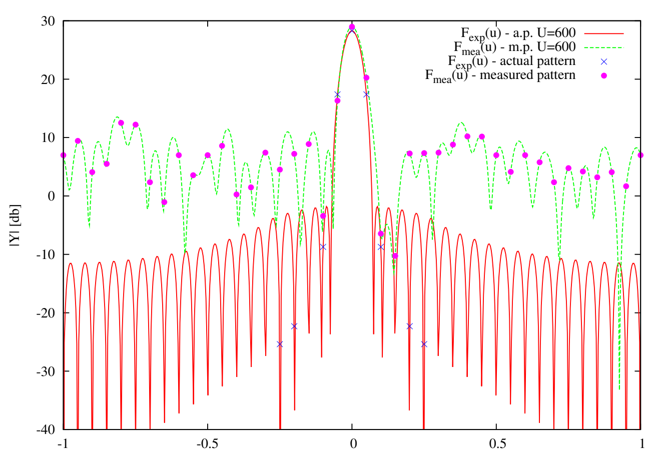

Fig.2 - Actual and measured patterns

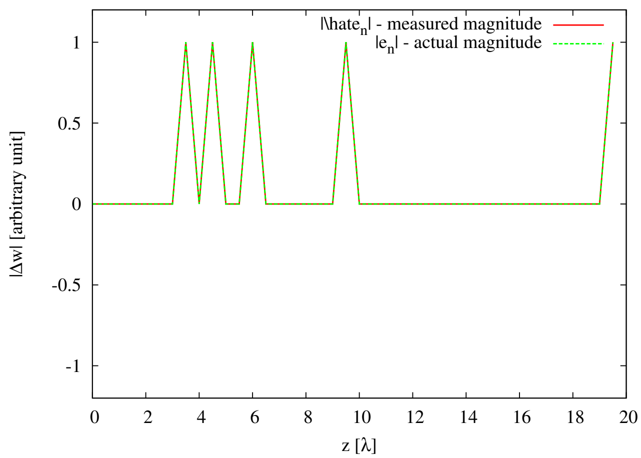

Fig.3 - Actual and measured magnitude

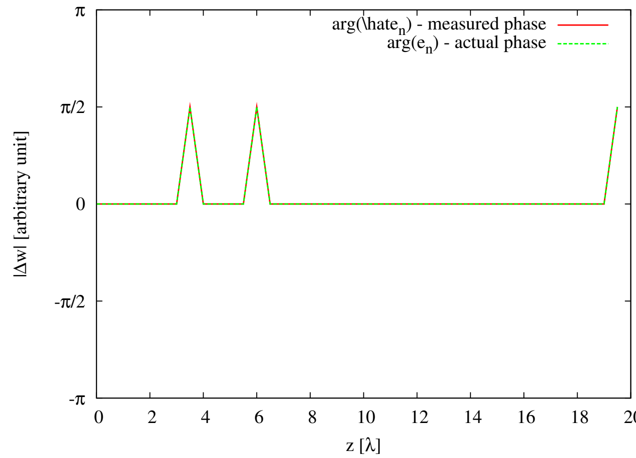

Fig.4 - Actual and measured phase

Results with $F = 15$:

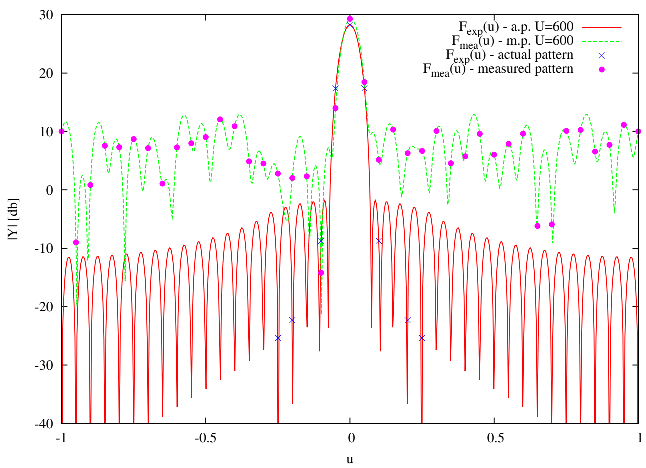

Fig.2 - Actual and measured patterns

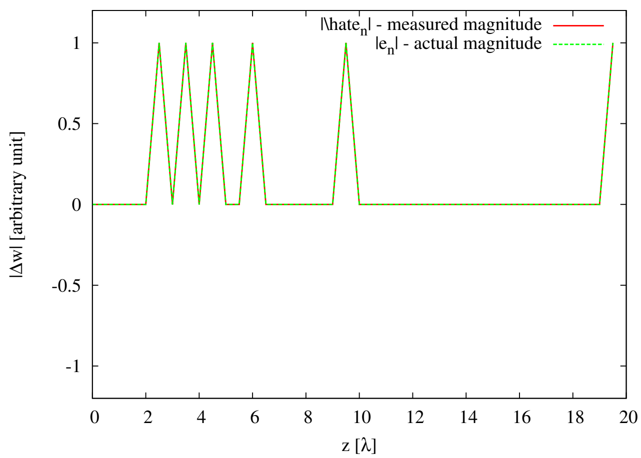

Fig.3 - Actual and measured magnitude

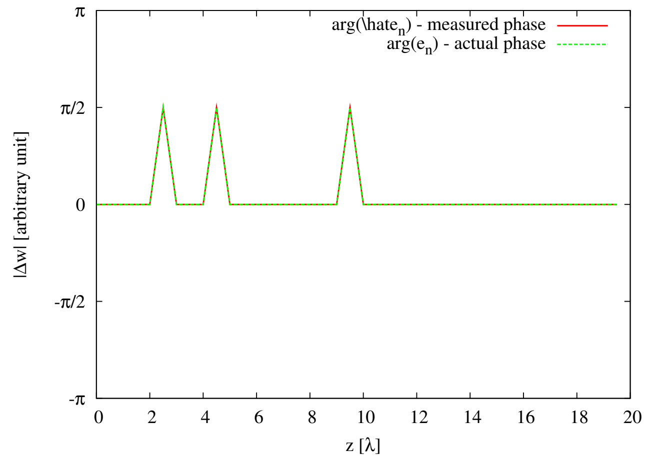

Fig.4 - Actual and measured phase

Results with $F = 18$:

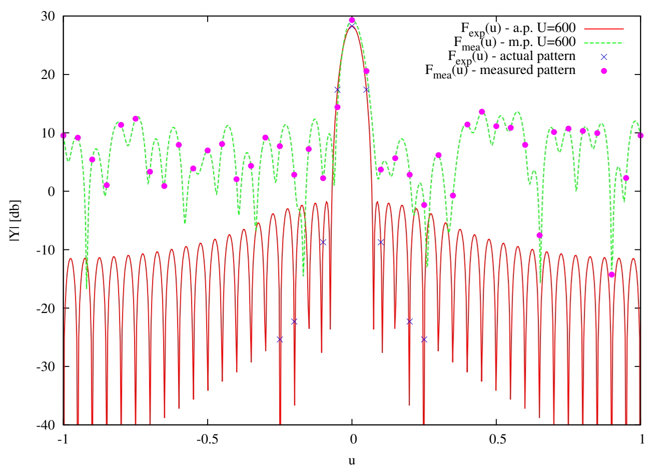

Fig.2 - Actual and measured patterns

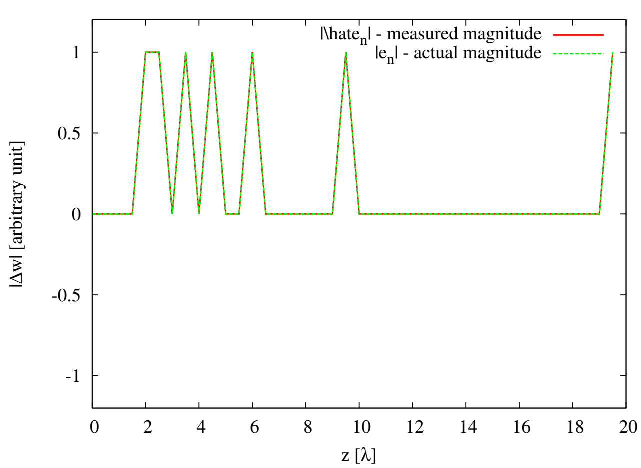

Fig.3 - Actual and measured magnitude

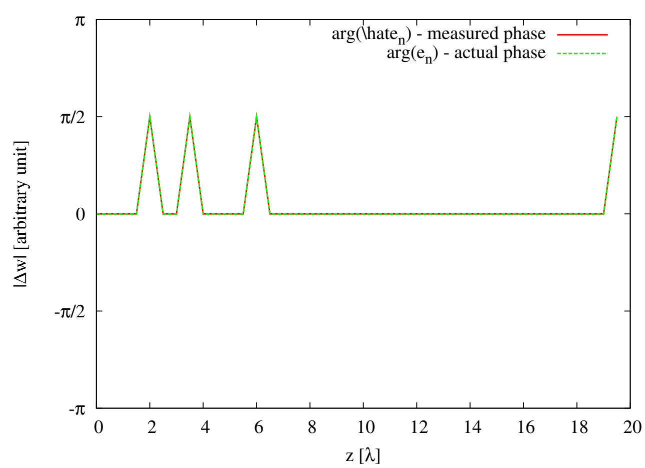

Fig.4 - Actual and measured phase

Results with $F = 20$:

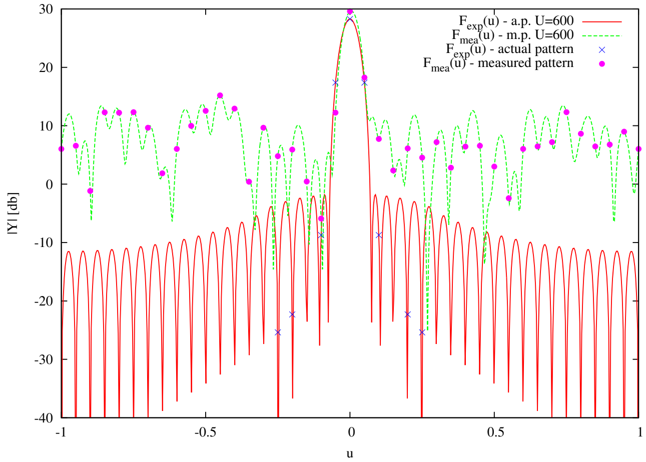

Fig.2 - Actual and measured patterns

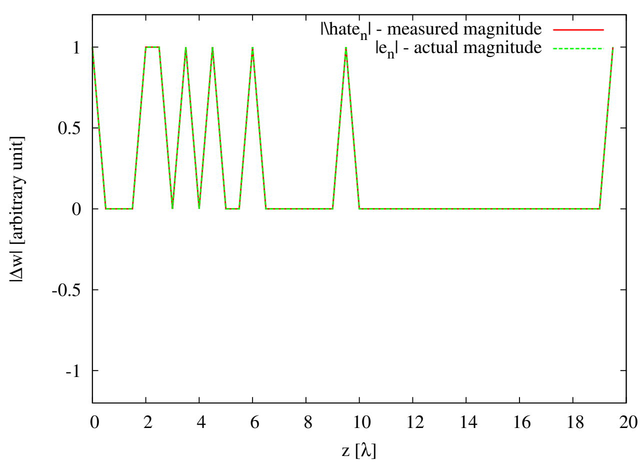

Fig.3 - Actual and measured magnitude

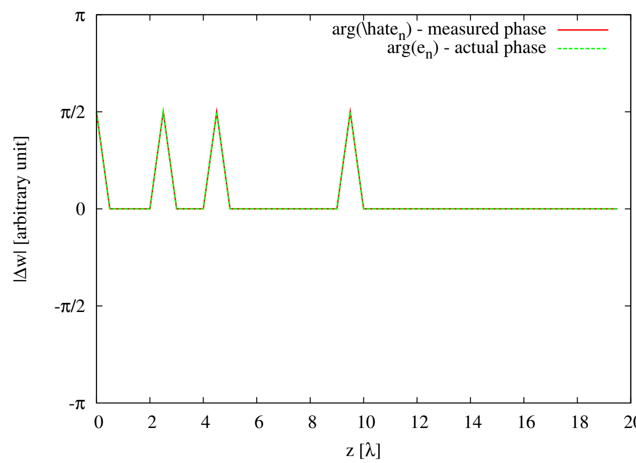

Fig.4 - Actual and measured phase

Observations

As we expected, the reliability trend shows that the more you add errors in the array antenna and the less reliable will be the failure detection.

1.3 THIRD SIMULATION RESULTS

1.3.1 First Case

Test Case:

- Linear Array of point sources
- Reference pattern: Dolph
- Number of elements: $N \in [20, 40, 100, 200]$
- Observation angle number: $N + 1$
- Element Spacing: $\lambda/2$
- $dB = -20$
- Percentage of failures: 5%

Reliability about all simulations:

N	η
20	0
40	0
100	$5.12 * 10^{-8}$
200	$1.14 * 10^{-6}$

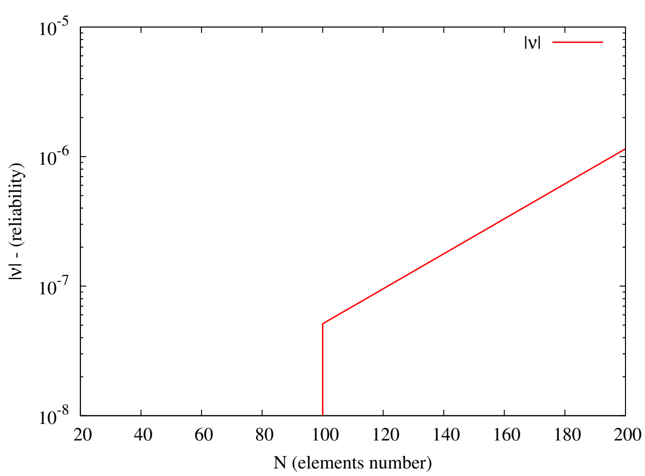

Fig.1 - Reliability

Results with $N = 20$:

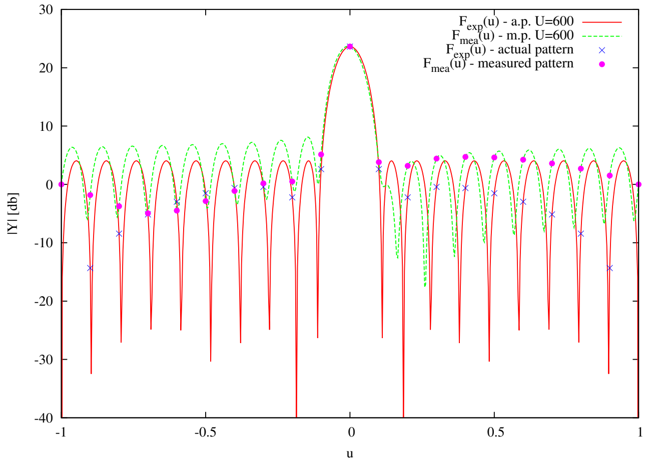

Fig.2 - Actual and measured patterns

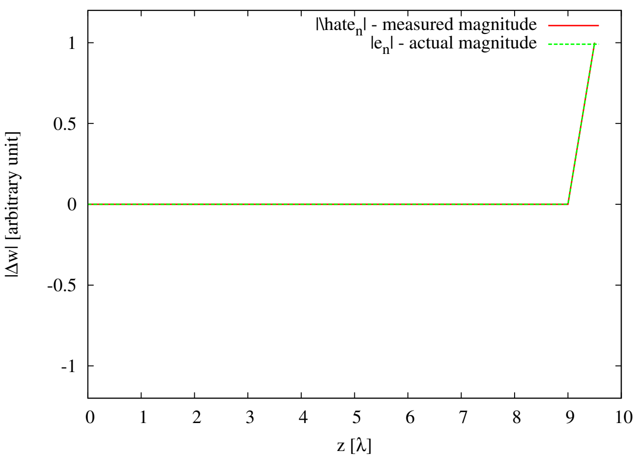

Fig.3 - Actual and measured magnitude

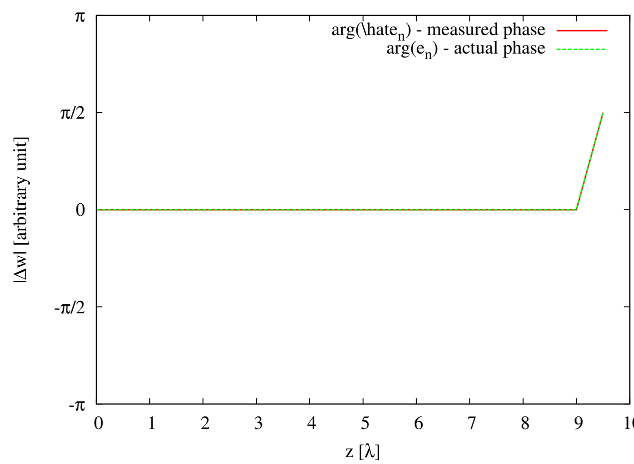

Fig.4 - Actual and measured phase

Results with $N = 40$:

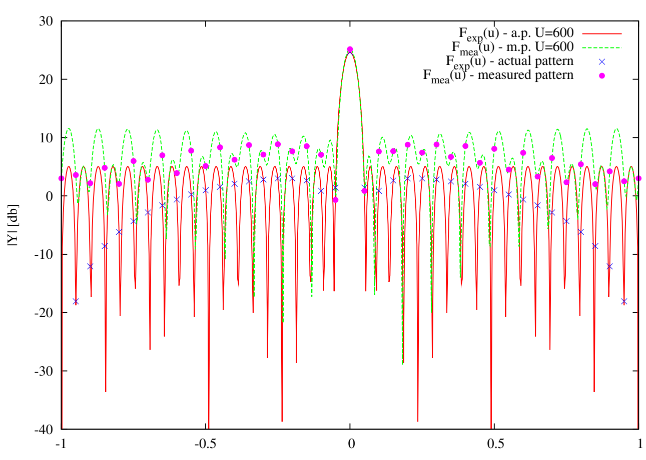

Fig.2 - Actual and measured patterns

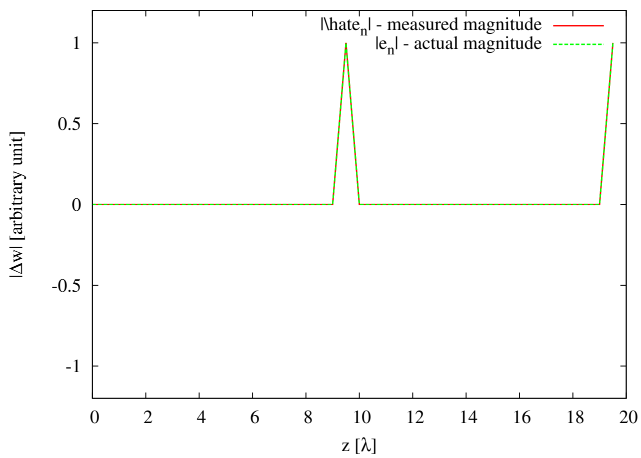

Fig.3 - Actual and measured magnitude

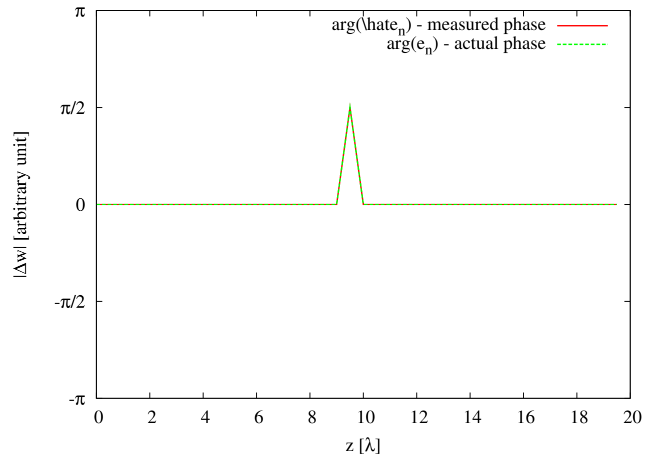

Fig.4 - Actual and measured phase

Results with $N = 100$:

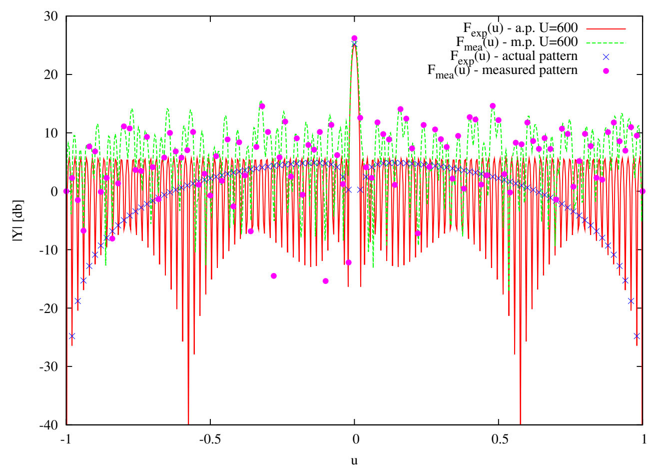

Fig.2 - Actual and measured patterns

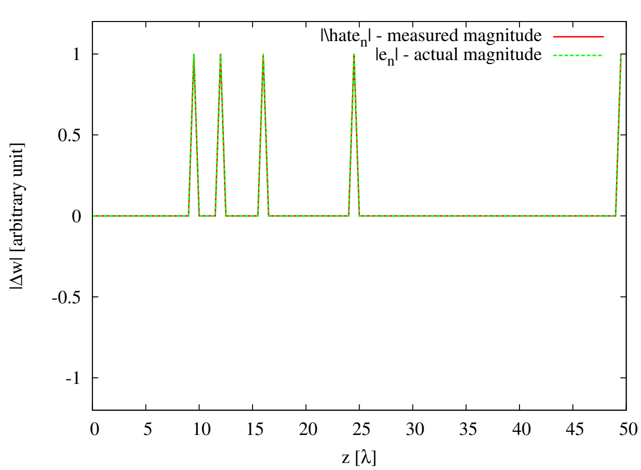

Fig.3 - Actual and measured magnitude

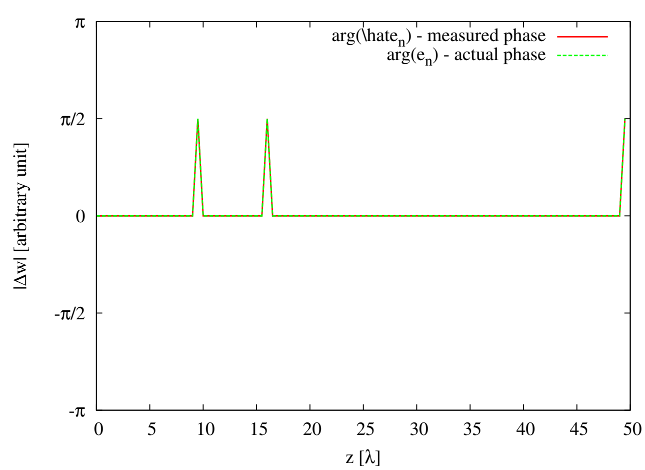

Fig.4 - Actual and measured phase

Results with $N = 200$:

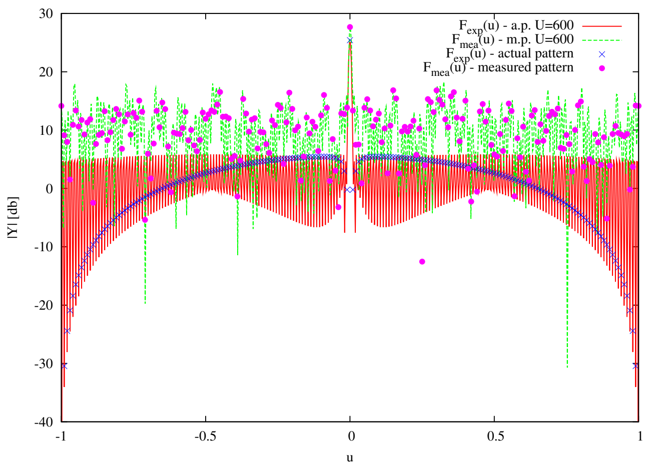

Fig.2 - Actual and measured patterns

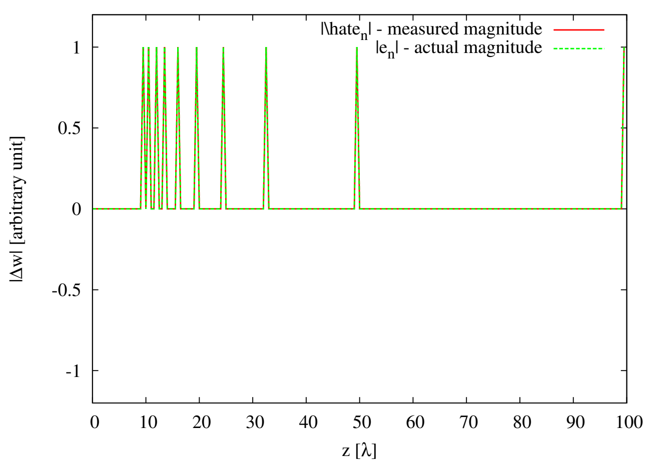

Fig.3 - Actual and measured magnitude

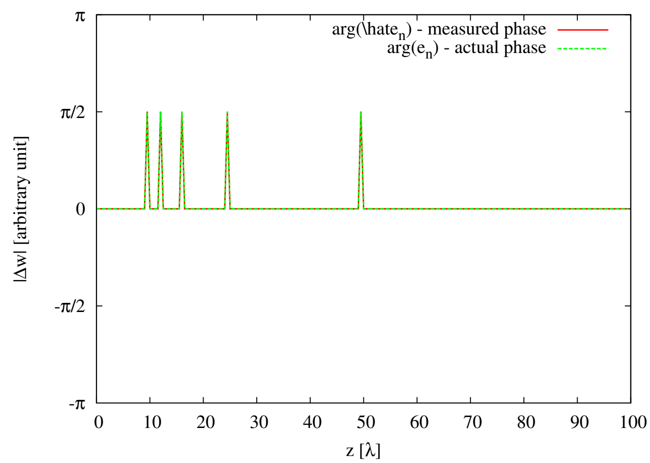

Fig.4 - Actual and measured phase

1.3.2 Second Case

Test Case:

- Linear Array of point sources
- Reference pattern: Dolph
- Number of elements: $N \in [20, 40, 100, 200]$
- Observation angle number: $N + 1$
- Element Spacing: $\lambda/2$
- $dB = -25$
- Percentage of failures: 5%

Reliability about all simulations:

N	η
20	0
40	0
100	$3.35 * 10^{-9}$
200	$5.68 * 10^{-7}$

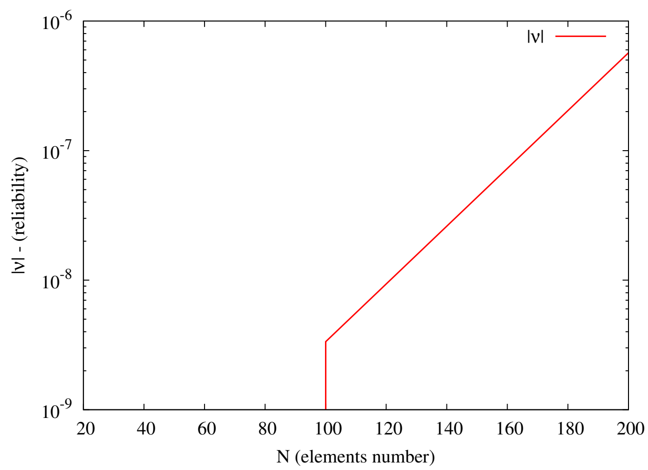

Fig.1 - Reliability

Results with $N = 20$:

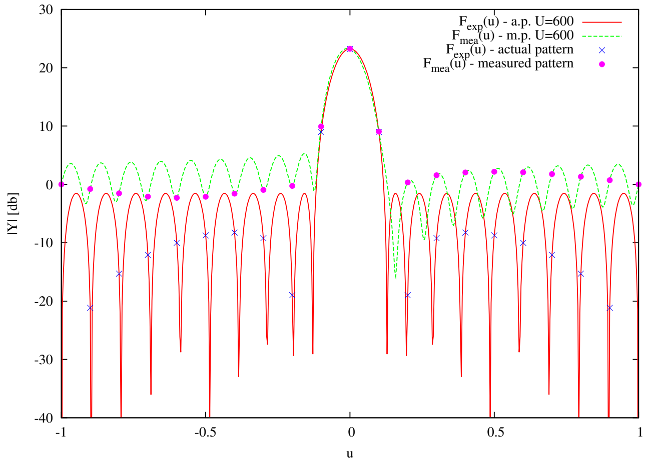

Fig.2 - Actual and measured patterns

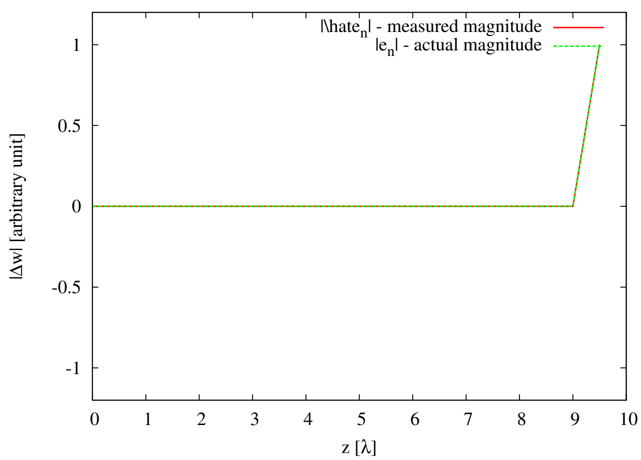

Fig.3 - Actual and measured magnitude

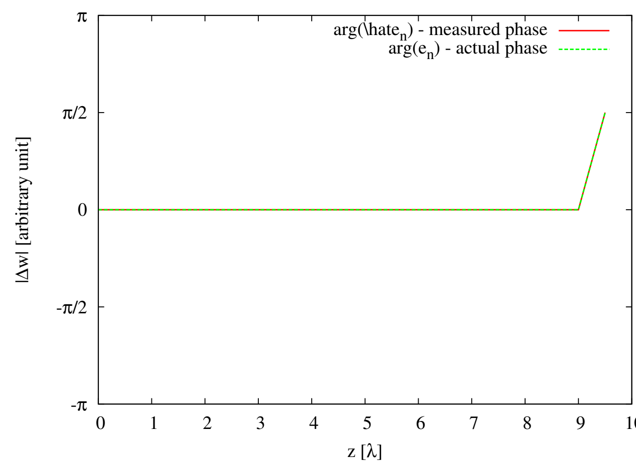

Fig.4 - Actual and measured phase

Results with $N = 40$:

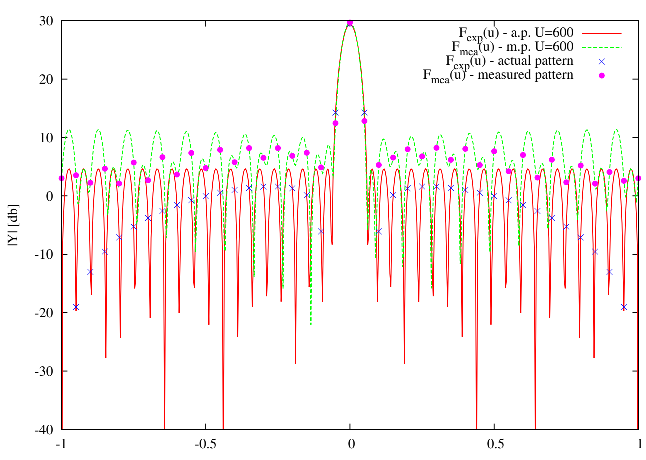

Fig.2 - Actual and measured patterns

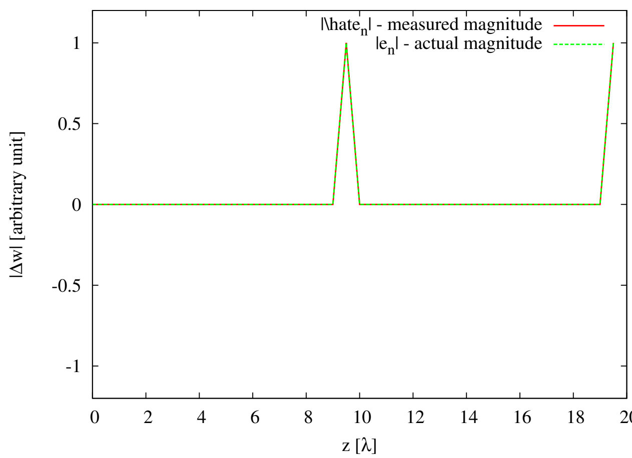

Fig.3 - Actual and measured magnitude

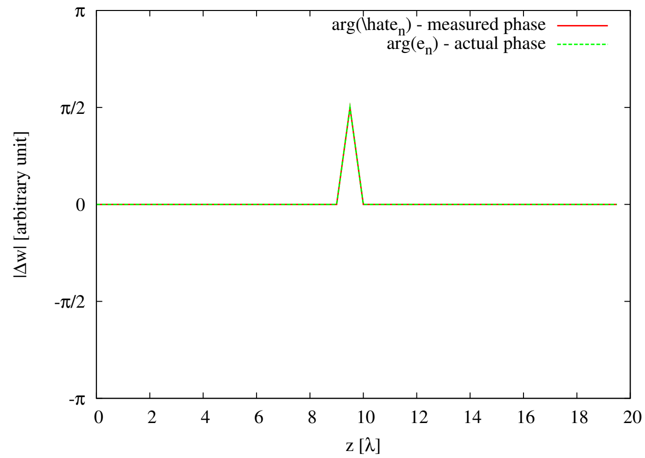

Fig.4 - Actual and measured phase

Results with $N = 100$:

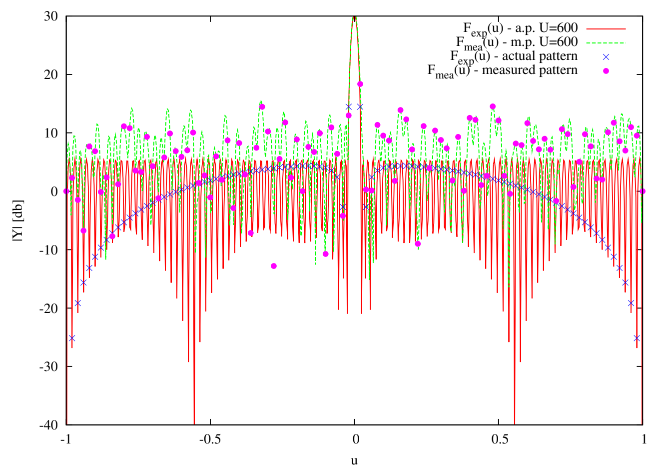

Fig.2 - Actual and measured patterns

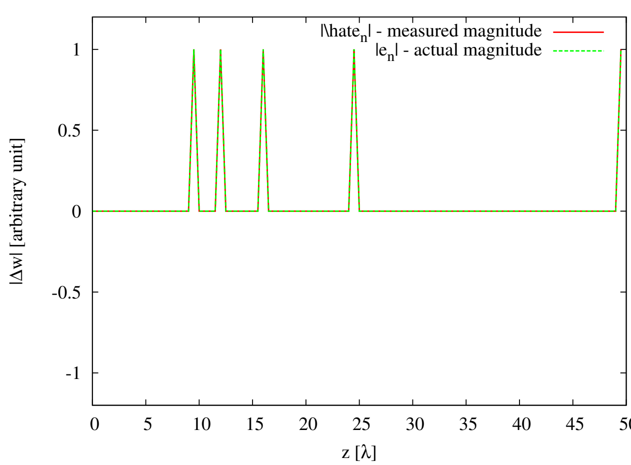

Fig.3 - Actual and measured magnitude

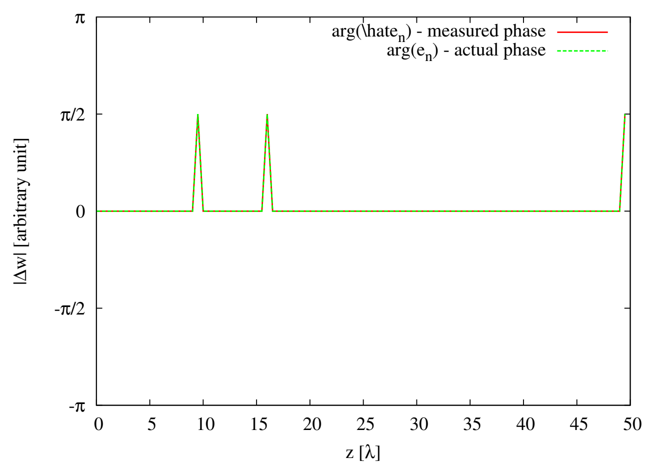

Fig.4 - Actual and measured phase

Results with $N = 200$:

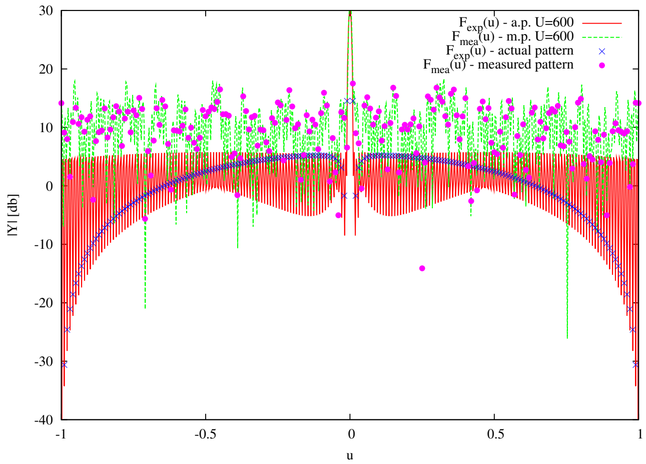

Fig.2 - Actual and measured patterns

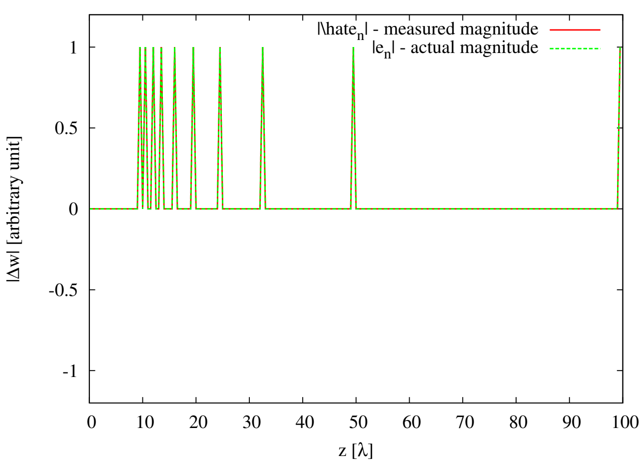

Fig.3 - Actual and measured magnitude

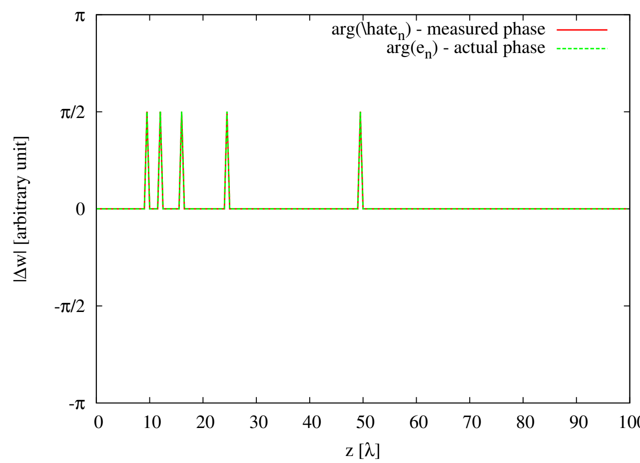

Fig.4 - Actual and measured phase

1.3.3 Third Case

Test Case:

- Linear Array of point sources
- Reference pattern: Dolph
- Number of elements: $N \in [20, 40, 100, 200]$
- Observation angle number: $N + 1$
- Element Spacing: $\lambda/2$
- $dB = -30$
- Percentage of failures: 5%

Reliability about all simulations:

N	η
20	0
40	$8.92 * 10^{-10}$
100	$4.45 * 10^{-9}$
200	$1.65 * 10^{-7}$

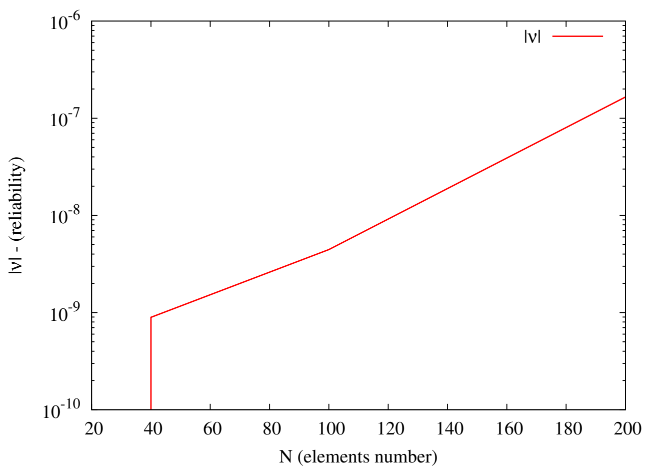

Fig.1 - Reliability

Results with $N = 20$:

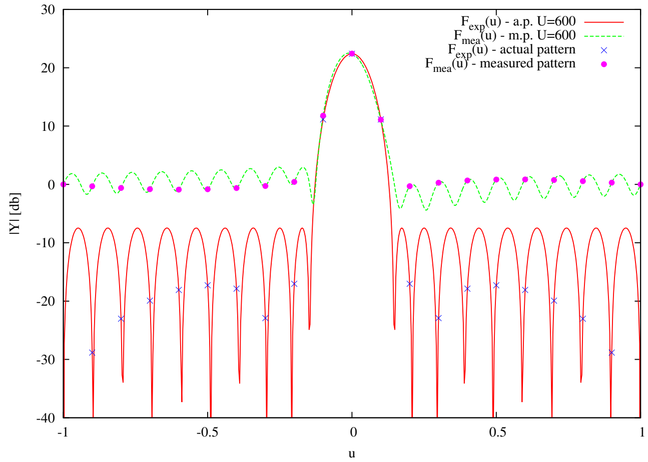

Fig.2 - Actual and measured patterns

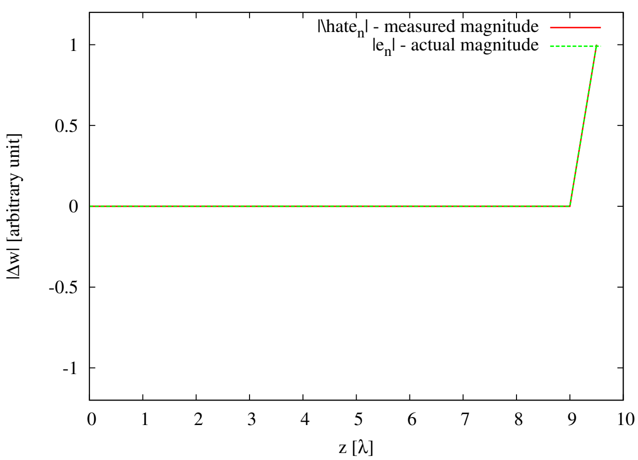

Fig.3 - Actual and measured magnitude

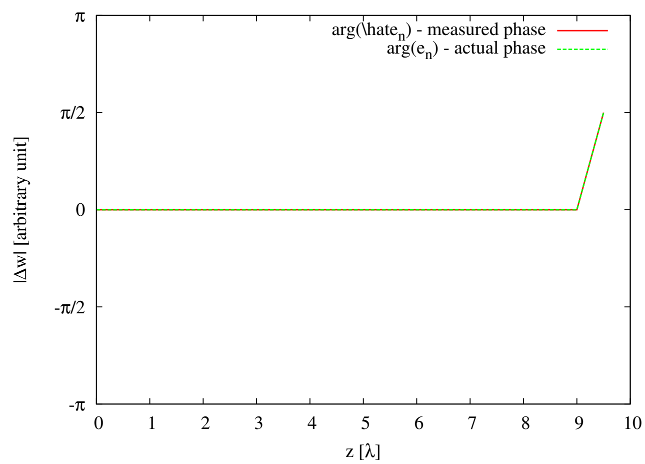

Fig.4 - Actual and measured phase

Results with $N = 40$:

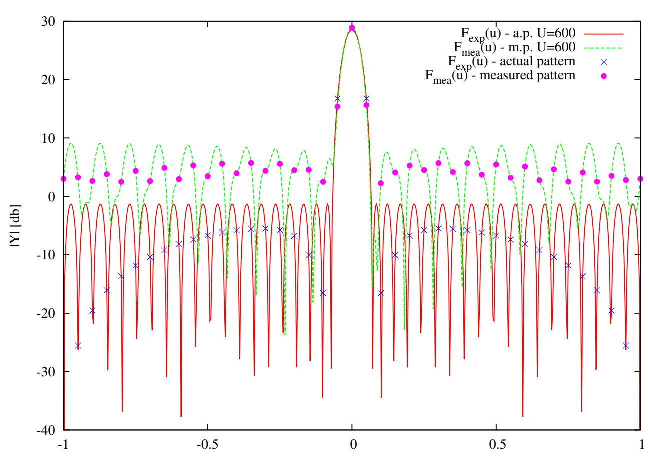

Fig.2 - Actual and measured patterns

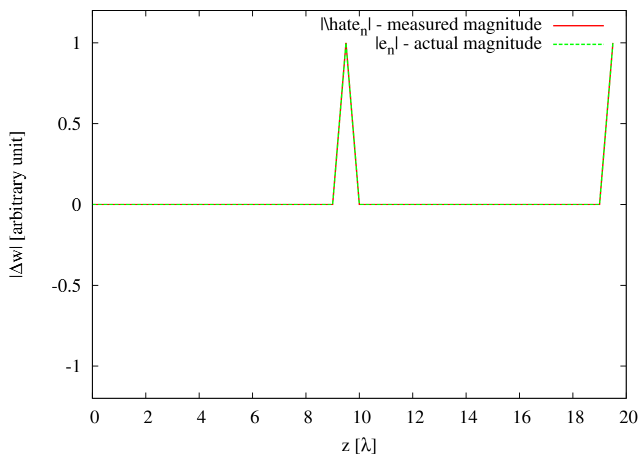

Fig.3 - Actual and measured magnitude

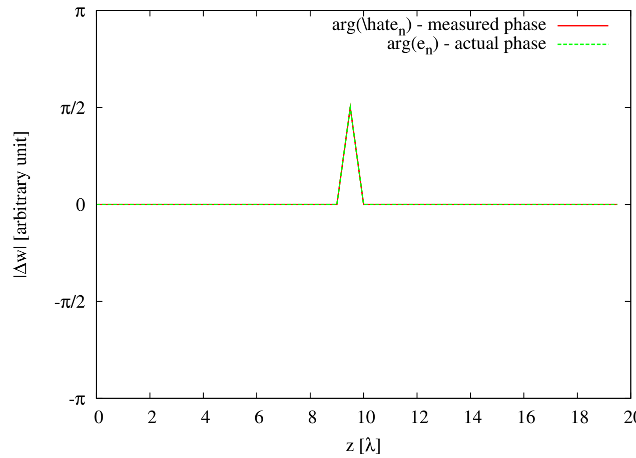

Fig.4 - Actual and measured phase

Results with $N = 100$:

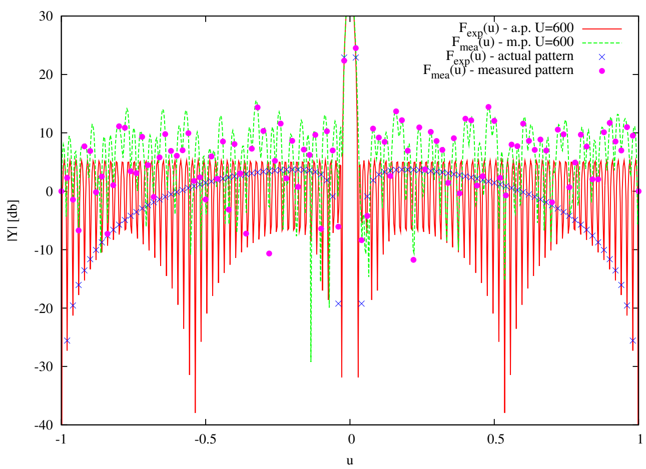

Fig.2 - Actual and measured patterns

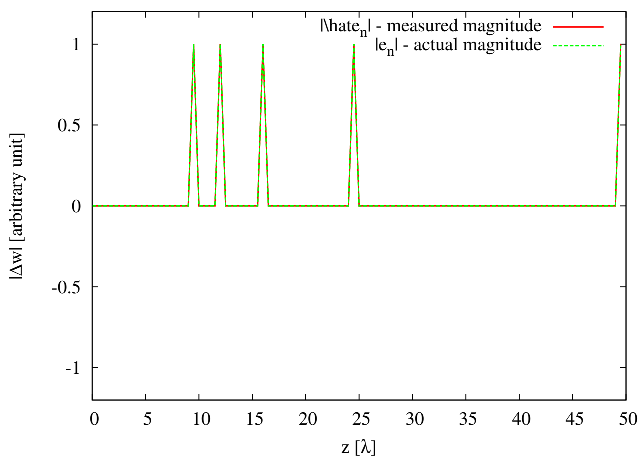

Fig.3 - Actual and measured magnitude

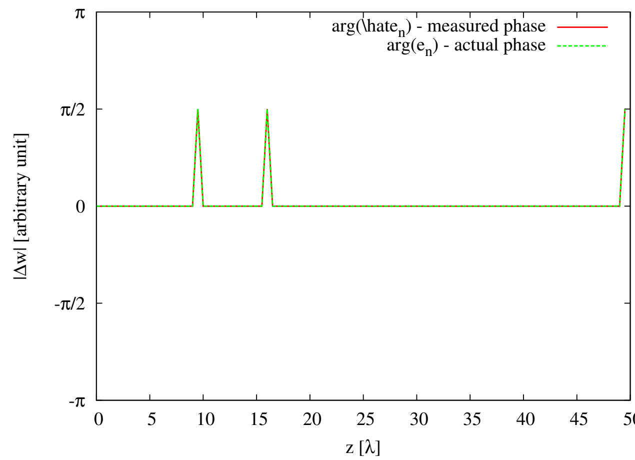

Fig.4 - Actual and measured phase

Results with $N = 200$:

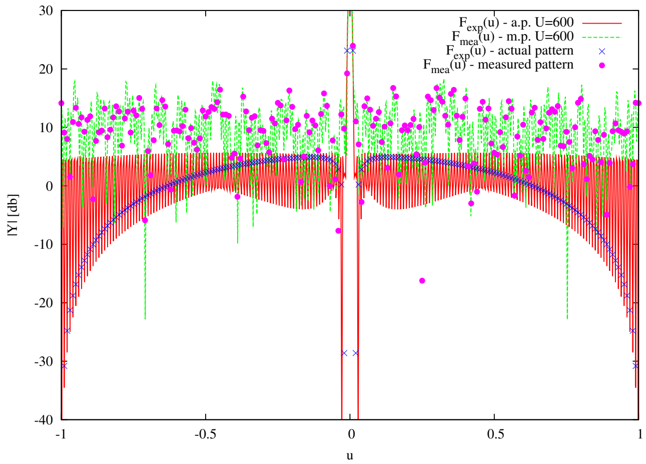

Fig.2 - Actual and measured patterns

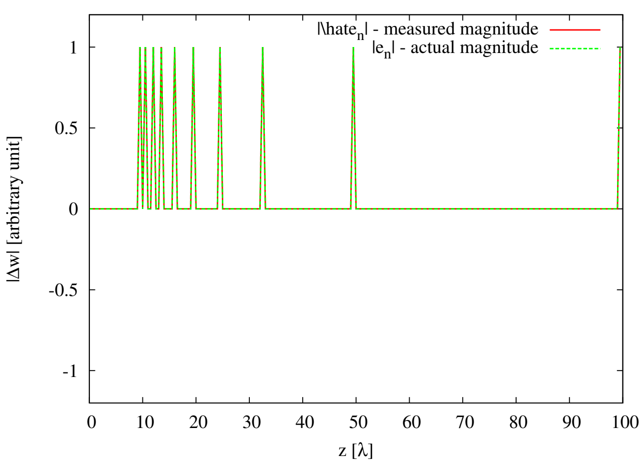

Fig.3 - Actual and measured magnitude

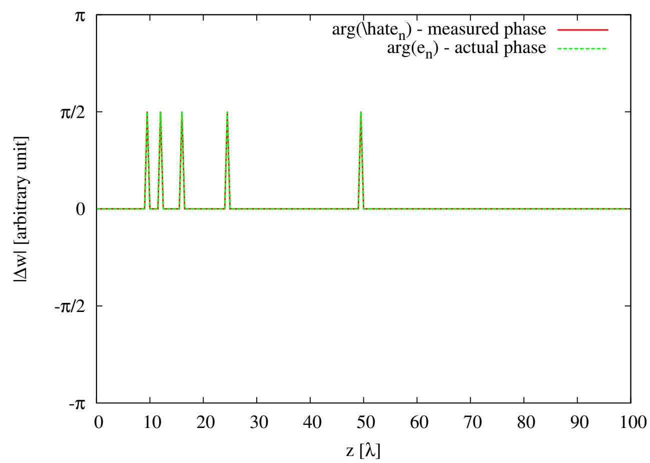

Fig.4 - Actual and measured phase

1.3.4 Fourth Case

Test Case:

- Linear Array of point sources
- Reference pattern: Dolph
- Number of elements: $N \in [20, 40, 100, 200]$
- Observation angle number: $N + 1$
- Element Spacing: $\lambda/2$
- $dB = -35$
- Percentage of failures: 5%

Reliability about all simulations:

N	η
20	0
40	$1.84 * 10^{-9}$
100	$4.92 * 10^{-10}$
200	$9.39 * 10^{-8}$

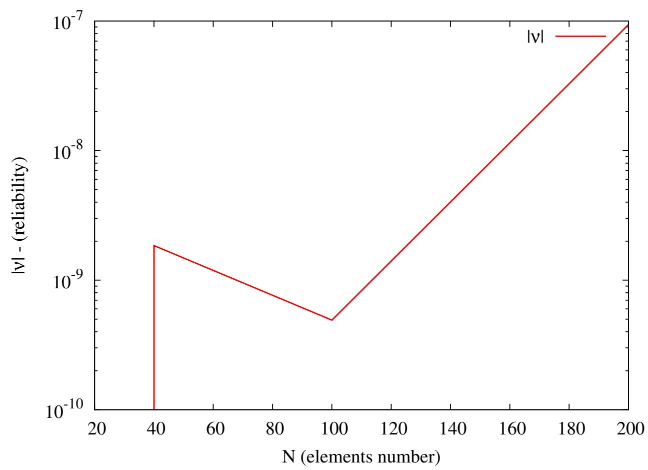

Fig.1 - Reliability

Results with $N = 20$:

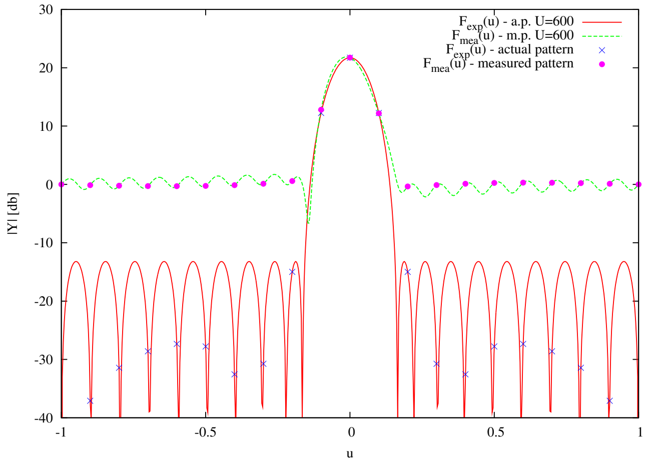

Fig.2 - Actual and measured patterns

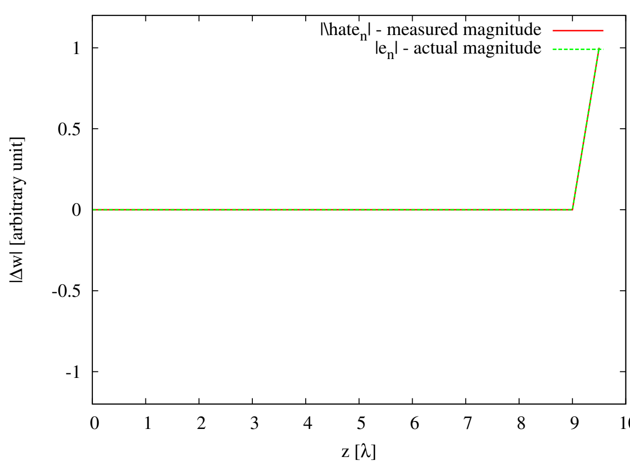

Fig.3 - Actual and measured magnitude

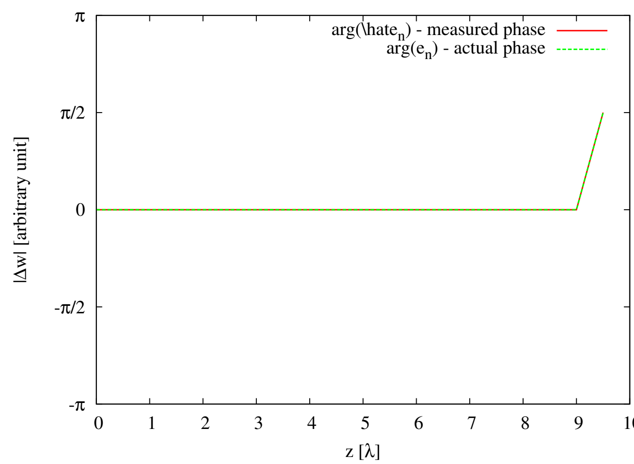

Fig.4 - Actual and measured phase

Results with $N = 40$:

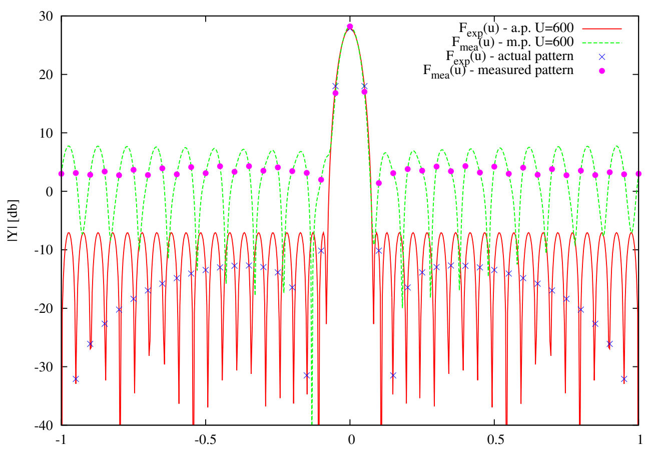

Fig.2 - Actual and measured patterns

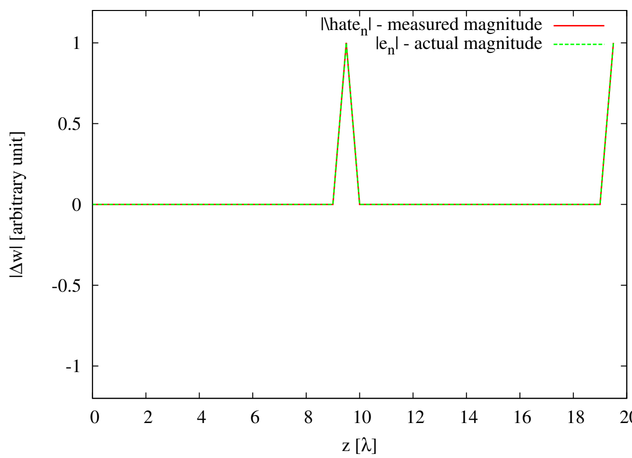

Fig.3 - Actual and measured magnitude

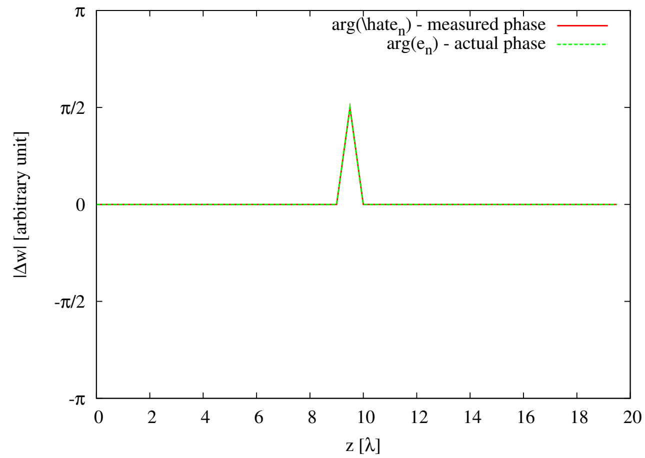

Fig.4 - Actual and measured phase

Results with $N = 100$:

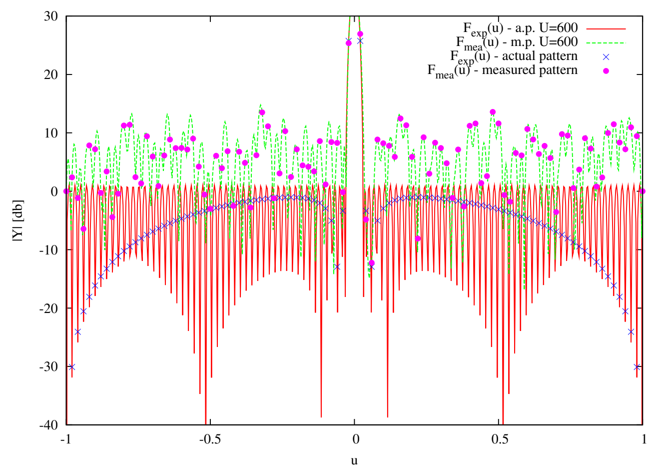

Fig.2 - Actual and measured patterns

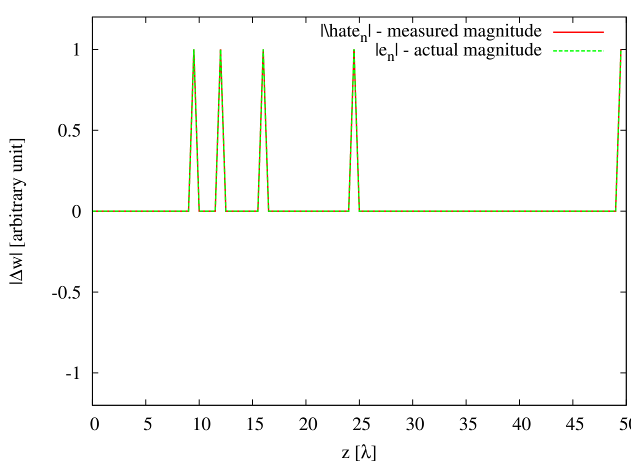

Fig.3 - Actual and measured magnitude

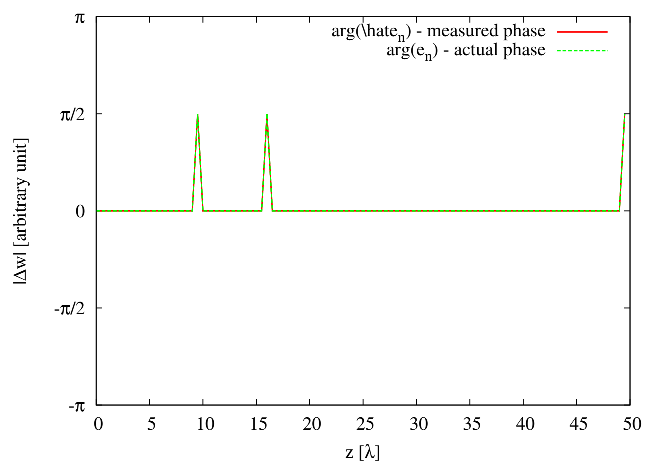

Fig.4 - Actual and measured phase

Results with $N = 200$:

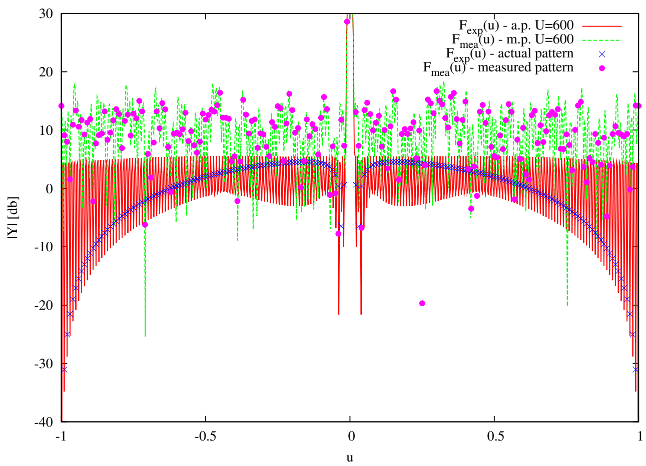

Fig.2 - Actual and measured patterns

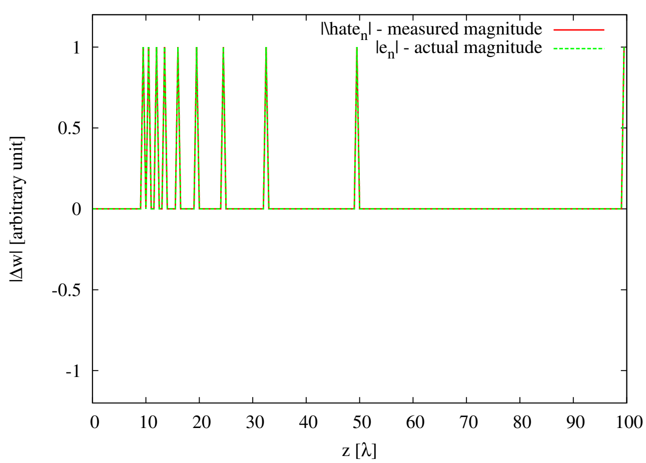

Fig.3 - Actual and measured magnitude

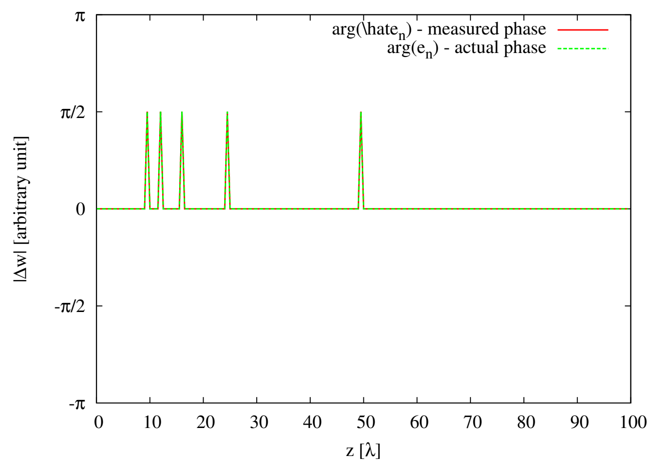

Fig.4 - Actual and measured phase

1.3.5 Fifth Case

Test Case:

- Linear Array of point sources
- Reference pattern: Dolph
- Number of elements: $N \in [20, 40, 100, 200]$
- Observation angle number: $N + 1$
- Element Spacing: $\lambda/2$
- $dB = -40$
- Percentage of failures: 5%

Reliability about all simulations:

N	η
20	0
40	$1.60 * 10^{-8}$
100	$4.71 * 10^{-11}$
200	$3.15 * 10^{-8}$

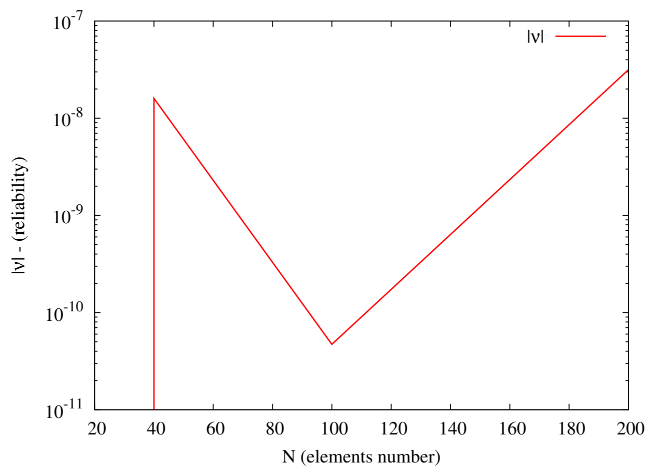

Fig.1 - Reliability

Results with $N = 20$:

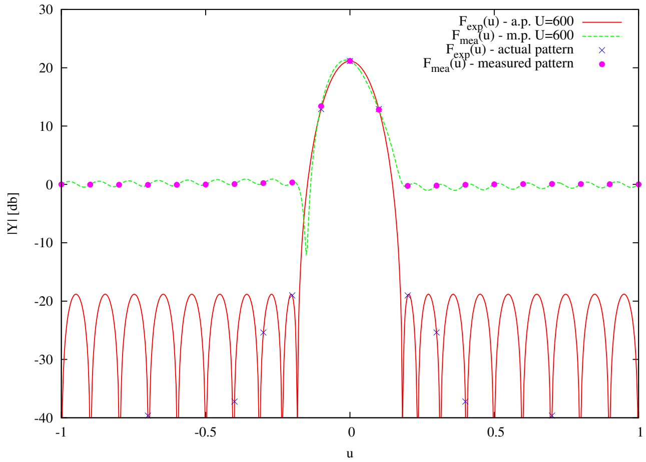

Fig.2 - Actual and measured patterns

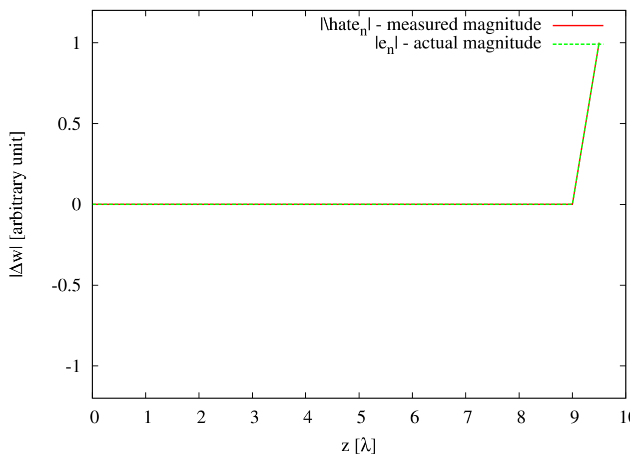

Fig.3 - Actual and measured magnitude

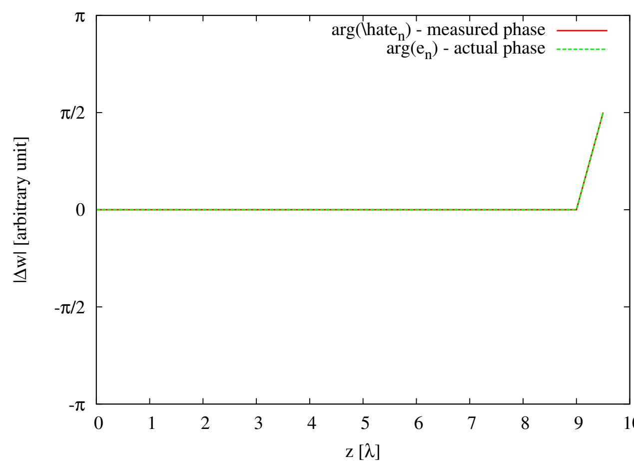

Fig.4 - Actual and measured phase

Results with $N = 40$:

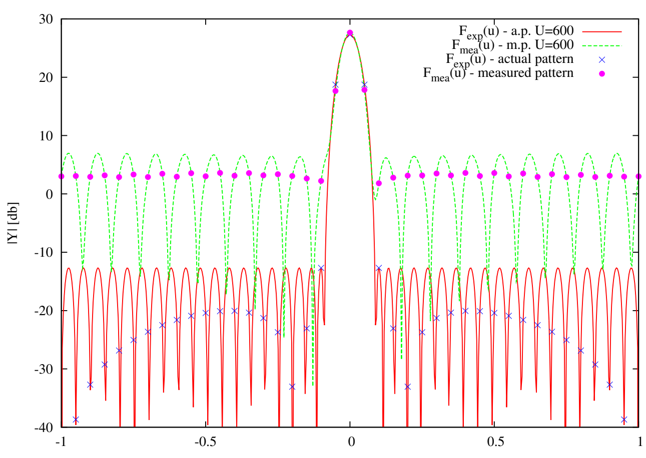

Fig.2 - Actual and measured patterns

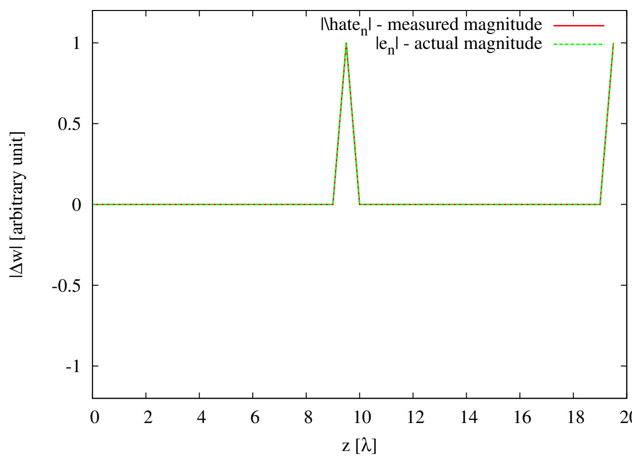

Fig.3 - Actual and measured magnitude

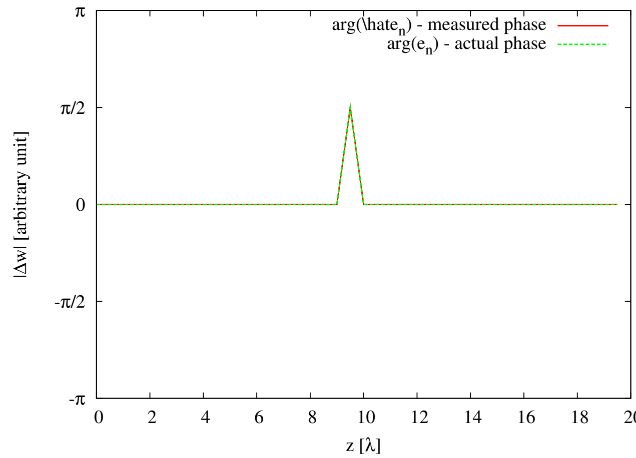

Fig.4 - Actual and measured phase

Results with $N = 100$:

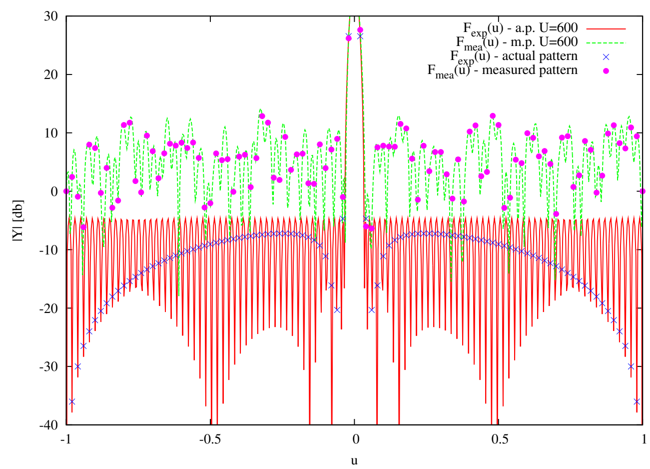

Fig.2 - Actual and measured patterns

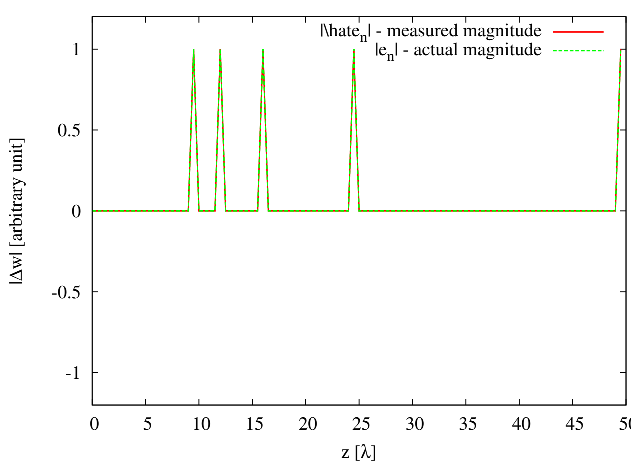

Fig.3 - Actual and measured magnitude

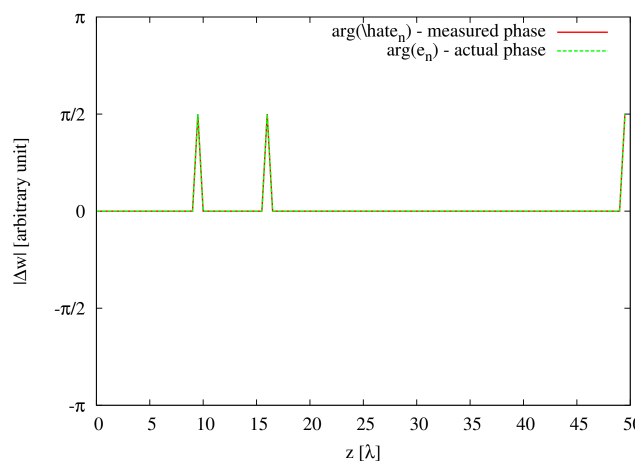

Fig.4 - Actual and measured phase

Results with $N = 200$:

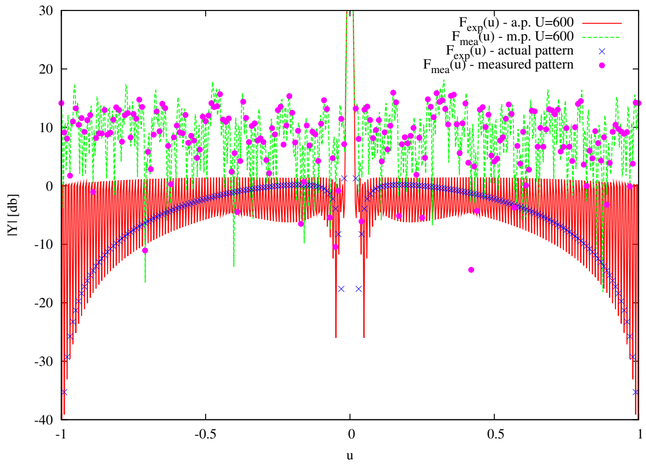

Fig.2 - Actual and measured patterns

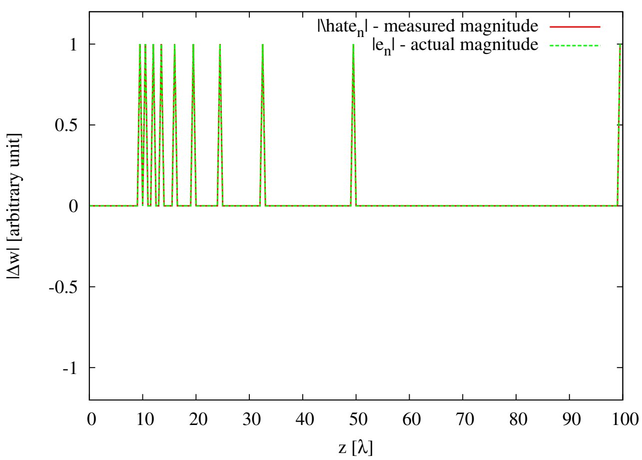

Fig.3 - Actual and measured magnitude

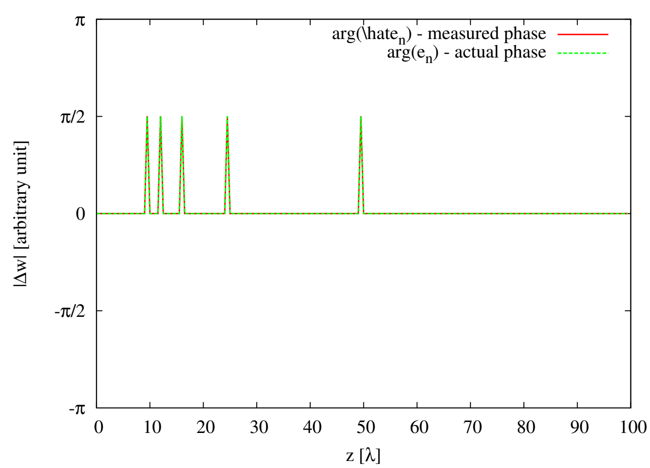

Fig.4 - Actual and measured phase

1.3.6 Sixth Case

Test Case:

- Linear Array of point sources
- Reference pattern: Taylor
- Number of elements: $N \in [20, 40, 100, 200]$
- Observation angle number: $N + 1$
- Element Spacing: $\lambda/2$
- $dB = -20$
- Percentage of failures: 5%

Reliability about all simulations:

N	η
20	0
40	$1.56 * 10^{-10}$
100	$2.21 * 10^{-9}$
200	$5.01 * 10^{-8}$

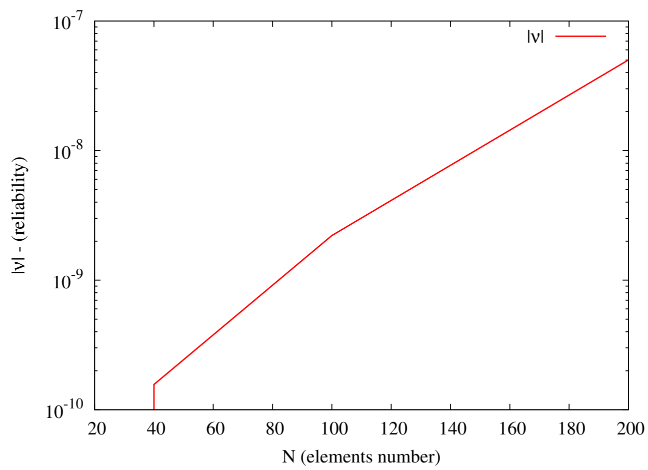

Fig.1 - Reliability

Results with $N = 20$:

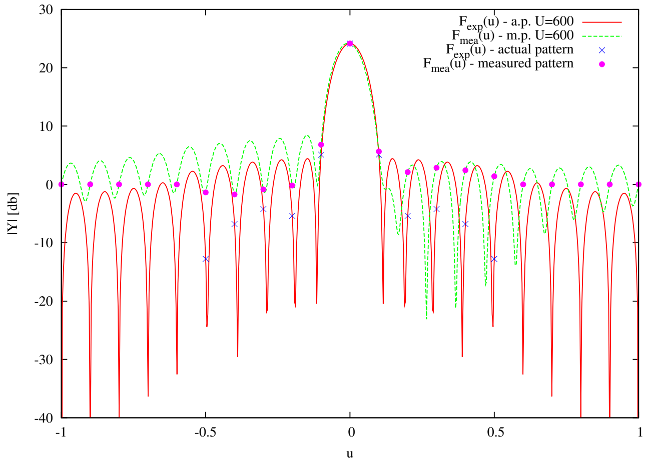

Fig.2 - Actual and measured patterns

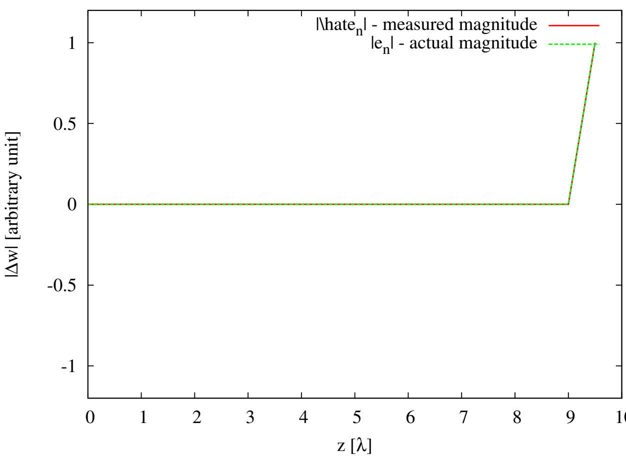

Fig.3 - Actual and measured magnitude

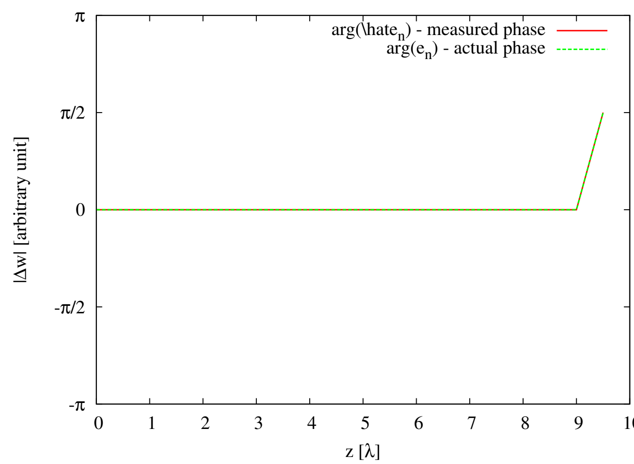

Fig.4 - Actual and measured phase

Results with $N = 40$**:**

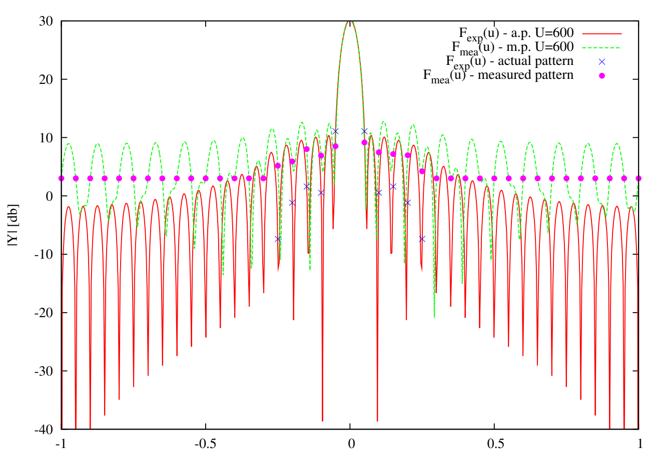

Fig.2 - Actual and measured patterns

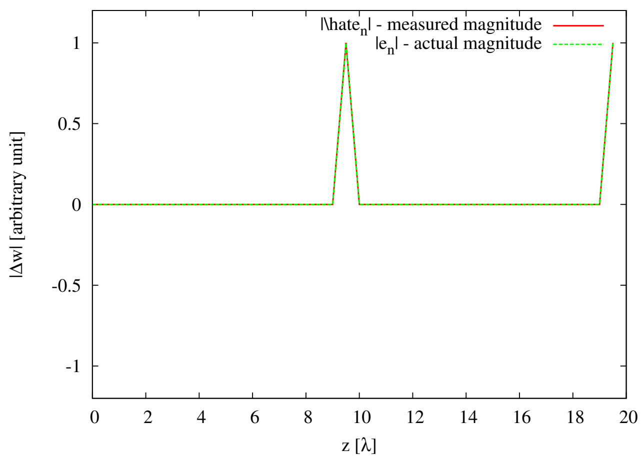

Fig.3 - Actual and measured magnitude

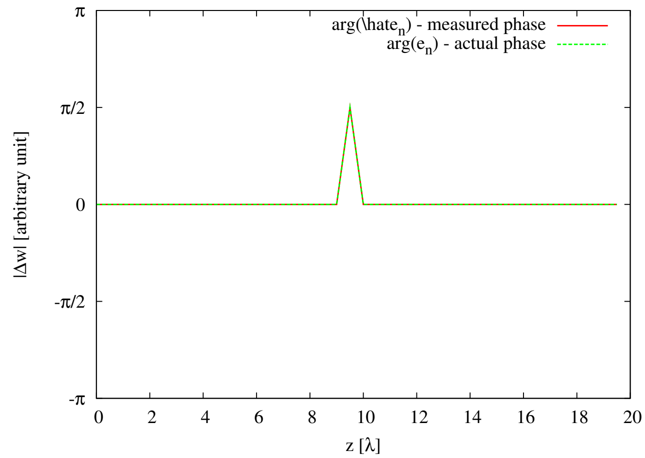

Fig.4 - Actual and measured phase

Results with $N = 100$:

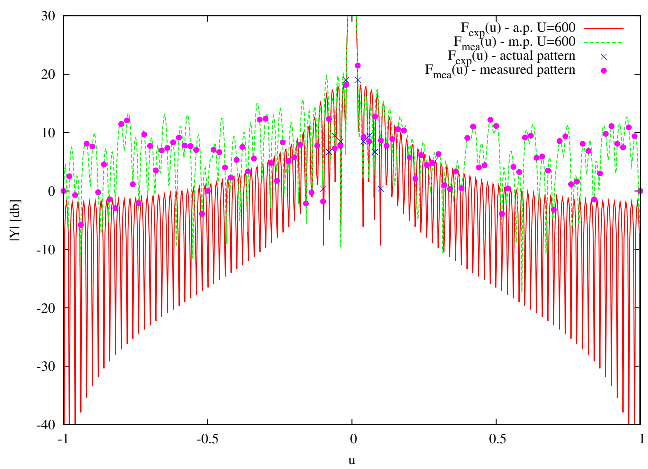

Fig.2 - Actual and measured patterns

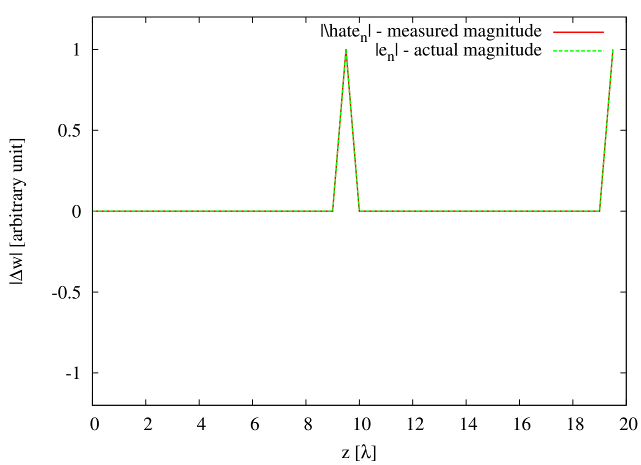

Fig.3 - Actual and measured magnitude

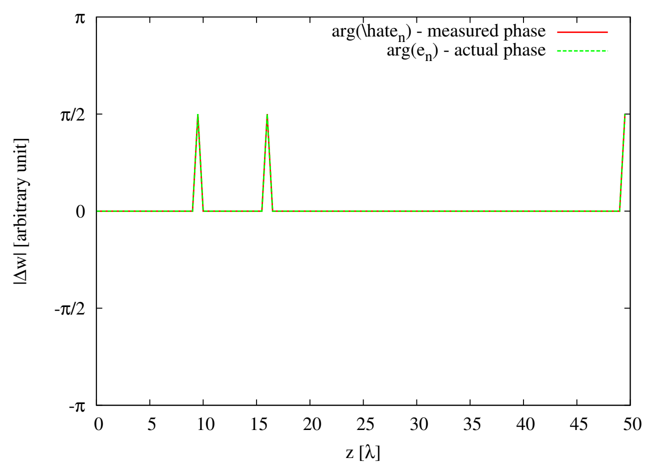

Fig.4 - Actual and measured phase

Results with $N = 200$:

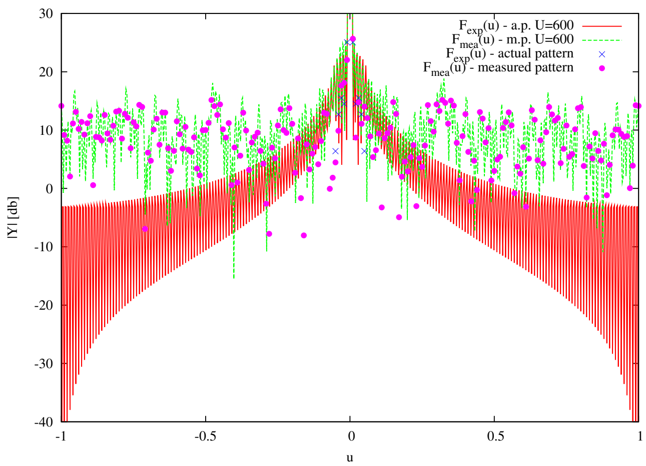

Fig.2 - Actual and measured patterns

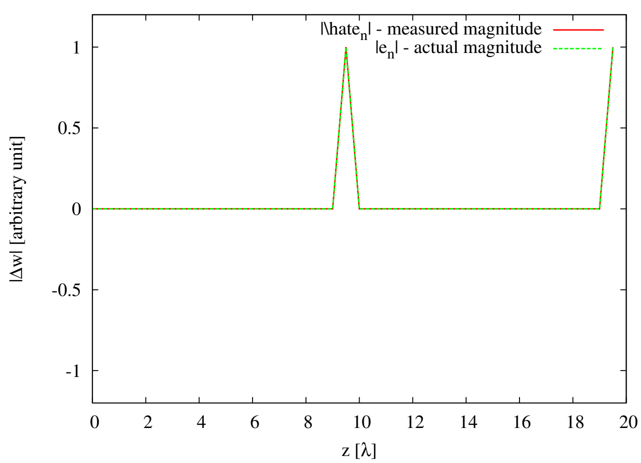

Fig.3 - Actual and measured magnitude

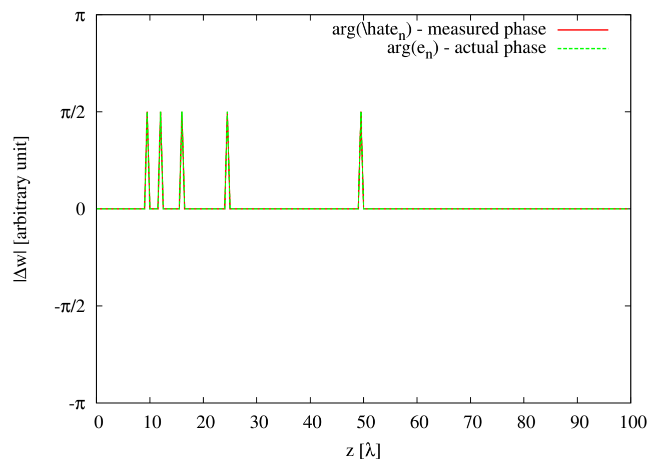

Fig.4 - Actual and measured phase

1.3.7 Seventh Case

Test Case:

- Linear Array of point sources
- Reference pattern: Taylor
- Number of elements: $N \in [20, 40, 100, 200]$
- Observation angle number: $N + 1$
- Element Spacing: $\lambda/2$
- $dB = -25$
- Percentage of failures: 5%

Reliability about all simulations:

N	η
20	0
40	$1.24 * 10^{-10}$
100	$3.10 * 10^{-9}$
200	$3.37 * 10^{-8}$

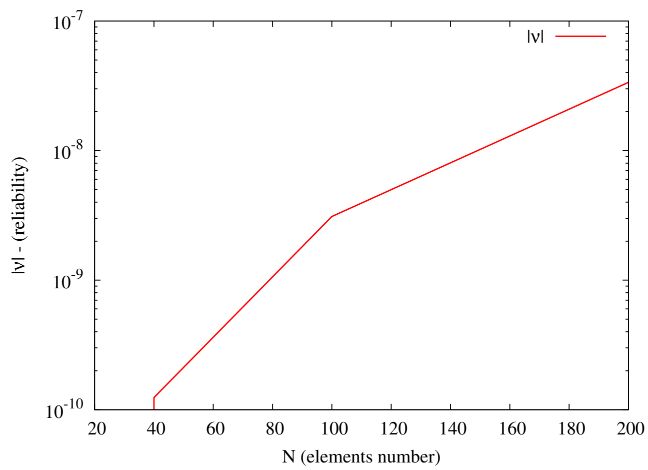

Fig.1 - Reliability

Results with $N = 20$:

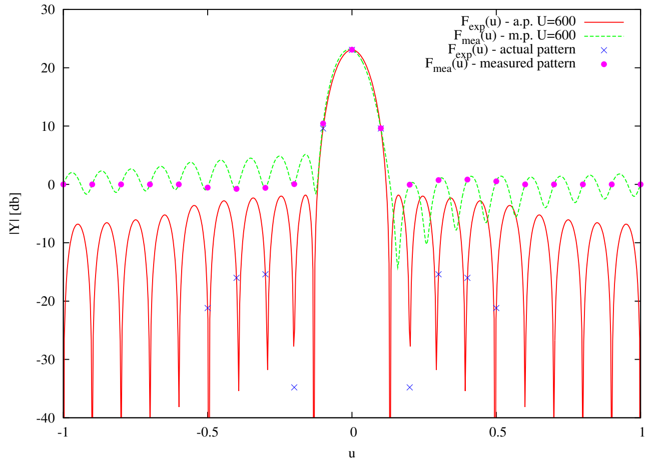

Fig.2 - Actual and measured patterns

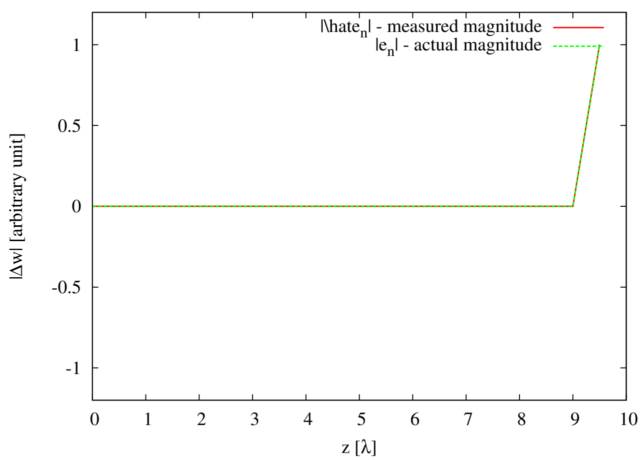

Fig.3 - Actual and measured magnitude

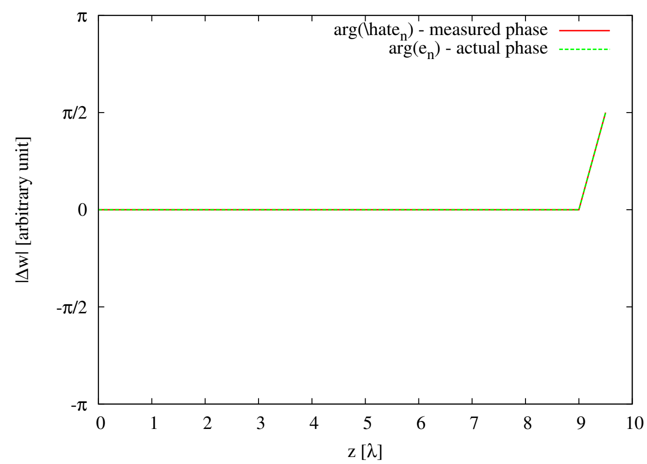

Fig.4 - Actual and measured phase

Results with $N = 40$:

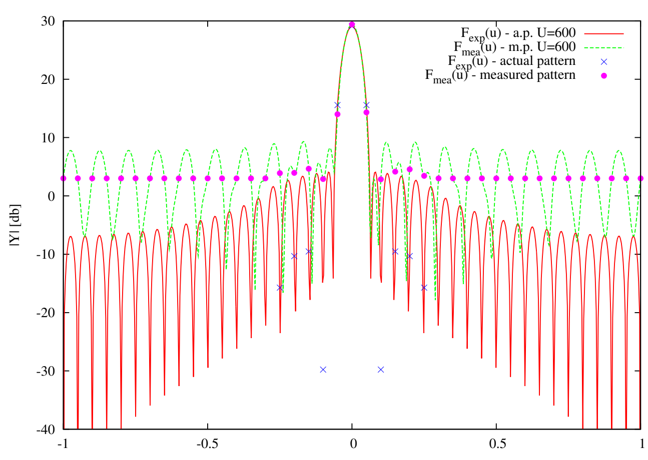

Fig.2 - Actual and measured patterns

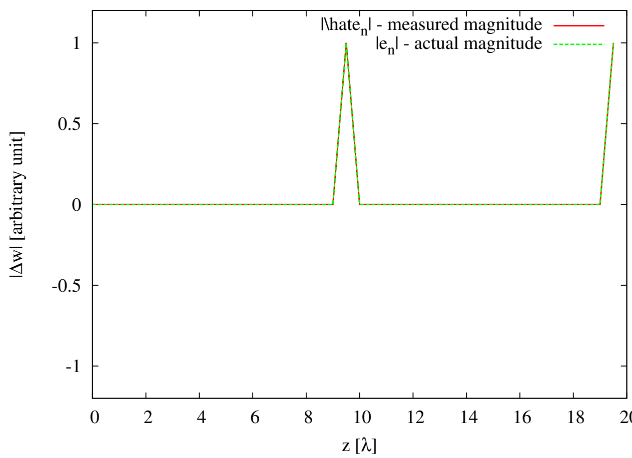

Fig.3 - Actual and measured magnitude

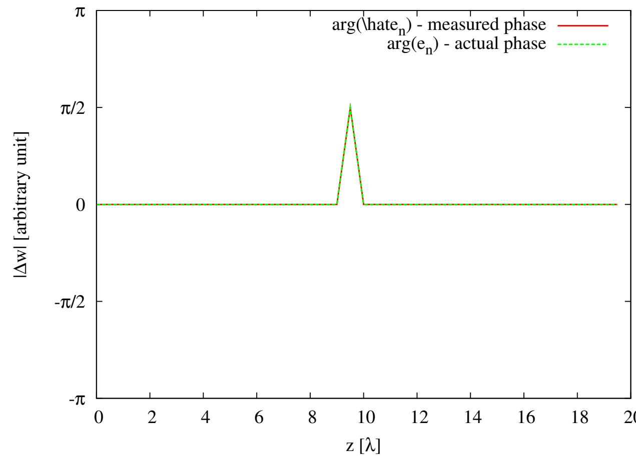

Fig.4 - Actual and measured phase

Results with $N = 100$:

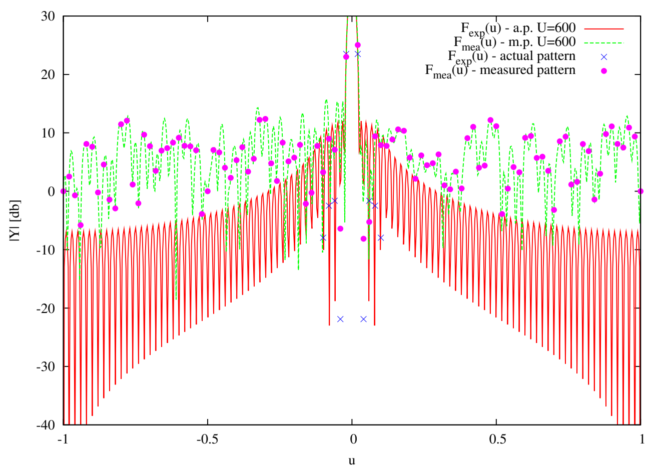

Fig.2 - Actual and measured patterns

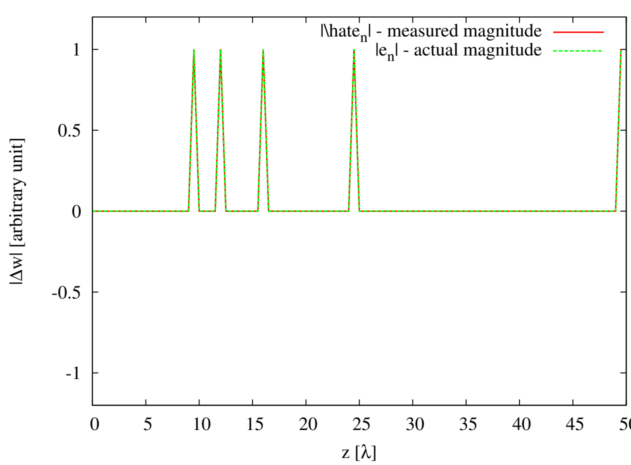

Fig.3 - Actual and measured magnitude

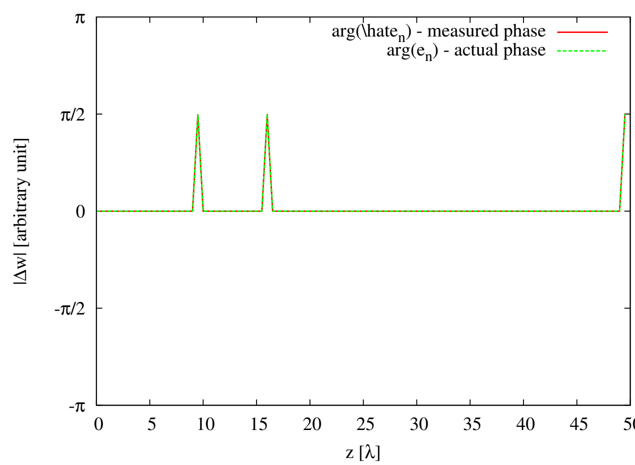

Fig.4 - Actual and measured phase

Results with $N = 200$:

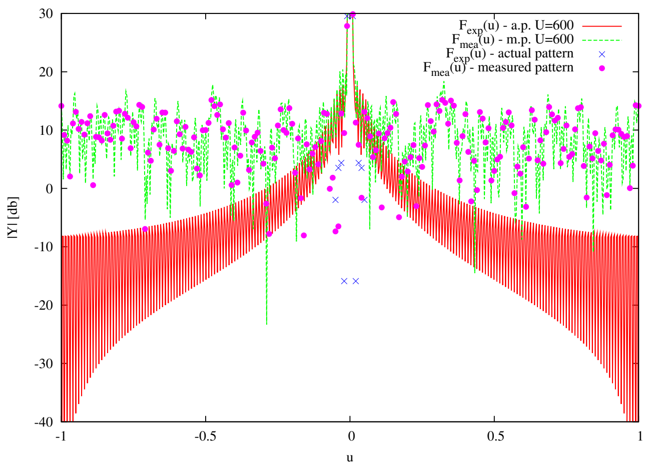

Fig.2 - Actual and measured patterns

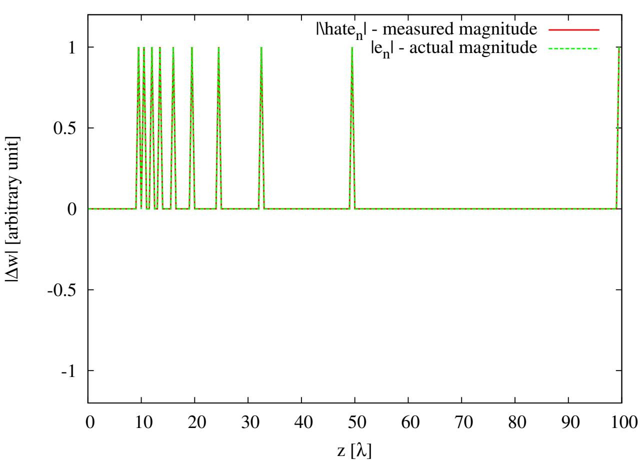

Fig.3 - Actual and measured magnitude

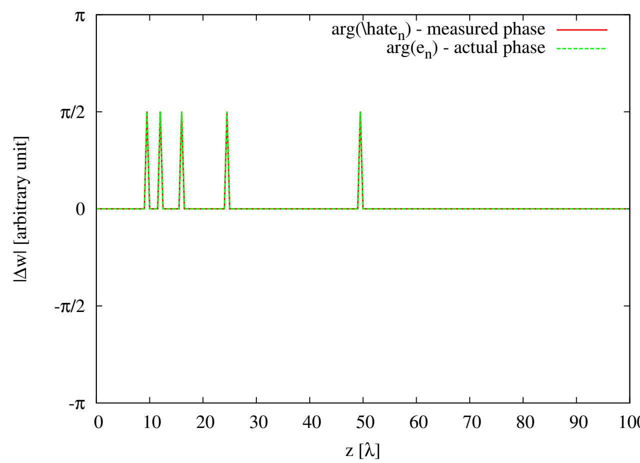

Fig.4 - Actual and measured phase

1.3.8 Eighth Case

Test Case:

- Linear Array of point sources
- Reference pattern: Taylor
- Number of elements: $N \in [20, 40, 100, 200]$
- Observation angle number: $N + 1$
- Element Spacing: $\lambda/2$
- $dB = -30$
- Percentage of failures: 5%

Reliability about all simulations:

N	η
20	0
40	$1.70 * 10^{-8}$
100	$2.98 * 10^{-9}$
200	$6.46 * 10^{-8}$

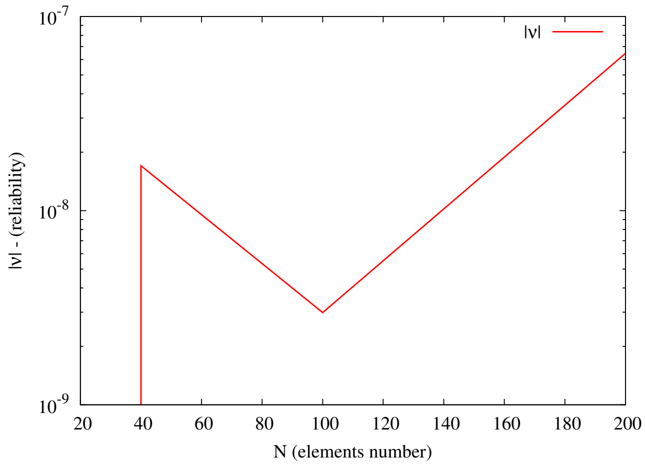

Fig.1 - Reliability

Results with $N = 20$:

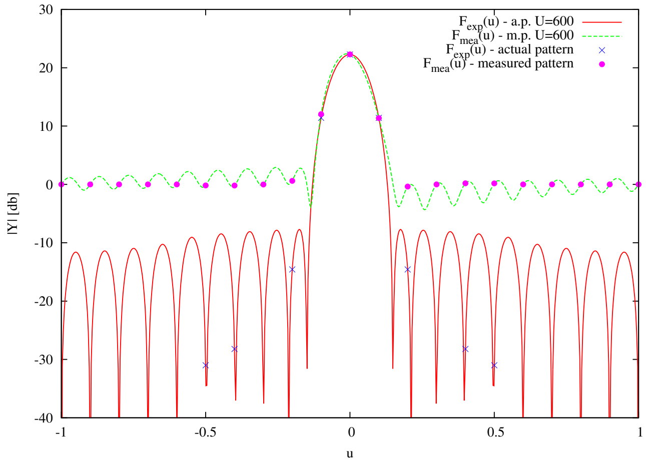

Fig.2 - Actual and measured patterns

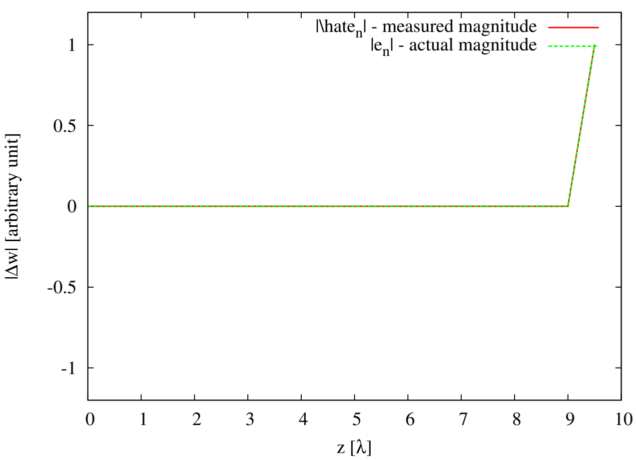

Fig.3 - Actual and measured magnitude

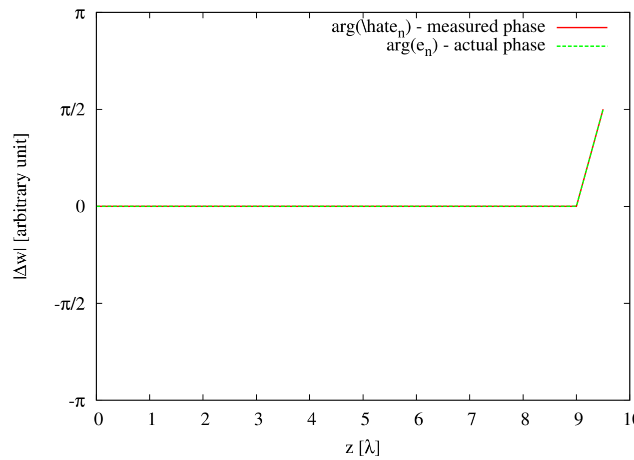

Fig.4 - Actual and measured phase

Results with $N = 40$:

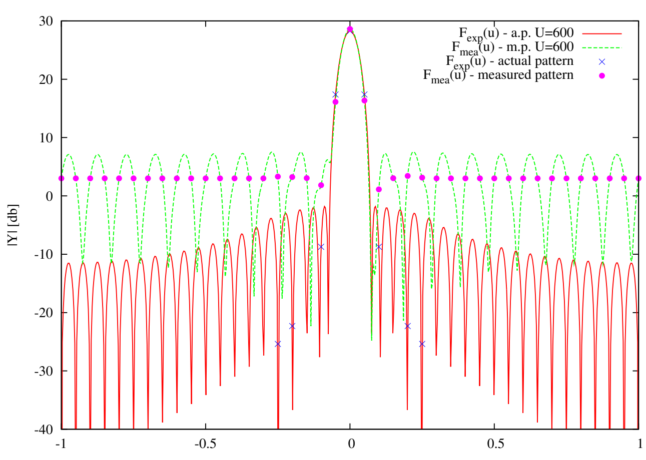

Fig.2 - Actual and measured patterns

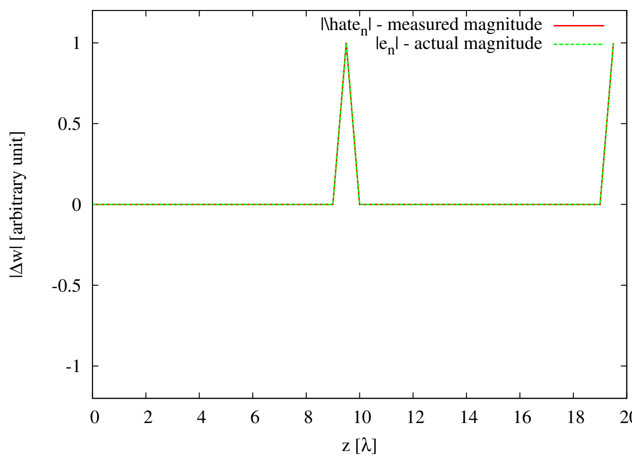

Fig.3 - Actual and measured magnitude

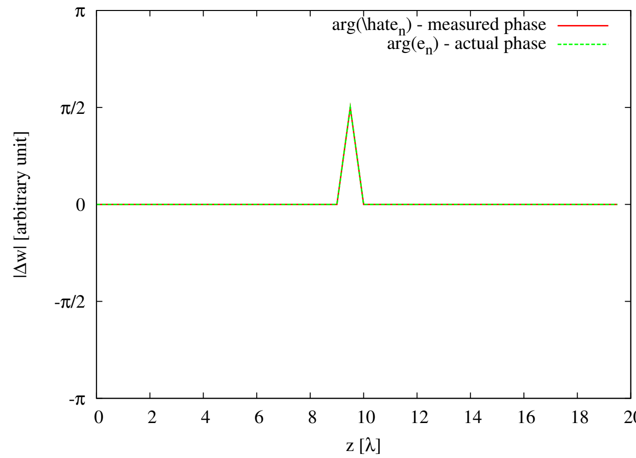

Fig.4 - Actual and measured phase

Results with $N = 100$:

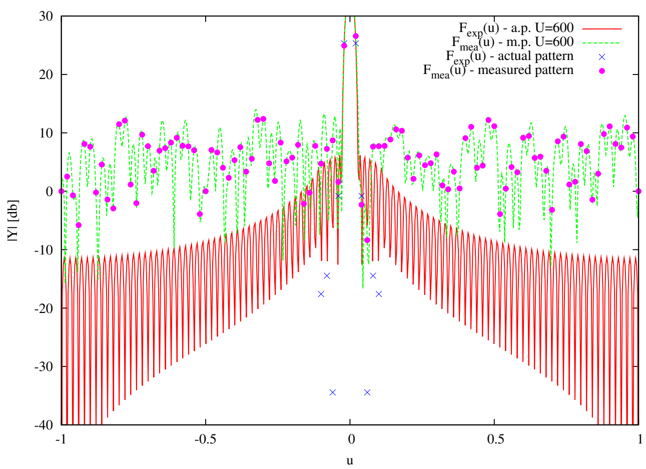

Fig.2 - Actual and measured patterns

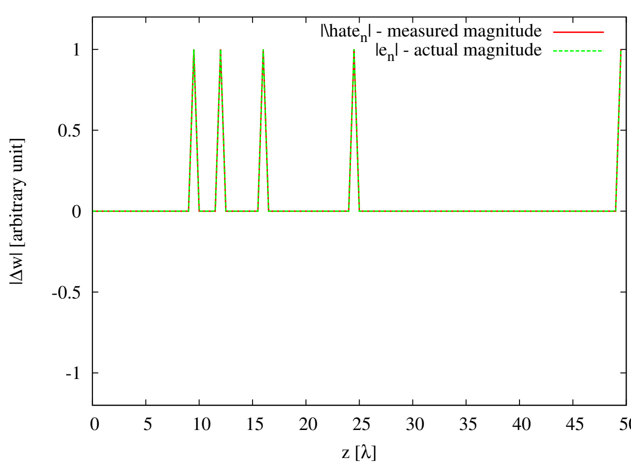

Fig.3 - Actual and measured magnitude

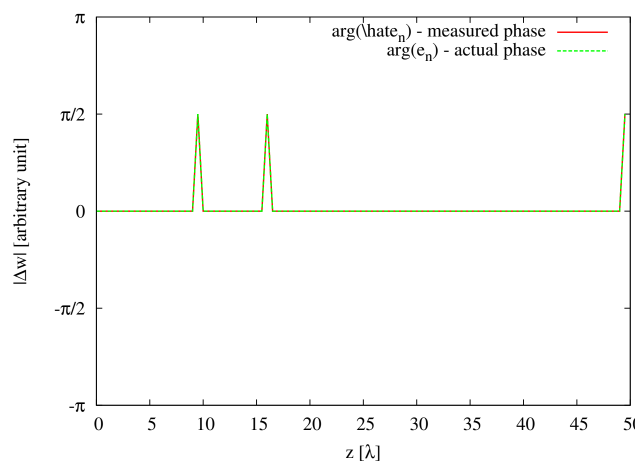

Fig.4 - Actual and measured phase

Results with $N = 200$:

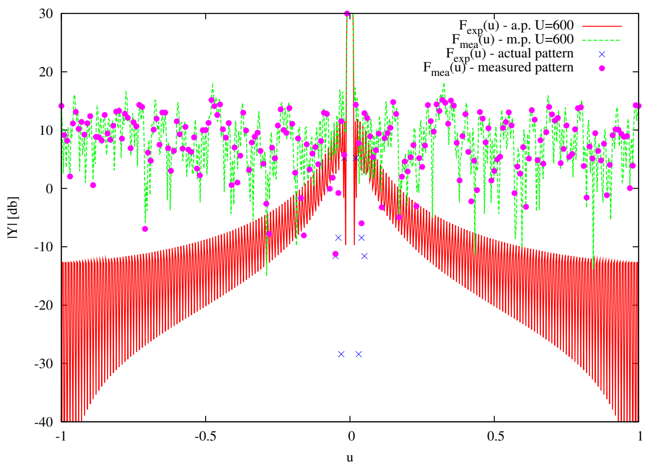

Fig.2 - Actual and measured patterns

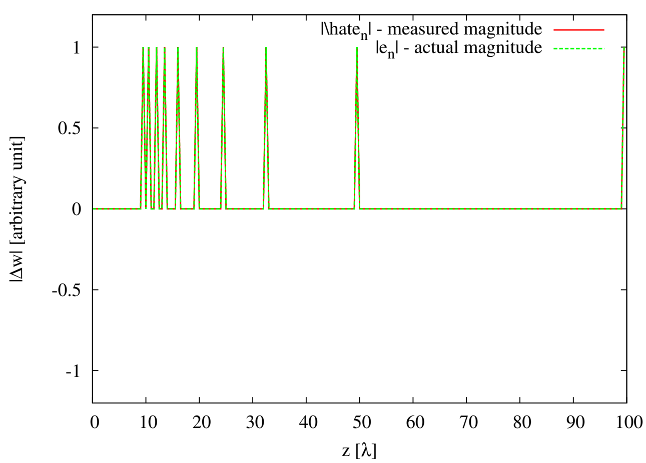

Fig.3 - Actual and measured magnitude

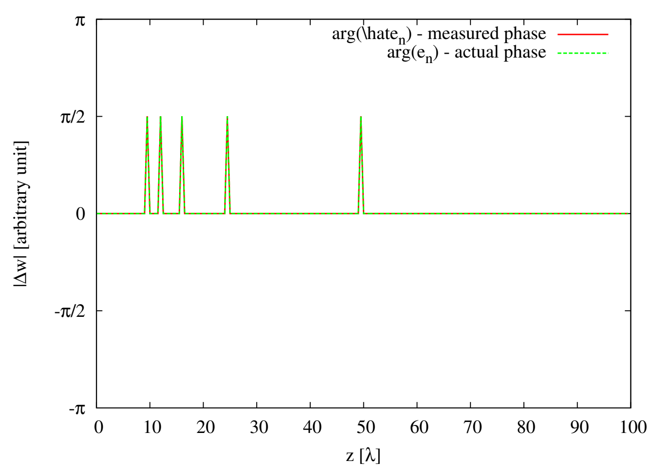

Fig.4 - Actual and measured phase

1.3.9 Ninth Case

Test Case:

- Linear Array of point sources
- Reference pattern: Taylor
- Number of elements: $N \in [20, 40, 100, 200]$
- Observation angle number: $N + 1$
- Element Spacing: $\lambda/2$
- $dB = -35$
- Percentage of failures: 5%

Reliability about all simulations:

N	η
20	0
40	$3.87 * 10^{-8}$
100	$3.71 * 10^{-9}$
200	$1.33 * 10^{-7}$

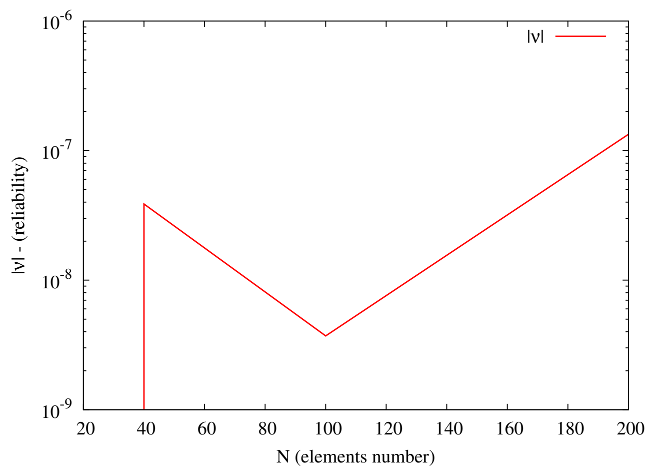

Fig.1 - Reliability

Results with $N = 20$:

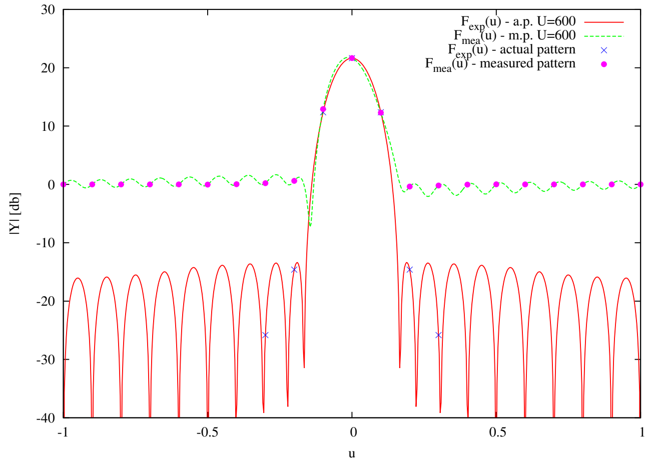

Fig.2 - Actual and measured patterns

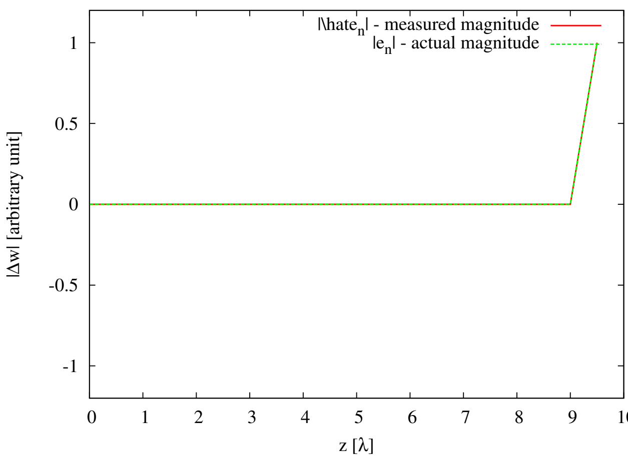

Fig.3 - Actual and measured magnitude

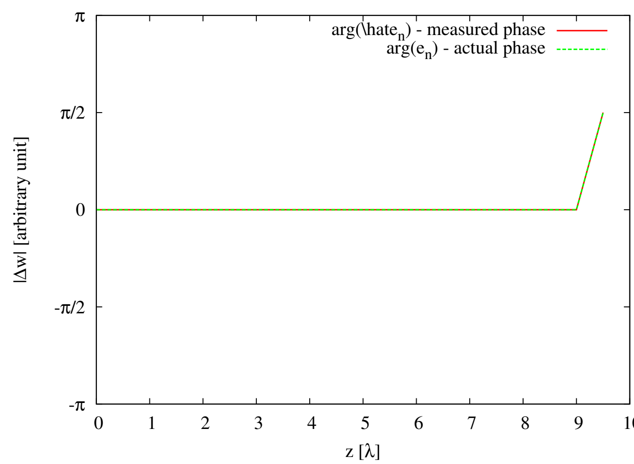

Fig.4 - Actual and measured phase

Results with $N = 40$**:**

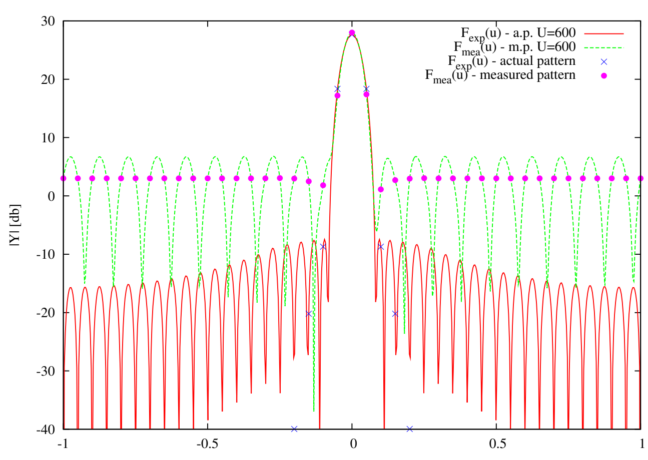

Fig.2 - Actual and measured patterns

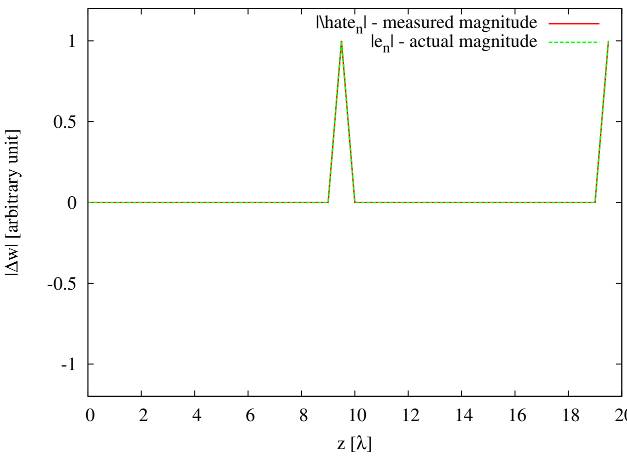

Fig.3 - Actual and measured magnitude

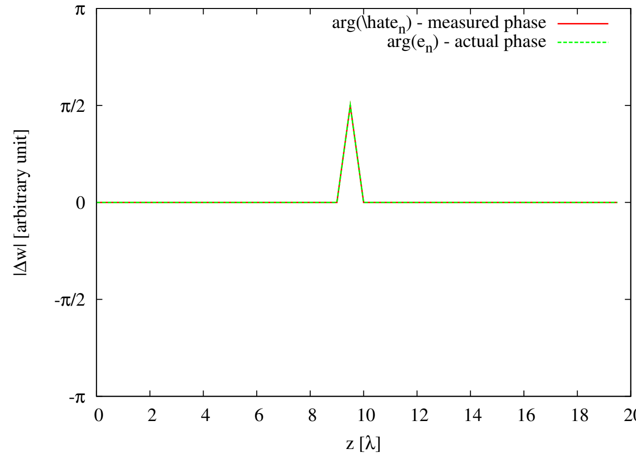

Fig.4 - Actual and measured phase

Results with $N = 100$:

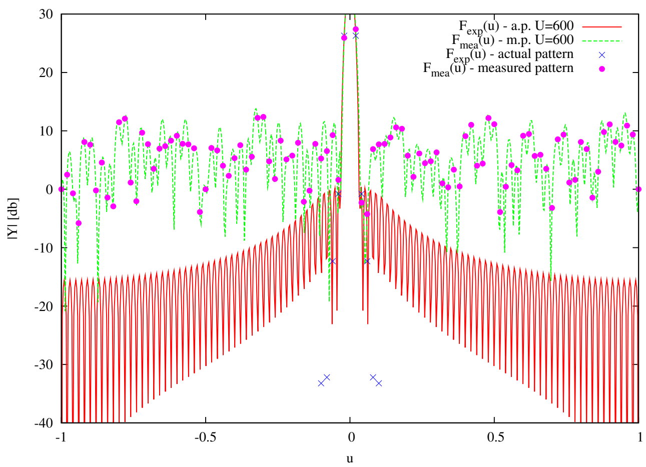

Fig.2 - Actual and measured patterns

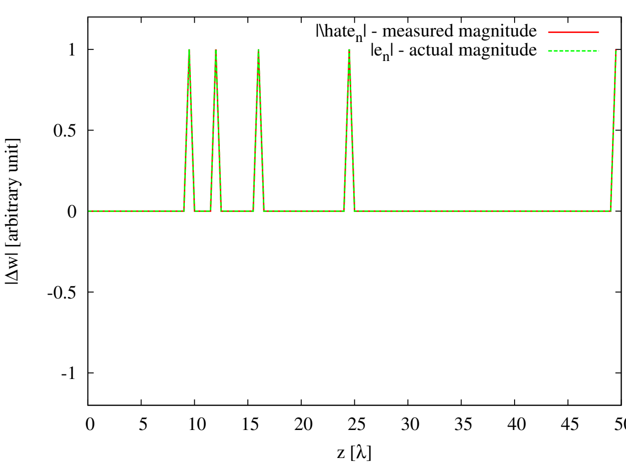

Fig.3 - Actual and measured magnitude

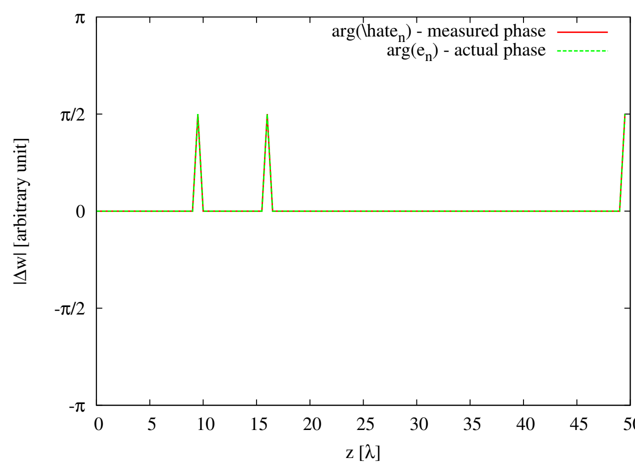

Fig.4 - Actual and measured phase

Results with $N = 200$:

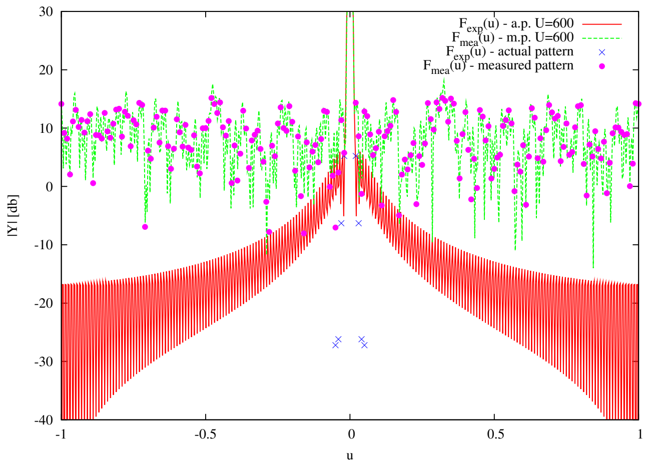

Fig.2 - Actual and measured patterns

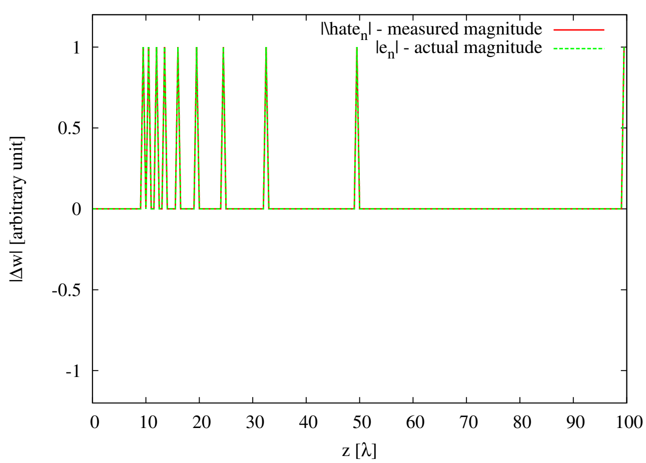

Fig.3 - Actual and measured magnitude

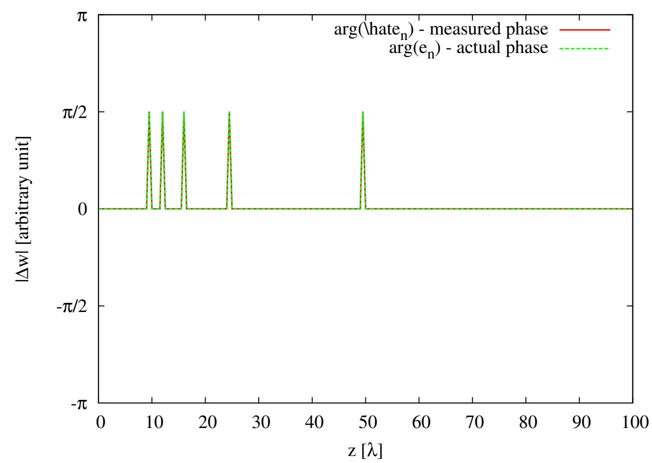

Fig.4 - Actual and measured phase

1.3.10 Tenth Case

Test Case:

- Linear Array of point sources
- Reference pattern: Taylor
- Number of elements: $N \in [20, 40, 100, 200]$
- Observation angle number: $N + 1$
- Element Spacing: $\lambda/2$
- $dB = -40$
- Percentage of failures: 5%

Reliability about all simulations:

N	η
20	0
40	$6.17 * 10^{-8}$
100	$2.56 * 10^{-10}$
200	$2.16 * 10^{-7}$

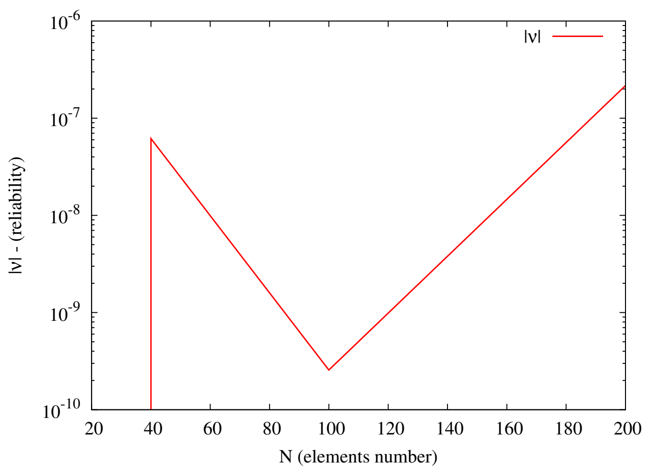

Fig.1 - Reliability

Results with $N = 20$:

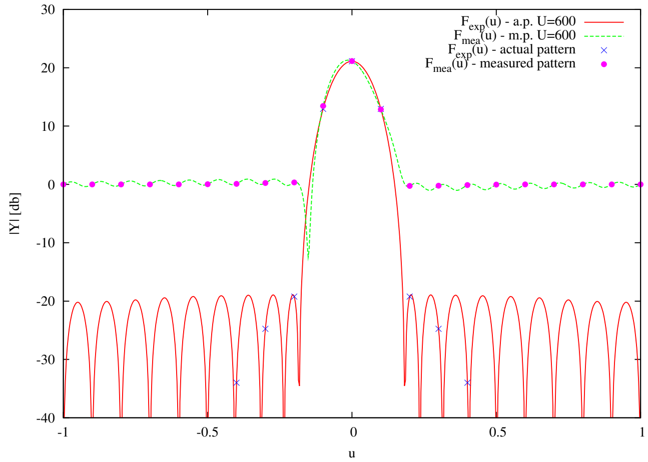

Fig.2 - Actual and measured patterns

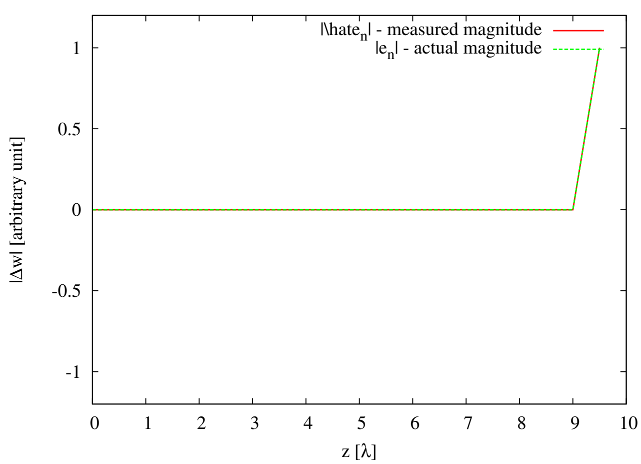

Fig.3 - Actual and measured magnitude

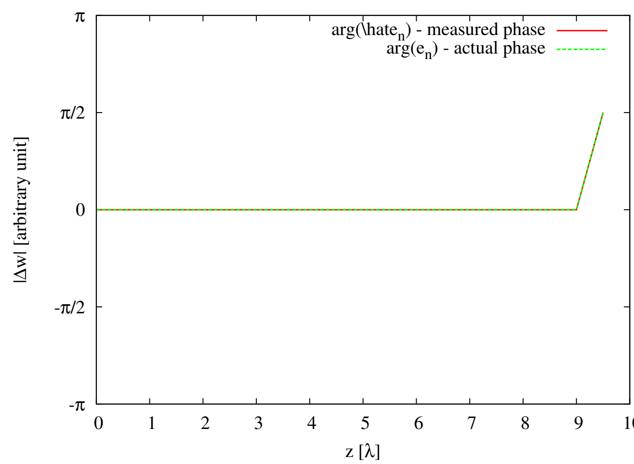

Fig.4 - Actual and measured phase

Results with $N = 40$:

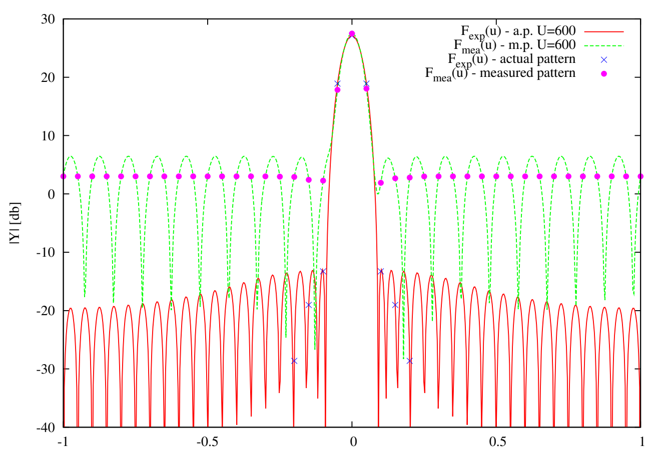

Fig.2 - Actual and measured patterns

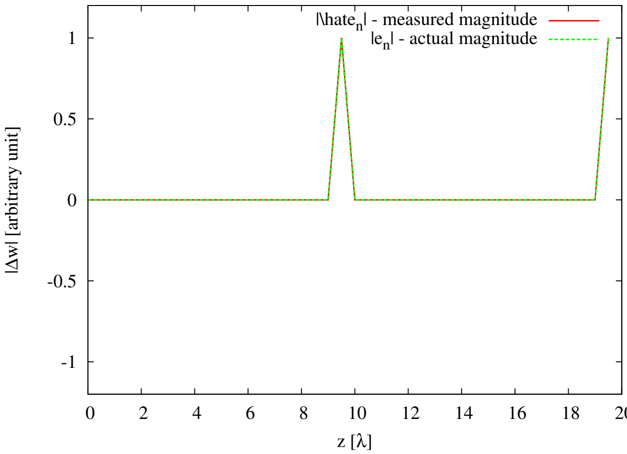

Fig.3 - Actual and measured magnitude

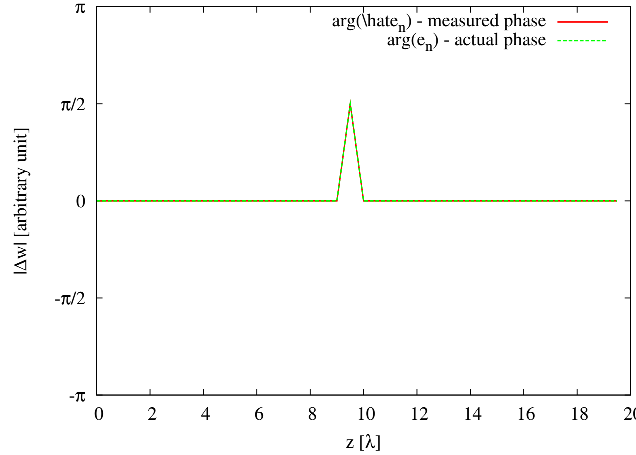

Fig.4 - Actual and measured phase

Results with $N = 100$:

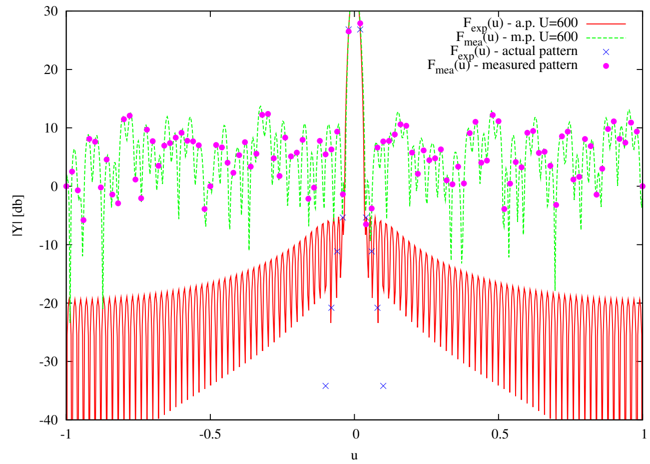

Fig.2 - Actual and measured patterns

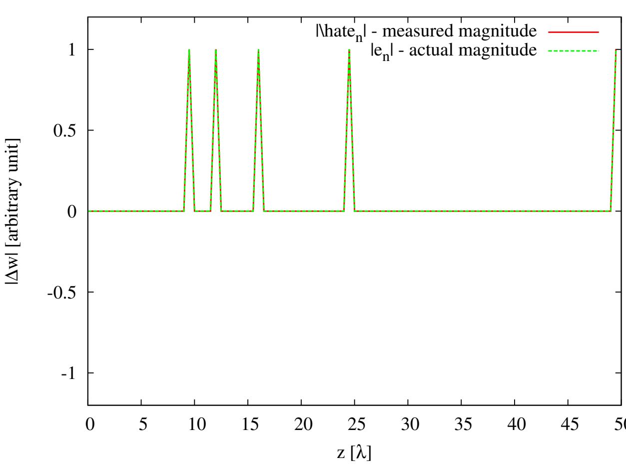

Fig.3 - Actual and measured magnitude

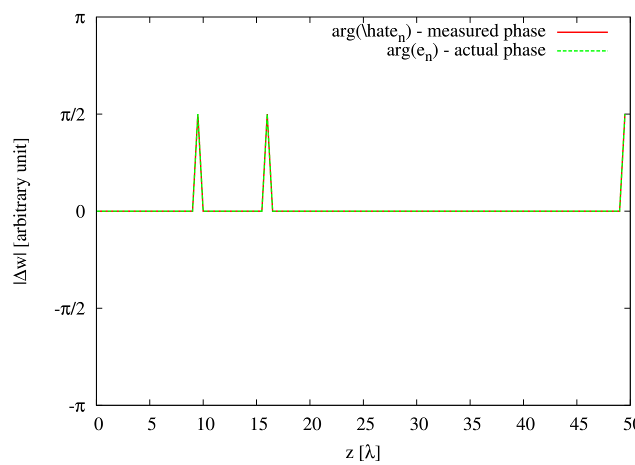

Fig.4 - Actual and measured phase

Results with $N = 200$:

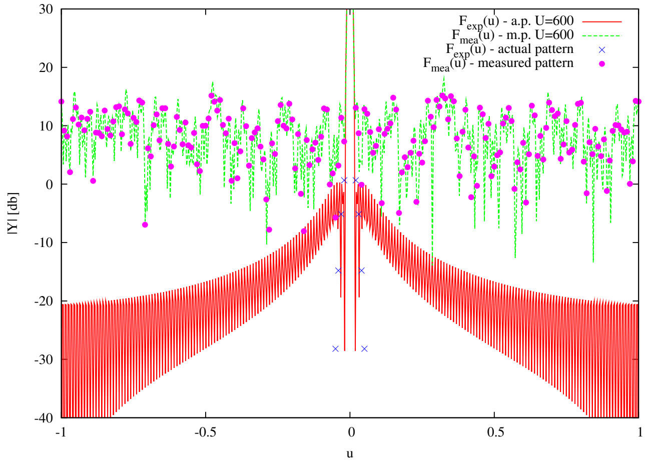

Fig.2 - Actual and measured patterns

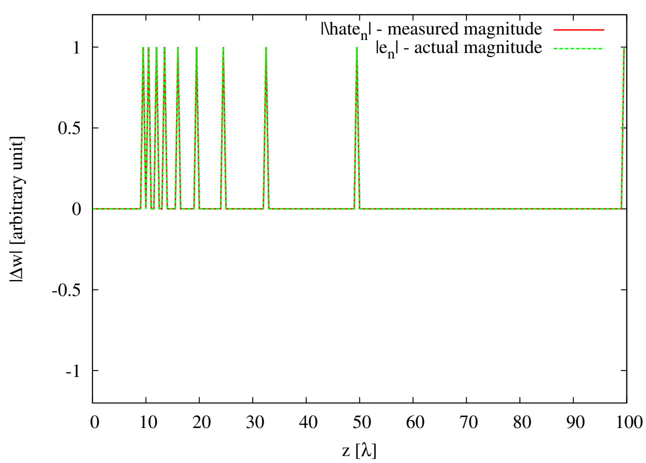

Fig.3 - Actual and measured magnitude

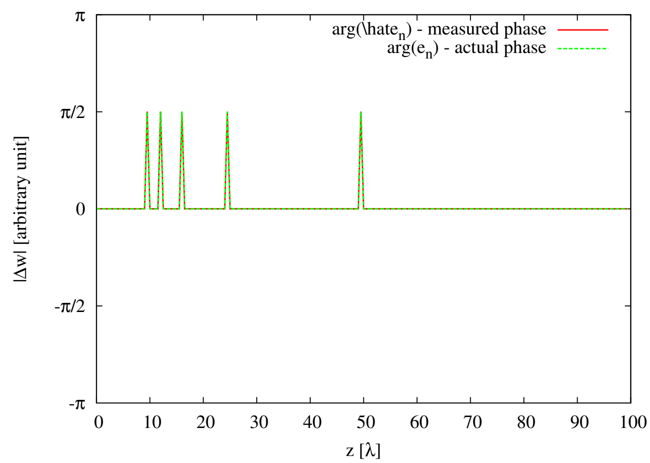

Fig.4 - Actual and measured phase

Observations

As we could imagine before simulating, the results we obtain show that the more you add elements in the array antenna and the less you will be able to find all the array failures (keeping constant the proportion of number of elements with respect to number of failures).

Final observations

In cases in which I had one failure and that failure was in the immaginary part of the complex weight error I have noticed that I have, in the beam pattern plot, a big difference in the shape of the measured pattern with respect to the actual one.

References

[1] L. Poli, G. Oliveri, and A. Massa, "Imaging sparse metallic cylinders through a Local Shape Function Bayesian Compressive Sensing approach," Journal of Optical Society of America A, vol. 30, no. 6, pp. 1261-1272, 2013.

[2] F. Viani, L. Poli, G. Oliveri, F. Robol, and A. Massa, "Sparse scatterers imaging through approximated multitask compressive sensing strategies," Microwave Opt. Technol. Lett., vol. 55, no. 7, pp. 1553-1558, Jul. 2013.

[3] L. Poli, G. Oliveri, P. Rocca, and A. Massa, "Bayesian compressive sensing approaches for the reconstruction of two-dimensional sparse scatterers under TE illumination," IEEE Trans. Geosci. Remote Sensing, vol. 51, no. 5, pp. 2920-2936, May. 2013.

[4] L. Poli, G. Oliveri, and A. Massa, "Microwave imaging within the first-order Born approximation by means of the contrast-field Bayesian compressive sensing," IEEE Trans. Antennas Propag., vol. 60, no. 6, pp. 2865-2879, Jun. 2012.

[5] G. Oliveri, P. Rocca, and A. Massa, "A bayesian compressive sampling-based inversion for imaging sparse scatterers," IEEE Trans. Geosci. Remote Sensing, vol. 49, no. 10, pp. 3993-4006, Oct. 2011.

[6] G. Oliveri, L. Poli, P. Rocca, and A. Massa, "Bayesian compressive optical imaging within the Rytov approximation," Optics Letters, vol. 37, no. 10, pp. 1760-1762, 2012.

[7] L. Poli, G. Oliveri, F. Viani, and A. Massa, âMT-BCS-based microwave imaging approach through minimum-norm current expansion,â IEEE Trans. Antennas Propag., in press. doi:10.1109/TAP.2013.2265254

[8] G. Oliveri and A. Massa, "Bayesian compressive sampling for pattern synthesis with maximally sparse non-uniform linear arrays," IEEE Trans. Antennas Propag., vol. 59, no. 2, pp. 467-481, Feb. 2011.

[9] G. Oliveri, M. Carlin, and A. Massa, "Complex-weight sparse linear array synthesis by Bayesian Compressive Sampling," IEEE Trans. Antennas Propag., vol. 60, no. 5, pp. 2309-2326, May 2012.

[10] G. Oliveri, P. Rocca, and A. Massa, "Reliable Diagnosis of Large Linear Arrays - A Bayesian Compressive Sensing Approach," IEEE Trans. Antennas Propag., vol. 60, no. 10, pp. 4627-4636, Oct. 2012.

[11] F. Viani, G. Oliveri, and A. Massa, âCompressive sensing pattern matching techniques for synthesizing planar sparse arraysâ IEEE Trans. Antennas Propag., in press. doi:10.1109/TAP.2013.2267195

[12] M. Carlin, P. Rocca, G. Oliveri, F. Viani, and A. Massa, "Directions-of-Arrival Estimation through Bayesian Compressive Sensing strategies," IEEE Trans. Antennas Propag., in press.

[13] M. Carlin, P. Rocca, "A Bayesian compressive sensing strategy for direction-of-arrival estimation," 6th European Conference on Antennas Propag. (EuCAP 2012), Prague, Czech Republic, pp. 1508-1509, 26-30 Mar. 2012.

[14] M. Carlin, P. Rocca, G. Oliveri, and A. Massa, âBayesian compressive sensing as applied to directions-of-arrival estimation in planar arraysâ, Journal of Electrical and Computer Engineering, Special Issue on âAdvances in Radar Technologiesâ, in press.